7.4.2 Artvin Project

(1) Reservoir

(a) Topography

As described in 7.1, two alternative plans are under review in regard to the project; one is an upstream dam site, and the other a downstream dam site in the same river. The data related to the reservoir and others in connection with both sites are as follows.

Upstream dam site
High water level of the reservoir: EL500.0 m
Reservoir capacity: $23.^{7} \times 10^{6}$ m^{3}

Downstream dam site
High water level of the reservoir: EL500.0 m
Reservoir capacity: $166.^{8} \times 10^{6}$ m^{3}

i) Reservoir of upstream dam

The upstream dam site is about 3 kilometers upstream of the original dam site. The major tributaries in the reservoir are Hev valley and Pikal valley on the left bank and Avresi valley and Citliyan valley on the right bank. All these valleys are, however, extremely small compared with the tributaries in the Yusufeli reservoir area. Therefore, the principal reservoir under the upstream dam site locates in the mainstream of the Coruh River that runs northeastward slightly meandering from the Yusufeli dam site.

The reservoir upto 1 - 2 kilometers upstream of the dam site is situated on Yusufeli formation consisting of gabbro, and the area from there to the Yusufeli dam site is situated on Ikizdere granitic rocks. Thus the riverbed in this reservoir shows topographic features of a narrow valley without flood plain. Also, except for small flatlands formed at the exits of small valleies and

alluvial cones at the feet of steep cliffs, the river generally forms a steep ravine. The width of the reservoir is about 200 meters at the high water level of EL.500.00 meters.

No landslide area is seen in the reservoir area of the upstream dam site.

ii) Reservoir of downstream dam

The downstream dam site is planned to be about 10 kilometers downstream from the upstream dam site. The major tributaries in the reservoir are Esenkaya valley and Tarakcilar valley on the left bank and Nagal valley and Hars valley on the right bank. As in case of the reservoir of the upstream dam site, each valley is small compared with the tributaries in the Yusufeli reservoir area.

The reservoir of the downstream dam site is situated on the main stream of the Coruh River, which runs northeastward, repeating several meanders.

The main area of the reservoir is situated on Yusufeli formation, which consists of gabbro and phyllite in the upstream area, mainly phyllite in the midstream and extremely hard green rocks considered to be made up of diabase and basic tuff in the downstream area, respectively. Consequently, the general topography exhibits a wide-river in the phyllite area except for the gabbro and hard green rock areas. That is, the river immediate downstream of the upstream dam site and near the original dam site lies on the gabbro area, in which the width of the riverbed is generally narrow, about 120 - 150 meters, thereby forming a ravine.

Also, in the vicinity of the downstream dam site, ravine is formed, as in case of the gabbro area, because of the distribution of hard green rocks. In other areas, however, because of distribution of phyllite, a gently-

sloping wide valley is formed with large scale slope washes and terrace deposits in many places on both sides of the river. In this reservoir area, two large landslides of Havuzlu and Demirkent are situated; the former is about eight kilometers upstream, and the latter about 6.5 kilometers upstream from the downstream dam site.

(b) Geology distributed

The geology distributed in both reservoirs under the Artvin Project is follows.

Quaternary	Surface deposits	Slope wash	Reservoirs of both upstream and downstream dam sites
		Landslide material	Reservoir of downstream dam site
		Riverbed deposits	Reservoirs of both upstream and downstream dam sites
		Terrace deposits	Ditto
Tertiary	Basement rocks	Ikizdere granitic rocks	Upstream end of both reservoirs
Mesozoic		Yusufeli formation	Reservoirs of both upstream and downstream dam sites

i) Surface deposits in the reservoir of the upstream dam

Slope wash

The slope washes are seen here and there in the reservoir area. As in case of the Yusufeli reservoir area, there are two kinds of the slope wash; one is talus and the other alluvial cone. However, since the greater part of

these materials locate higher than the high water level of 500 meters, they may not directly affect the reservoir.

The greatest slope wash in this reservoir area is that lies on the south slope (see DWG.AP.3-26) of the right bank of the upstream dam site. The material principally consists of rock fragments; so-called detritus. Although the thickness of the slope wash has not yet been confirmed, judging from their appearance, it seems not to be very thick.

Riverbed deposits

The riverbed deposits in the reservoir area have not yet been investigated. The riverbed deposits in the Yusufeli dam site were found to be about 50 meters, and it is considered that this also can be roughly applied to this reservoir. And it is considered that the kinds and shapes of gravel forming the deposits are nearly same as those of the Yusufeli reservoir. Note that there is no remarkable flood plain.

Terrace deposits

The distribution area and thickness of the terrace deposits are small in the reservoir of the upstream dam site. However, small scale terrace deposits lie on the left bank of the immediate downstream of the Yusufeli dam site and on the left bank of the Artvin upstream dam site. These consist of sand, silt, and gravel, and their sorting is not necessarily good. The tops of terrace deposits are estimated to be approximately EL.510 meters. Also one test sample were collected from the terrace deposits immediate downstream of the Yusufeli dam site and that the pollen analysis has been performed. The details are described in 7.4.1, (1)-(b).

ii) Basement rocks in the reservoir of the upstream dam

Ikizdere granitic rocks

The basement rock from the midstream to the upstream area of the reservoir, namely, the area upto about five kilometers downstream from the Yusufeli dam site, consists of Ikizdere granitic rocks.

These rocks are as same as those of the Ikizdere granitic rocks described in 7.4.1, (1)-(b)-ii).

Yusufeli formation

The Yusufeli formation in this reservoir area mainly consists of gabbro. This gabbro is green and extremely hard. Many aplite veins can be seen in the gabbro along the left bank of the dam site and along the Hev valley. In the reservoir area, the gabbro is distributed from the dam site to about 2.5 kilometers upstream of it.

iii) Surface deposits in the reservoir of the downstream dam

Slope wash

As previously described in 7.4.2, (1)-(a)-ii), the Yusufeli formation in the reservoir of the downstream dam site consists of gabbro, phyllite, and green rocks of basic tuff and diabase. Due to the variation of the basement rocks, the distribution of the slope wash changes.

All the slope wash in this reservoir area is talus-type, and the alluvial cone distributed in the upstream area is seldom seen in this area. Generally, there are remarkable distributions of slope wash in the area of phyllite. The typical examples are on the right bank immediate downstream of the upstream dam site, the opposite banks of Havuzlu and Demirkent landslides, and on the right bank downstream of Demirkent landslide, where the slope wash is considered to be made up of principally of rock fragments, and the thickness is estimated to be between 5 and 10 meters.

Landslide Material

In the reservoir area of the downstream dam site, two large-scale landslides exist; one is Havnzlu landslide locating on the left bank 8 kilometers upstream of the downstream dam site, and the other is Demirkent landslide on the right bank about 6.5 kilometers upstream of the dam site. It seems that both landslides are stable in present.

The area of Havuzlu landslide is 772,000 m^2 and according to the results of the electric prospecting, the maximum thickness of the landslide is approximately 150 meters with the slope inclination within the landslide being about 23 degrees. The materials constituting the mass of landslide consists of rock fragments of sandstone, shale, and phyllite, etc. Note that the EIE has executed electric prospectings and three drillholes in the landslide, the results are shown in DWG.AP.3-27.

No geological investigation has been performed for Demirkent landslide. However, the scale of the landslide is considered to be greater than Havuzlu landslide. Although no microscopic identification has been made in regard to the material constituting this landslide, it is assuemed that it is made up of weathered residual soil of gabbro or amphibolite. Further, on the opposite bank (left bank) of Demirkent landslide, talus material lies accompanied by greenish grey and brown earth pillars. It is assumed that this material is the remnants of the slidden mass reached the opposite riverbank burying the Coruh River when occurred. The top of the material remaining on the left bank of the river is estimated to be about EL.550 meters or more.

Riverbed deposits

The thickness of the riverbed deposits at the downstream dam site has been confirmed by the drillhole (SID-1) and it was about 34 meters. Therefore, it is assumed that the thickness of the riverbed deposits in this reservoir area is about 34 - 50 m (at Yusufeli dam site).

Terrace deposits

Generally, the reservoir area exhibits no noticeable typical terrace. However, as previously described, thin gravel layers deposited on the slope wash locating at the right bank immediate downstream of the upstream dam site, and on the slope wash locating at the right bank downstream of Demirkent landslide. It is assumed that these terrace deposits were produced when the Coruh River was buried by the landslide mass forming temporary lakes. The thickness of these layers are as thin as less than several meters.

iv) Basement rocks in the reservoir of the downstream dam

Yusufeli formation

The basement rock distributed in the reservoir of the downstream dam site consists of Yusufeli formation. As previously described, however, Yusufeli formation in this reservoir area is made of a variety of rocks such as gabbro, phyllite, diabase, and basic tuff, etc.

Gabbro is green and extremely hard. The distribution of gabbro is seen in the vicinity of the original dam site and in the downstream area of Essenkaya valley in the midstream area of the reservoir. Phyllite is widely distributed from Havuzlu landslide to the downstream area of Essenkaya village. In these areas, besides phyllite, thin layers of shale and sandstone are intercalated. Green rocks, such as diabase and basic tuff, are disbributed in the downstream area of the reservoir, namely, in the vicinity of the downstream dam site. This green rocks are hard.

(c) Considerations from the viewpoint of engineering geology

In both reservoir areas of the upstream and downstream dam sites, the geological factors that may adversely affect the watertightness of the reservoir, such as soluble rocks, cavities, and thin ridges cannot be found. Consequently, it

is considered that the watertightness of both reservoirs are assured. Hereafter, the stability of slope is described.

i) Slope stability in the reservoir of the upstream dam

As described above, in the reservoir of the upstream dam site, there is no existing landslide and no geographical features capable of producing a new landslide when the reservoir is filled. It is expected that as described in 7.4.2, (1)-(b)-i), there will be no particular problem with respect to the slope wash developing on the south-west slope of the mountain on the right bank of the dam site, because the slope wash does not face to the reservoir and the elevation of the foot of the slope wash is expected to be higher than the high water level of EL.500 m. However, a detailed surface investigation for this is necessary at the detail design stage together with investigations on the stability of steep slope (see 7.4.1, (1)-(c)-ii)).

ii) Slope stability in the reservoir of the downstream dam

As mentioned previously, two large landslides of Havuzlu and Demirkent lie in this reservoir. Besides these, there is no particular topography that has any possibilities to cause landslide when the reservoir is filled. The followings are considerations in regard to the influences of the reservoir on the thick unconsolidated deposits distributed on the right bank downstream of the upstream dam site, the opposite bank of Havuzlu landslide, on the opposite bank of Demirkent landslide, and on the right bank of the downstream of Demirkent landslide, and also the influence of the reservoir on the previously described two large-scale landslides.

Influence of the reservoir on the unconsolidated deposits

In three (all are on the right bank of the Coruh River) of the four places mentioned above except for the opposite bank of Demirkent landslide, slope washes crop out 5 - 10 meter high above the road. These slope washes are detritus consisting mainly of rock fragments, and the tops of the detritus are covered with thin layers of gravel. All these materials are unconsolidated. The elevations of the tops of these unconsolidated deposits are estimated to be about EL.500 meters in the upstream area (upstream of Havuzlu landslide) and EL.500 - 525 meters in the downstream area (downstream of Demirkent landslide).

Consequnetly, these three unconsolidated deposits will be submerged entirely or partially when the reservoir is filled. The submersion of these areas under water could cause collapse of the unconsolidated deposits. In the event that large back-deposits exist in the areas mentioned above, these deposits may continuously collapse. Therefore, the sizes of these three areas should be investigated in the future. Furthermore, if there are any other thick deposits other than the above areas, their sizes should also be investigated.

As previously described, the unconsolidated deposits accompanied by earth pillars that can be seen in the opposite bank of Demirkent landslide is assumed to be the remnants of the slidden mass of Demirkent landslide. This is considered to be the weathered residual material of basic rock, such as gabbro or amphybolite. Should it be covered with water, causing them to become soft, it can possibly slide into the reservoir. The results of field investigations have revealed that the amount of the deposits above the high water level of the reservoir is not large, and the greater part of them will be submerged under the high water level of the reservoir. It is

desirable, however, that more detailed investigations be made on the matter in the future.

Havuzlu landslide

The only one reason for our recommendation to abolish the original dam site upon the review of the Artvin Development Project was the existence of Havuzlu landslide having a great mass of landslide material amounting to about 86×10^6 m^3 on the left bank about one kilometer upstream from the original dam site.

The scale of this landslide material mass is quite large, with the lowest elevation of about EL.480 m, the elevation of its top of about EL.1150 m, the area 772,000 m^2, the maximum thickness about 150 m (based on the results of the electric prospecting performed by the EIE), and the assumed volume of slide material of 86×10^6 m^3. Judging from the cross-section of the landslide obtained by three drillholes and the electric prospecting by the EIE, the lower part of the slip surface (so-called leg of the landslide) is estimated to be about EL.600 meters, accordingly, there is little possibility of the reservoir water infiltrating into the slip surface. The greater part of the tougue of the landslide, however, will be submerged under water. In addition, the inclination of the ground surface of the landslide mass is about 22 degrees and the inclination of the slip surface (slope of bedrock) is 30 - 50 degrees, indicating steep inclination in general.

It is extremely difficult to determine whether Havuzlu landslide will be reactivated as the result of the impounding of the reservoir water. Especially, substantial expense and time will be required to investigate how the present balance will be affected after the completion of the reservoir. In addition, besides the new condition of the reservoir, a simulation must be performed with respect to natural phenomena, such as heavy rain and an earthquake. Based on these various considerations, the

original dam site about one km downstream from Havuzlu landslide was abandoned on the condition that the selection of alternative dam sites for the Artvin development project are possible.

The Artvin upstream dam site has no relationship to Havuzlu landslide. The downstream dam site, however, is situated about eight kilometers downstream of the landslide, and due consideration should be given to the influence of Havuzlu landslide.
The problems that may be confronted in case the mass of landslide should flow into the reservoir are the influence of the waves and floods on the dam and also the influence of the blocked reservoir on the upstream area resulting from the mass of landslide.

The sliding speed of landslide mass may vary depending on each landslide. For example, in the case of the Vaiont dam, the sliding speed in the middle period of activity was reported as being several millimeters to several centimeters per day. (Some report describes that the sliding speed was 15 - 30 meters per second during the extreme landslide period.) On the other hand, the evalation of the bottom of the slip surface of the Havuzlu landslide is about EL.600 meters, which is higher than the high water level of the reservoir, in addition, the form of the slip surfce (equal to the top of the bed rock) along the profile of electric prospecting line shows "stairs form" (partly steep 30° - 50°, partly flat-within 10°) at the main part and "ski jump form" at the end of the landslide (see DWG.AP.3-27).

Considering the above conditions, given that Havuzlu landslide is reactivated, the landslide speed will not reach an exceedingly high speed. Further, the reservoir from the landslide to the downstream dam site have several meanders, and the distance is about eight kilometers. In addition, a structure of concrete arch gravity or concrete arch is selected for the downstream dam to

withstand the landslide waves and floodwaters that could possibly be caused by a landslide. For these reasons, the reactivation of Havuzlu landslide may not greatly affect the downstream dam even if it is reactivated.

Conversely, since the water depth of the reservoir in front of Havuzlu landslide is about 50 meters, and the width of the tongue of the landslide is about 600 meters. The capacity of the reservoir in front of the landslide can be estimated as being about 3.7×10^6 m^3. Because the volume of the Havuzlu landslide mass is about 86×10^6 m^3, should an amount of about a twentieth of the total landslide mass flow into the reservoir, the reservoir will be almost blocked. Although there is little possibility of the total amount of landslide falling into the reservoir, the influence of such a case on the Yusufeli Power Plant needs to be reviewed.

Demirkent Landslide

Investigation excepting site reconnaissance has not yet been made in regard to Demirkent landslide.

The area of the landslide mass based on a map drawn on a greatly reduced scale can be determined as being about 950,000 m^2. The characteristic of this landslide is the gentle sloping of about 17 degrees, and the villages and trees on this mass area are very stable.

As mentioned, if the assumption is correct that the slope wash accompanied by the earth pillars, at the opposite bank of Demirkent landslide, is the portion of remnants of the landslide material, it can be said that Demirkent landslide moved a fairly long time ago and that the landslide material have been well compacted as time elapsed.

On the other hand, in consideration that the top of Demirkent landslide is flat and part of this landslide mass remains at a high place on the opposite bank (the elevation of about EL.550 meters), this landslide mass may have almost completed its slide, and it is presently

maintaining stable topographical and geological features. Also, the material of the landslide mass that can be seen at outcrops on the ground surface consists of well-consolidated, fine-grained materials and gravels.

The reservoir will cover the foot of Demirkent landslide with water. It is difficult to conclude how this landslide will react when it is covered with water as is the case of Havuzlu landslide. The stability of this landslide, however, as previously described, from the viewpoint of the geographical features and landslide materials, even when its foot area is covered with water, is judged to be better than the Havuzlu landslide area.
A further review is also necessary for this landslide with respect to its influence on the downstream dam and the upstream area (Yusufeli Power Plant) as in the previously described Havuzlu landslide.

(2) Dam

(a) Upstream Dam Site

i) Topography

This dam site is about 9 kilometers downstream from the Yusufeli dam site and about 3 kilometers upstream from the original dam site. It is also situated immediately downstream of the Hev valley which meets the Coruh River on the left bank. Near this area, the river forms a steep valley. At the elevation of the high water level (EL.500 m), the width of the valley is expected to be about 120 meters, and at the elevation of the present riverbed of EL.450 m, the width of the valley is about 35 to 40 meters. The average inclination of the slope at the dam axis is about 55 degrees at the left bank and about 60 degrees at the right bank respectively.
At the back of the left abutment, a fault fracture zone runs parallel with the mainstream of the Coruh River, resulting in an eroded ridge forming an saddle. The ele-

vation of the saddle is about 530 meters, and the thickness of the saddle in upstream to downstream direction at the high water level of EL.500 m, is about 60 meters.

In the meantime, the ridge at the right bank is extremely thick. However, a slope wash with its top being about EL.800 meters is widely distributed immediately downstream of the axis.

ii) Geology distributed

Basement rocks

The basement rock of the dam site is gabbro, of Yusufeli formation, and small aplite veins develop to intrude this. Although they are extremely hard, many faults, large and small and accompanied by aplite veins, are seen on the left abutment, showing a great degree of fracture as a whole. Also, the width of the fault fracture zone crossing the ridge is about 15 meters, and this fracture zone continuously runs upstream to downstream direction. This fault fractured zone is accompanied by many slickensides and quartz-calcite veinlets.

Conversely, a few faults develop in the bedrock of the right bank, which forms a massive hillside.

Alluvium

In the mainstream riverbed, alluvium, which is assumed to be made up of sand and gravel, is distributed. Although the thickness of the alluvium is not clear, judging from the general characteristics of the alluvium of the Coruh River, it is estimated to be about 50 meters.

An alluvium also lies in the riverbed of the Hev valley, which joins the left bank immediately upstream of the dam axis.

Terrace deposits

A thin narrow terrace deposit extending for about 90 meters in upstream to downstream direction lies in the left abutment of the dam site, with the elevation of approximately EL.470 meters. The terrace deposits consist of round gravel and sand.

Slope Wash

Small scale slope washes exist sporadically in the left bank of the dam site. The thicknesses of these slope washes are estimated to be less than several meters.

iii) Considerations from the viewpoint of engineering geology

Weathering

Weathering of the bedrock is generally remarkable at the left bank. Many faults having various sizes and cracks are found at the left abutment. They are generally influenced by oxidation or chloritization. The fracture zone of the main fault mentioned in ii) are loosened at the ground surface by weathering. No noticeable weathering has developed on the bedrock at the right bank.

Hardness

The fresh portions of the bedrocks are hard.
In the fault facture zone passing through the saddle part of the left bank, as previously described, weathering has developed, causing the bedrocks to become weakened.
Conversely, the bedrocks of the right bank are very hard.

Discontinuity

Analyses of the directionality of the discontinuities of bedrock have been performed by means of Schmidt net dividing the objectives into joint and fault. The same analyzing technique as that applied to the analyses of the discontinuity of the Yusufeli dam site bedrock is used. In these analyses, those having a fractured zone of more than one centimeter are treated as faults, and

those with a fractured zone of less than one centimeter are treated as joints for convenience.

(Fault)

The most conspicuous fault is the one that passes through the saddle part of the left bank. This fault runs in the strike of N20° - 40°E, and its dip of 63° - 70° NW. It runs almost parallel to the mainstream of the Coruh River and is dipped to the mountain-side.

The thickness of the fractured zone that goes together with this fault is about 15 meters, and as previously described, a marked weathering has developed on this fractured zone.

Besides this fault, there are many large and small faults in the left bank area that have affected the geographical features, thereby forming a marked uneven eroded geographical features.

As shown in the Schmidt net in Fig. AP.3-1, faults sporadically exist in each quadrant, and no specific directionality of faults is observed.

(Joint)

The distribution frequency by direction of joints is shown in the Schmidt net in Fig. AP.3-2. As in the case of the faults, joints do not also concentrate into a specific quadrant.

Also, in Fig. AP.3-3, a Schmidt net combining the above faults and joints is shown.

This also shows that the combination of joints and faults similarly scatters over the quadrants.

Water Permeability

No data for permeability of this area is available because no drillhole has been performed there. Consequently, it is presently impossible to describe the quantitative permeability of bedrock.

Qualitative observations indicate, however, that the per-

meability of the left bank area is generally large and that of the right bank is small if the weathering and cracks of bedrock that can affect the permeability of bedrock are taken into account.

Should the upstream dam site be adopted, the permeability of bedrock needs to be investigated in detail before the detailed design stage, regardless of the kind of dam to be employed.

(b) Downstream Dam Site

i) Topography

This dam site is situated about 19 kilometers downstream from the Yusufeli dam site and about 10 kilometers downstream from the Artvin upstream dam site. The river exhibits an extremely steep V shaped ravine in the vicinity of the dam site, and its width is about 150 meters at the high water level of EL.500 meters, the width of the ravine in the riverbed at about EL.380 meters of 25 to 30 meters. The inclination with respect to the hillside slope at the dam axis is 65 degrees at the left bank and 75 degrees at the right bank.

Relatively little uneveness is seen on the hillside slope of the left bank, which displays a smooth ground surface. Conversely, the right abutment forms a spur having the saddle at the east side, thereby pushing out to the mainstream of the Coruh River. The saddle that appears at a glance to be a thin saddle has a width of more than 100 meters in upstream to downstream direction at the high water level of EL.500 meters. Immediately upstream of the dam axis, a slide area is seen. This is a rockslide with the top of EL. about 630 meters, resulting in a narrow strip of fallen rocks deposit in the area with a height of less than EL.550 meters.

ii) Geology distributed

Basement rocks

The basement rocks of the dam site consist of phyllite, basic tuff, and diabase of Yusufeli formation to form bedded structures; the strata are formed with different layers with a thickness ranging from several centimeters to several meters. The greenish basic tuff and diabase in this formation have been identified by the EIE by microscopic observations. Phyllite is the least in terms of quantity, and green rock comprising basic tuff and diabase is predominant.

The basic tuff and diabase are extremely hard and their beds are closely adhered. Foliation has developed well in the phyllite portions, and phyllite tends to come off easily along the foliation.

The bedding planes run in the direction of N25° - 40°E, which is the same direciton as the river flow upstream the dam axis, and sharply inclines in the east-west direction at angles of more than 80 degrees. Thus the geological features of the downstream dam site apparently has a monoclinic structure.

Alluvium

Alluvium consisting of gravel and sand exists in the riverbed. In the riverbed area about 110 meters upstream from the dam axis, a drillhole (SID-1) was executed. Results of the drillhole revealed the thickness of alluvium to be 33.7 meters.

Slope Wash

In the right bank of the dam axis, a rock slide surface with the highest area being EL.630 meters, and slidden rock fragments extend in a narrow strip from here to the riverbed. No other noticeable slope wash is seen in this area.

iii) Considerations from the viewpoint of engineering geology (See Fig. 7-17)

Weathering

Generally, the bedrocks at the left abutment appears to be fresh, the bedrocks, however, at the right abutment seem to be somewhat weathered on the ground surface.

Hardness

The bedrocks of both abutments excepting near ground surface can be expected to be well hard. However, according to the results of unconfined compressive test by EIE, the drilled cores of SID-1 (located in the river bed) at the depth of 40.52 m - 40.78 m and 42.0 m - 42.30 m show 378.2 kgf/cm^2 and 135.1 kgf/cm^2 respectively. These values seem to be smaller than the expected one. It can be assumed as the reasons that even the cores appear very solid, the bedrocks at the river bed were affected by the fault confirmed at the depth of 65.30 m - 81.40 m of SID-1 (core descriptions are shown on the next item).

As the temporary values to estimate modulus of elasticity on the foundation rocks of both abutments, the following values are considered;

	Left abutment	Right abutment
unconfined compressive strength (kgf/cm^2) - (Assumed)	500	300
modulus of elasticity (kgf/cm^2) - (Assumed)	45,000	25,000

Discontinuity

(Fault)

Five small-scale faults with a width of fractured zone of less than 20 centimeters have been confirmed to exist on the left bank area. No detailed surface geological investigation at the right bank was carried out for lack of approach to the right abutment, however, according to

the observations from the vicinity, some faults seem to continue from the left bank to the right bank. In addition, considerably large fault shear zones are found in the river bottom and due to the shear zones, the bed rocks are somewhat cracky. The attitudes of faults are not known because of one drillhole.

The outlines of the drilled cores (SID-1) are as follows;

Depth (m)	Description
0 - 33.70	sand and gravels (alluvium)
33.70 - 36.85	somewhat cracky, cracks brown and slickensides.
36.85 - 57.00	Fair to good cores, core length 10 - 20 cm or more, no brown cracks.
57.00 - 59.50	no brown cracks, but many calcite veins, chloritization at 59.50 m.
59.50 - 61.50	1 - 3 cm gravely cores, many calcite films, shear zone.
61.50 - 65.30	As a whole sheared, many calcite veins and chlorite films.
65.30 - 81.40	shear zone, mainly gravely cores to flaky cores, clay not remarkable.
81.40 - 83.00	cracky zone, many chlorite films.
83.00 - 90.50	good cores, no brown cracks
90.50 - 92.00	cracky zone with shear zone (91.80 - 92.00)
92.00 - 95.00	somewhat cracky, but good cores
95.00 - 100.00	good cores

As mentioned before, the saddle is formed at the mountain side of the right abutment and it can be assumed that there may be a fault on this saddle site.

(Major joint)

Several major joints are seen at both abutments. Among them, one clear joint having the attitude of N30°W and 35°SW, located at the right abutment, has a long continuity and inclines to the river side, thus careful attention shall be paid for this joint.

(Bedding plane)

Generally, the strike and dip of strata are N25° to 40°E, and 85°NW to 80°SE, respectively. Consequently the bedding plane obliquely cross the dam axis (N85°W) at an angle of 45° to 60°. The bedidng planes closely adhere to one another.

(Foliation)

Generally, the strike and dip of phyllite foliation are N45° to 60°E and 60° to 75°NW, respectively. Phyllite tends to break off easily along the foliation but should phyllite develop on the bedrock mass, it will become hard.

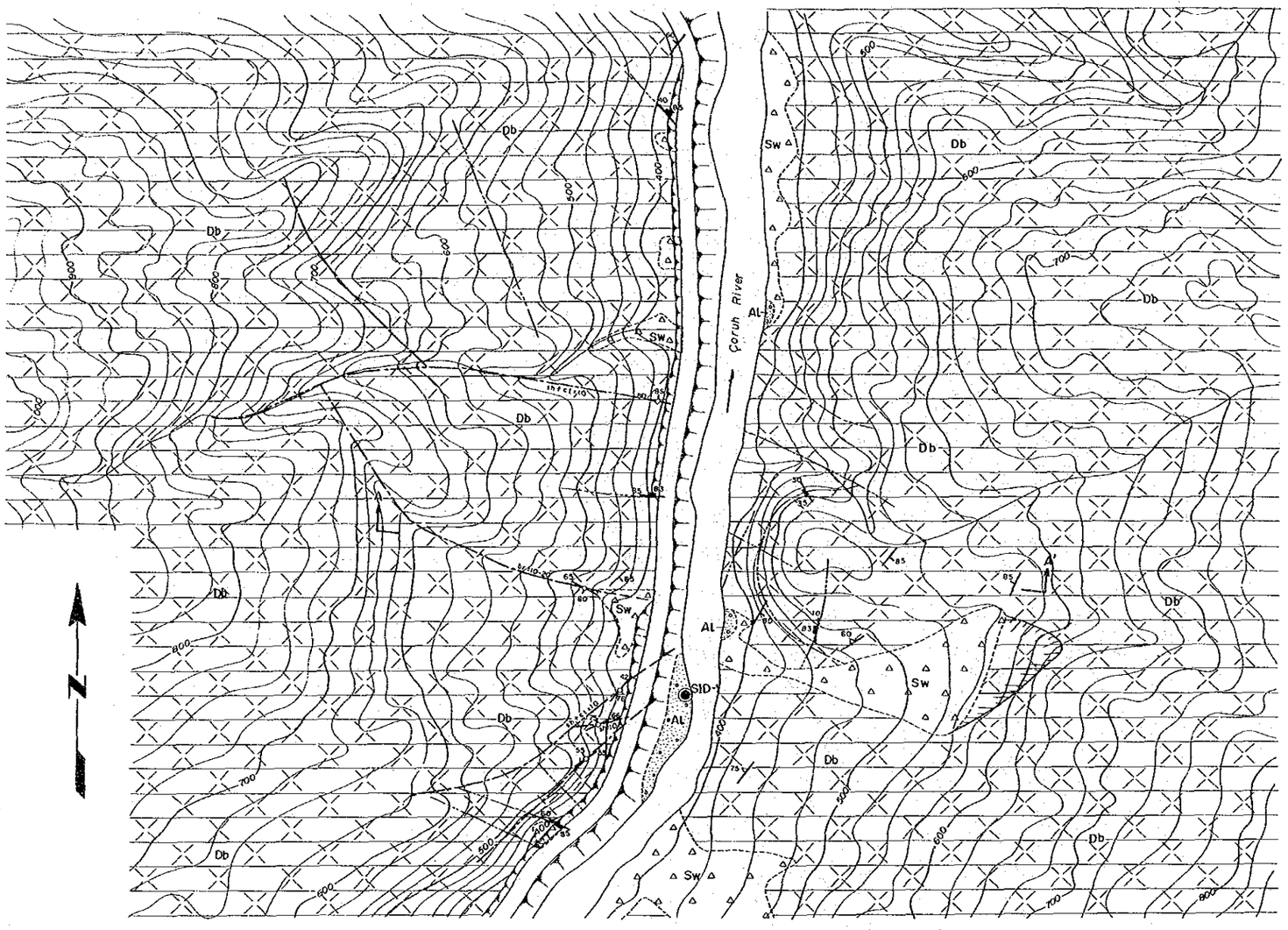

LEGEND

- Alluvium
- Slope wash
- Phyllite, basic tuff and diabase
- Geologic boundary
- Strike and dip of strata
- Strike and dip of foliation
- Fault and strike & dip
  - sh : Thickness of shear in cm
  - cl : Thickness of clay in cm
  - br : Thickness of breccia in cm
- Fault (assumed)
- Major joint and strike & dip
- Rock slide surface
- Drillhole SID-1
- Cross section A – A'

For LOG OF DRILLHOLE

Name of hole
Length
Direction
Log
Rock classification
W : Weathering
H : Hardness
C : Interval of cracks
See STANDARD OF ROCK CLASSIFICATION FOR DRILLED CORE
Lugeon value (l/m/min/10kgf/cm²)

Alluvium
Shear Zone
Diabase

0 200m

A – A'

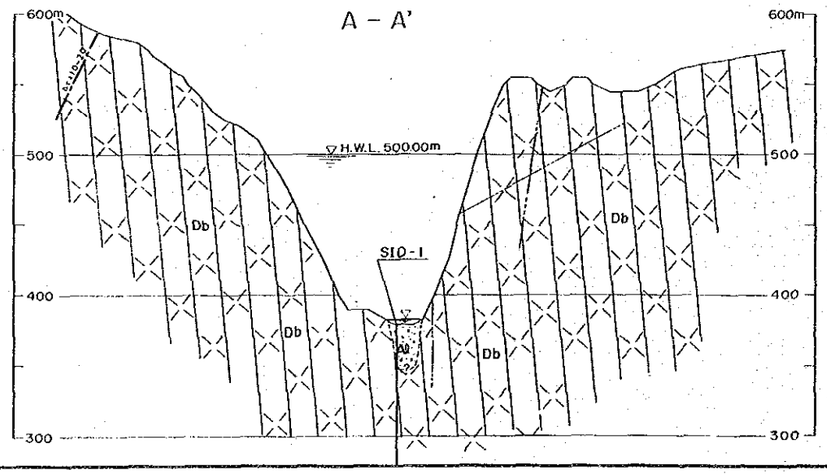

LOG OF DRILLHOLE

SID-1
L. 100m
Dir. Vertical

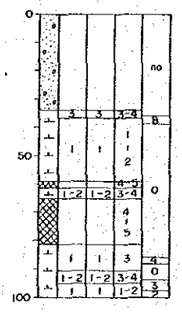

STANDARD OF ROCK CLASSIFICATION FOR DRILLED CORE

	Weathering		Hardness		Interval of Cracks
1	Very fresh. No weathering of mineral component.	1	Very hard. Broken into Knifedged pieces by strong hammer blow.	1	Over 30 cm
2	Fresh. Some minerals are weathered slightly. Usually no brown crack.	2	Hard. Broken into pieces by strong hammer blow.	2	10 - 30 cm
3	Fairly fresh. Some minerals are weathered. Cracks are stained and with weathered material.	3	Brittle. Broken into pieces by medium hammer blow.	3	3 - 10 cm
4	Weathered. Fresh portions still remain partially.	4	Very brittle. Easy broken into pieces by medium hammer blow.	4	1 - 3 cm
5	Strongly weathered. Most minerals are weathered and altered to second minerals.	5	Soft. Able to dig with hammer.	5	Under 1 cm

ÇORUH RIVER HYDROELECTRIC POWER DEVELOPMENT PROJECT

ARTVİN PROJECT
GEOLOGY
DOWNSTREAM DAM
PLAN AND SECTION

Fig. 7–17 | DECEMBER 1986

7.5 Material

7.5.1 Impervious Core Material

The total volume of core material to be used for the impervious core zone of the rockfill dam will be approximately 2.9 x 10^6 m^3. As a result of a rough investigation made by EIE and JICA Teams, the surroundings of Gorgulu Village located approximately 11 km upstream of the dam site was found to be a promising prospective site according to a comprehensive judgment of quantity, quality, borrowing operations, transportation, etc.

The basement rocks in this area are spilite (basalt) of the Yusufeli Formation, and limestone, red shale, and alternations of limestone, sandstone, marl, conglomerate, and shale of the Pugey Formation.

The site of a landslide called Gorgulu Landslide exists adjacent to Gorgulu Village. This is a landslide with the Yusufeli Formation distribution area as the top portion, which has an average inclination of 11 deg., width of approximately 750 m, and length of approximately 2 km. The total volume is estiamted to be 50 x $10^6 m^3$.

The material of the landslide is estimated to be weathered residual soil of spilite, with the main components being weathered gravels of spilite and sand, silt, and clay which are weathered products of the gravels, and are blackish. This material will be tentatively called "black soil" in this report.

There is slope wash estimated to have originated from red shale etc. of the Pugey Formation distributed from the gently-sloped mountainside of the Pugey Formation to the river terraces in a manner to surround this landslide. The amount existing is estiamted to be 1.5 x $10^6 m^3$ at just the flat area at the north side of the tip of the landslide, and it is considered that the required quantity will be amply exceeded when combined with the surroundings. The components consists of gravel, sand, silt, and clay, and a red color is presented. Similarly, this will be called "red soil" in this report.

The pits of Table 7-13 were excavated with the materials of the two kinds above as objects, the locations of which are shown in Fig.

7-18. The samples collected were tested at the laboratory of EIE. Further, as a result of surface reconnaissance by the EIE and JICA teams, it was feared that the swelling clay mineral montmorillonite might exist in the material, and therefore, a part of the testing and analyses was done additionally in Japan by the JICA Team.

Table 7-13 List of Pit for Soil Material

Subject	Name of pit	Remarks
Black soil	M-8	Performed by EiE before 1985
	M-9	"
	M-10	"
	AM-11	Performed by EiE in 1985, Additional
	AM-12	"
(Subtotal)	5 pits	
Red soil	AM-13	Performed by EiE in 1985, Additional
Grand total	6 pits	

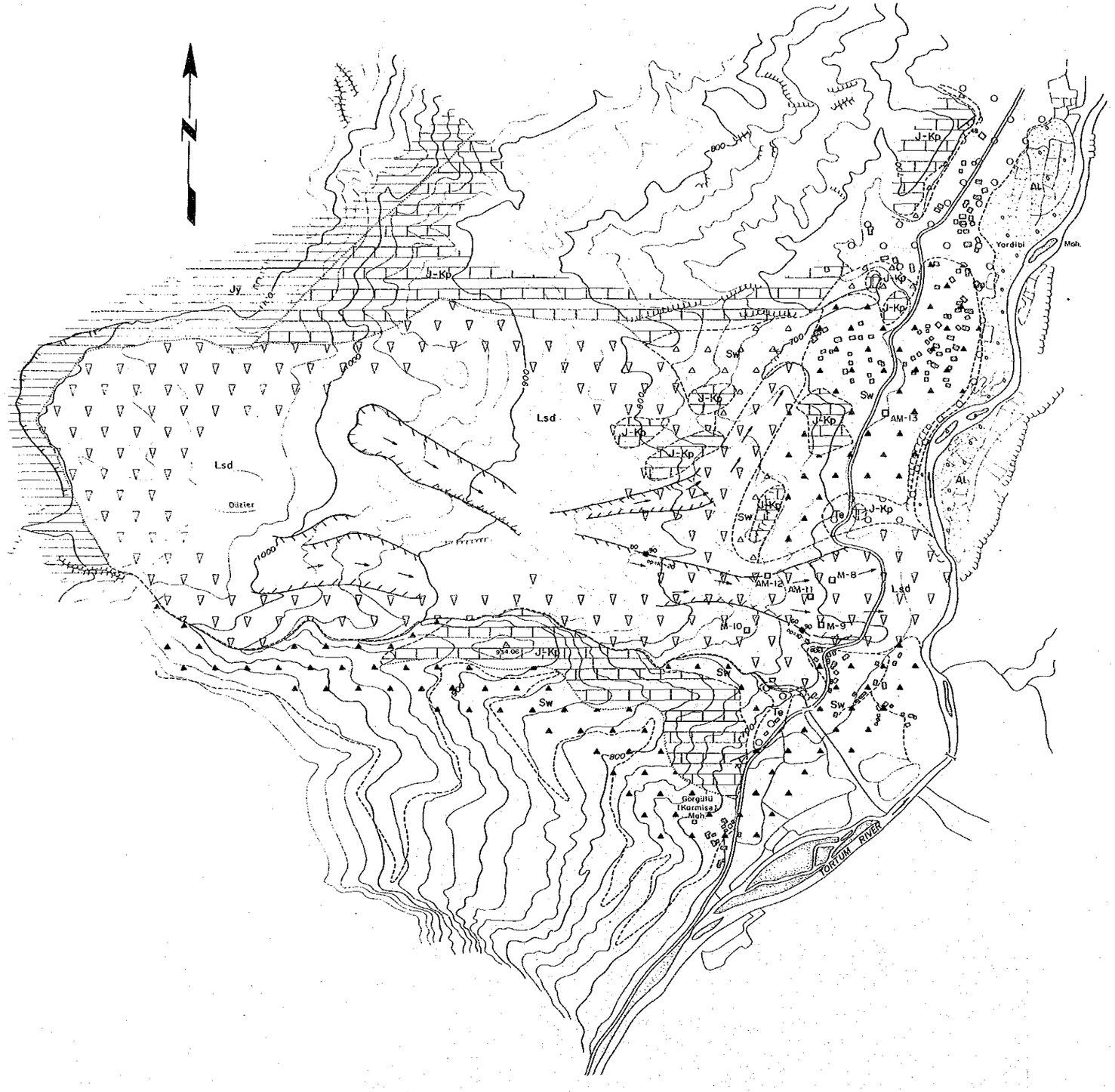

LEGEND

- Alt — Alluvium
- Sw — Slope wash
- Sw — Slope wash (red soil)
- Te — Terrace deposits
- Lsd — Landslide material (black soil)
- J-Kp — Püger Formation — Limestone, red shale, alternation of limestone, sandstone, marl, conglomerate and shale
- Jy — Yusufeli Formation — Spilite (or Basalt)
- Geologic boundary
- Geologic boundary (assumed)
- 30/48 — Strike and dip of strata
- 80/50 op:0-15 — Strike and dip of open crack; op: width of open crack in cm
- Top of landslide
- Secondary landslide
- M-8 — Test pit

0 — 500m

ÇORUH RIVER HYDROELECTRIC POWER DEVELOPMENT PROJECT

YUSUFELİ PROJECT

MATERIAL

BORROW AREA PLAN

Fig. 7–18 | DECEMBER 1986

(1) Laboratory Test Items and Quantities

The items of the laboratory tests and quantities are given in Table 7-14. The black soil of the samples for the items beginning with the swelling test in the table was collected by the JICA Team at the time of the surface reconnaissance, while the red soil was obtained by the JICA Team from EIE.

(2) Test Results

The test results of the impervious core material are given in Tables 7-15, 7-16, 7-17, and 7-18.

Summaries of the test results are given below for black soil and red soil, respectively.

(a) Black Soil

- Specific gravities were 2.54 to 2.80, while natural water contents were 9.2 to 12.0 percent.
- With regard to the Unified Soil Classification (ASTM D 2487), the material was found to be clayey sand (SC) or silty sand (SM) according to gradation tests and Atterberg's limits.
- Optimum water contents obtained in compaction tests were from 12.2 to 19.0 percent, while maximum dry densities were from 1.68 to 2.00 t/m^3. Coefficients of permeability at optimum water contents were from 1.2×10^{-7} to 2.4×10^{-6} cm/sec. The differences between natural water contents and optimum water contents were 3 to 5.5 percent, with the natural water contents lower.
- The cohesion and angle of internal friction according to direct shear tests (consolidated-undrained) were 0.09 to 0.48 kgf/cm^2 and 20.59 to 27.06 deg., respectively.
- Concerning grain-size distributions, the maximum grain size is 50 mm, while the quantitites of 19.1 mm and under are 86 to 99 percent, 4.75 mm and under 66 to 89

percnet, 0.075 mm and under 22 to 40 percent, and 0.005 and under 9 to 20 percent.
A comparatively wide distribution range is indicated.

. According to the results of X-ray analyses, plagioclases (anorthite, anorthite sodian, albite) are the main components, while there are small quantities of montmorillonite and quartz, and minute quantities of chlorite (see Table 7-17). According to microscope observations made at the same time, the volumetric percentage of montmorillonite was 15 to 17 percent.

(b) Red Soil

. Specific gravities were 2.66 to 2.70, while the natural water content was 11.4 percent.

. Optimum water contents obtained in compaction tests were 13.6 to 15.2 percent, while maximum dry densities were from 1.81 to 1.88 t/m^3.
Coefficients of permeability at optimum water contents were from 1.8×10^{-7} to 1.7×10^{-6} cm/sec.
The differences between natural water contents and optimum water contents were 4.2 to 7.7 percent, with the natural water contents lower.

. With regard to the Unified Soil Classification (ASTM D 2487), the material was found to be clayey sand (SC) according to gradation tests and Atterberg's limits.

. The cohesion and angle of internal friction according to direct shear tests (consolidated-undrained) were 0.26 to 0.58 kgf/cm^2 and 15.55 to 29.02 deg., respectively.

. Concerning grain-size distribution, the maximum grain size is 42 mm, while the quantities of 19.1 mm and under are 91 to 97 percent, 4.75 mm and under 76 to 79 percent, 0.075 mm and under 30 to 38 percent, and 0.005 mm and under 17 to 23 percent.
A comparatively wide distribution range is indicated.

- According to the results of swelling tests (see Table 7-16), swelling of the red soil is 0.67 percent, at 3 percentage points on the dry side of the optimum water content, and a minute 0.05 percent at the optimum water content.

- According to pinhole tests, the red soil is non-dispersable*.

- According to X-ray analyses, calcite, quartz, and plagioclases (anorthite, albite) are the main components with minute amounts of hematite, montmorillonite, and kaolinite also contained. According to microscope observations made at the same time, the volumetric percentage of montmorillonite is approximately 5 percent (see Table 7-17).

Note) * Non-dispersable soil

A dispersable soil is a soil that spontaneously assumes a dispersed or suspended condition due to existence of water and becomes the cause of chemical piping in an embankment.

(c) Evaluation

To evaluate the above test results, both the black soil and red soil belong to clayey sand (SC) to silty sand (SM) according to the Unified Classification Method, and are materials of good grain-size distribution containing 22 to 40 percent fines (0.075 mm and under). Coefficients of permeability are 2.4×10^{-6} to 1.2×10^{-7} cm/sec, and the soils possess ample imperviousness. However, both contain montmorillonite, a swelling clay mineral, the contents of which are 15 to 17 percent for black soil and approximately 5 percent for red soil. Generally speaking, when the fact that montmorillonite is contained is considered, there would be concern about deformation and collapse of the impervious soil core due to swelling, and erosion of the core due to dispersion.

Swelling of the red soil is extremely slight, and it is thought that the swelling can be adequately suppressed with the load applied on top in case of use as core material. As for dispersion faculty, it is known from the results of pinhole tests that the red soil is non-dispersable. Consequently, it may be evaluated as being usable as impervious core material. However, since test quantities are small with regard to the content of mont-morillonite, the swelling property, and the dispersion faculty, it is desirable for detailed investigations and testing to be carried out at the time of definite design and construction.

On the other hand, the black soil contains a fairly large amount of montmorillonite, and since there is concern with regard to swelling and dispersion faculty, it is thought necessary for thorough care to be exercised regarding these points even more than in connection with red soil in case the black soil is to be contemplated as impervious core material in the future.

Quantity-wise, it will be possible for more than the requirements for the impervious core material to be borrowed in both the cases of black soil and red soil.

Table 7-14 Items and quantities of test

Items	Quantities		Remarks
	Black soil	Red soil	
Specific gravity	9	3	
Water content	2	1	
Atterberg limit	9	3	
Grain size analysis	9	3	
Compaction	9	3	
Permeability	9	3	
Direct shear	5	3	
Swelling test*	—	1	
Pinhole test*	—	1	
X-ray analysis*	1	1	include microscopic observation
Chemical analysis*	1	1	

Note 1: * marked items were tested by JICA team in Japan.

Note 2: Pinhole test

A method of test for judging the dispersion faculty of soil developed by J.L. Sherard. A hole of 1-mm diameter is made in a cylindrical specimen of 36-mm diameter and 38-mm length (grain size 2-mm and under, water content adjusted to neighborhood of plastic limit), in which distilled water is made to penetrate under various heads, and the dispersion faculty of the soil is judged by the erosion condition of the hole, flow quantity, and drainage water color.

Table 7-15 Results of Tests (Soil Materials)

	Name of Pit	Sample No.	Depth of Sample (m)	Soil Classification (Unified System)	Specific Gravity	Water content (%)	Atterberg Limit			Grain Size Analysis						Compaction		Coefficient of Permeability (cm/sec)	Direct Shear (CU)			
							LL (%)	PL (%)	PI	Max. Grain Size (mm)	mm -63.5 (%)	mm -19.1 (%)	mm -4.75 (%)	mm -0.075 (%)	mm -0.005 (%)	Opt. Water Content (%)	Max. Dry Density (t/m^3)		Water content (%) (before test)	Wet Unit Weight (t/m^3)	C (kgf/cm^2)	ϕ (deg.)
Black Soil	M-8	—	—	SC	2.68	—	31.3	22.3	9.0	20	100	99	75	22	9	16.3	1.88	1.8×10^{-6}	—	—	—	—
	M-9	—	—	SC	2.57	—	36.5	21.5	15.0	22	100	97	71	30	19	16.3	1.77	2.4×10^{-6}	—	—	—	—
	M-10	—	—	SC	2.54	—	37.8	21.9	15.9	30	100	98	89	40	20	19.0	1.68	1.2×10^{-7}	—	—	—	—
	AM-11	I	0.2~1.2	SM	2.66	12.0	38.0	25.6	12.4	22	100	98	80	36	20	15.8	1.84	2.3×10^{-7}	—	—	—	—
	"	II	1.2~2.2	SM	2.64	12.0	37.5	26.0	11.5	25	100	95	76	32	18	15.6	1.83	2.2×10^{-6}	17.3	2.03	0.34	27.06
	"	III	2.2~3.5	SC	2.67	12.0	39.6	24.4	15.2	30	100	93	74	30	16	15.6	1.84	1.2×10^{-7}	19.3	2.03	0.20	20.59
	AM-12	I	0.2~1.2	SC	2.77	9.2	32.0	20.0	12.0	32	100	92	73	30	15	14.0	1.93	1.7×10^{-7}	17.6	2.20	0.09	24.86
	"	II	1.2~2.2	SC	2.80	9.2	26.0	18.4	7.6	22	100	98	69	24	13	14.7	1.87	1.3×10^{-7}	16.8	2.17	0.29	23.35
	"	III	2.2~3.5	SC-SM	2.76	9.2	24.2	17.9	6.3	50	100	86	66	24	12	12.2	2.00	2.4×10^{-7}	14.4	2.23	0.48	21.29
		(Average)			(2.68)	(10.6)	(33.7)	(22.0)	(11.7)	(28)	(100)	(95)	(75)	(30)	(16)	(15.5)	(1.85)	(8.2×10^{-7})	(17.1)	(2.13)	(0.28)	(23.43)
Red Soil	AM-13	I	0.3~1.3	SC	2.66	11.4	34.3	20.0	14.3	25	100	97	79	35	20	14.0	1.85	2.3×10^{-7}	15.6	2.09	0.26	29.02
	"	II	1.3~2.3	SC	2.70	11.4	34.3	19.9	14.4	25	100	96	76	30	17	13.6	1.88	1.7×10^{-6}	17.0	2.06	0.58	20.67
	"	III	2.3~3.5	SC	2.64	11.4	36.2	20.4	15.5	42	100	91	77	38	23	15.2	1.81	1.8×10^{-7}	19.1	2.04	0.34	15.55
		(Average)			(2.67)	(11.4)	(34.9)	(20.1)	(14.7)	(31)	(100)	(95)	(77)	(34)	(20)	(14.3)	(1.85)	(7.0×10^{-7})	(17.2)	(2.06)	(0.39)	(21.75)

Table 7-16 Results of Swelling Test

Specimen No.	Initial condition		Elapsed time (hour)	Swelling percentages (%)	Remarks
	Water content (%)	Dry density (g/cm^3)			
No. 1	12.2	1.76	168	0.67	
No.2	15.2	1.81	162	0.05	Optimum water content = 15.2%
No. 3	16.7	1.78	167	0.07	
No. 4	12.2	1.81	168	1.86	

Note: Initial conditions of the water content and the dry density were based on the test results of AM-13III shown on Table 7-15.

Table 7-17 Results of X-ray Analysis

Mineral	Black Soil	Red Soil
Quartz	C	A
Calcite	A	AA
Anorthite Sodian	AA	—
Anorthite	AA	C
Albite	—	C
Hematite	—	E
Montmorillonite	C *	E **
Chlorite	E	—
Kaolinite	—	E

Note: * Swelling ratio of montmorillonite was 12.3%.

** Swelling ratio of montmorillonite was 9.3%.

AA	Very strong	$\geqq$ 1000 cps (counts per second)
A	Strong	600 ~ 1000 cps
B	Medium	400 ~ 600 cps
C	Weak	200 ~ 400 cps
D	Very weak	100 ~ 200 cps
E	Trace	$<$ 100 cps

Table 7-18 Results of Chemical Analysis

(wt %)

Component	Black Soil	Red Soil
H_2O^+	4.3	2.4
Ignition loss *	4.7	20.8
SiO_2	48.1	35.4
Al_2O_3	14.4	8.9
Fe_2O_3	9.2	4.3
CaO	5.2	22.9
Na_2O	3.1	0.7
K_2O	1.7	1.3
MgO	4.4	0.9
MnO	0.22	0.08
Total	95.32	97.68

Note: * Ignition loss includes H_2O^-, Carbonate, organism etc.

7.5.2 Concrete Aggregate

River bed deposits in the Yusufeli dam site are about 50 m thick. However, the topography in and around the dam site is very steep and the river bed is narrow (approximately 50 m in the dam site), to make collection of concrete aggregates in large quantities very difficult. Nearest alternative places are found at around the confluence of the Oltu River and the Tortum River, 6 - 8 km upstream of the dam site, and at around the confluence of the Coruh River and the Barhal River, 9 - 10 km upstream of the same. In this field investigation, the former (the confluence of the Oltu River and the Tortum River) was selected as the suitable gravel deposits for concrete aggregate.

In this area, the Oltu River is 200 m or more wide, largely made up of sandbars. The river bed deposits of 3 test pits (G-1, 2 and 3) were tested at laboratory by the EIE. Judging from rock types in and upstream area, the gravals in the area appear to be made up of the following types of rock:

Limestone, calcareous rocks (marl etc.), sedimentary rocks such as sandstone, conglomerate and shale, basic igneous rocks such as spilite, basalt and gabbro, acidic-intermediate volcanic rocks such as rhyolite, rhyolitic tuff, dacite, and andesite. Among the aboves, acidic - intermediate volcanic rocks such as rhyolite contain glass components, so that alkali aggregate reaction was included in the aggregate test. Furthermore, pyroclastic rocks in Tertiary are widely found in the upstream of the Oltu River, and thus it is highly possible that tuffaceous materials are contained in fine materials. Thus, it is necessary to pay attensions to the grain size distribuiton of fine materials. In any case, the proposed gravel area is quite large and a sufficient amount of aggregate is available so far as its quality and gradation are suitable for concrete required for the dam.

In addition to the tests on natural aggregate, the EIE is conducting the test on crushed aggregates to be obtained from quarries.

The quarries will be around the dam site, probably Ikizdere granitic rocks. They are made up of very hard granite, granodiorite, granophyre and diabase. Except for fractured part of diabase etc., these rocks are very hard and suitable for crushed aggregates. Samples for the aggregate test were collected from adit LA-2 of the dam site. Test items for natural aggregate and crushed aggregate are shown in Table 7-4.

The comments on concrete aggregate test are as follows;

Alkali-aggregates reaction test

Test results of the chemical test ASTM C 289 are indicated on a diagram of Fig. 7-19.

Sample No.	Location	Classification
Y-1	Adit LA-2	Diabase
Y-2	"	Microgranite
G-1	Oltu river	River deposit
G-2	"	"
G-3	"	"

It can be judged that every test specimen is innocuous for the alkali aggregates reaction.

Grading, Specific gravity, Absorption, etc.

Test results and the standards of both fine and coarse aggregates are shown on Table 7-19. And the grading curves are indicated on Fig. 7-20.

Fine aggregates of G-3 should not be used because it is abundant in silt and also its grain-size distribution is not good. As to G-1 and G-2, if they are used for the concrete being subjected to erosion, they should be washed by water to decrease the quantities of silt up to less than 3%. Though, there is no problem besides the above-mentioned points.

Every specimen is available on coarse aggregates. However, in case that they are used as ASTM size number 467 (37.5 - 4.75 mm), they

should be sorted using a grizzly because the quantities over 37.5 mm are too large.

7.5.3 Rockfill Material

A quarry site for rockfill materials is proposed near the Yusufeli damsite. Quantities and qualities of the rocks near the damsite seem to be suitable judging from the data of adits and drillholes at the damsite. However, tests for this material shall be done according to the items listed on Chapter 14.

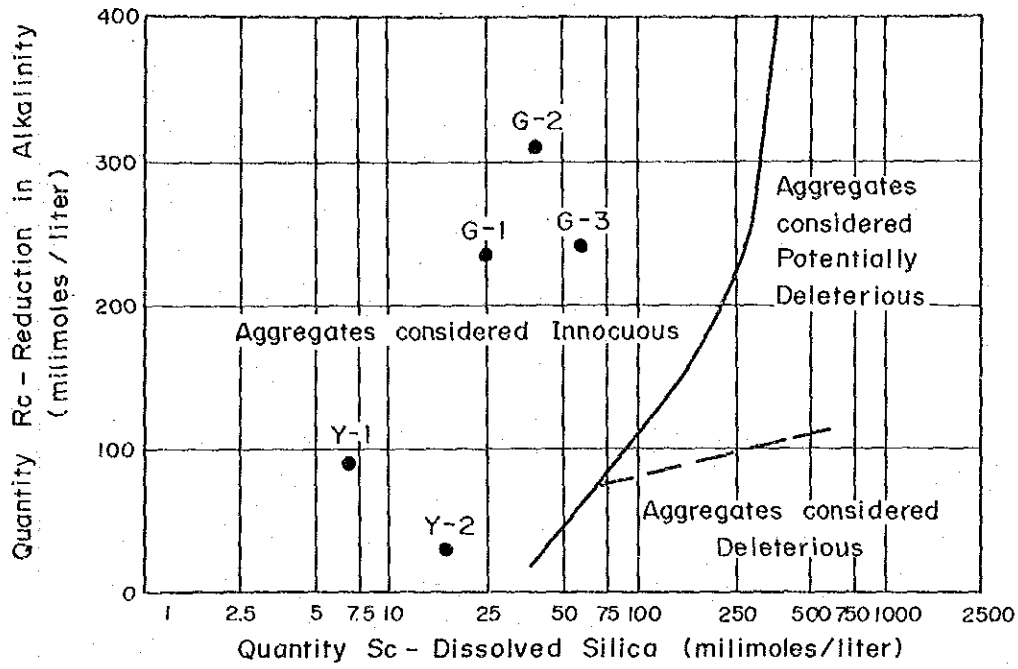

Fig. 7-19 Results of Alkali – Aggregate Reactivity Tests

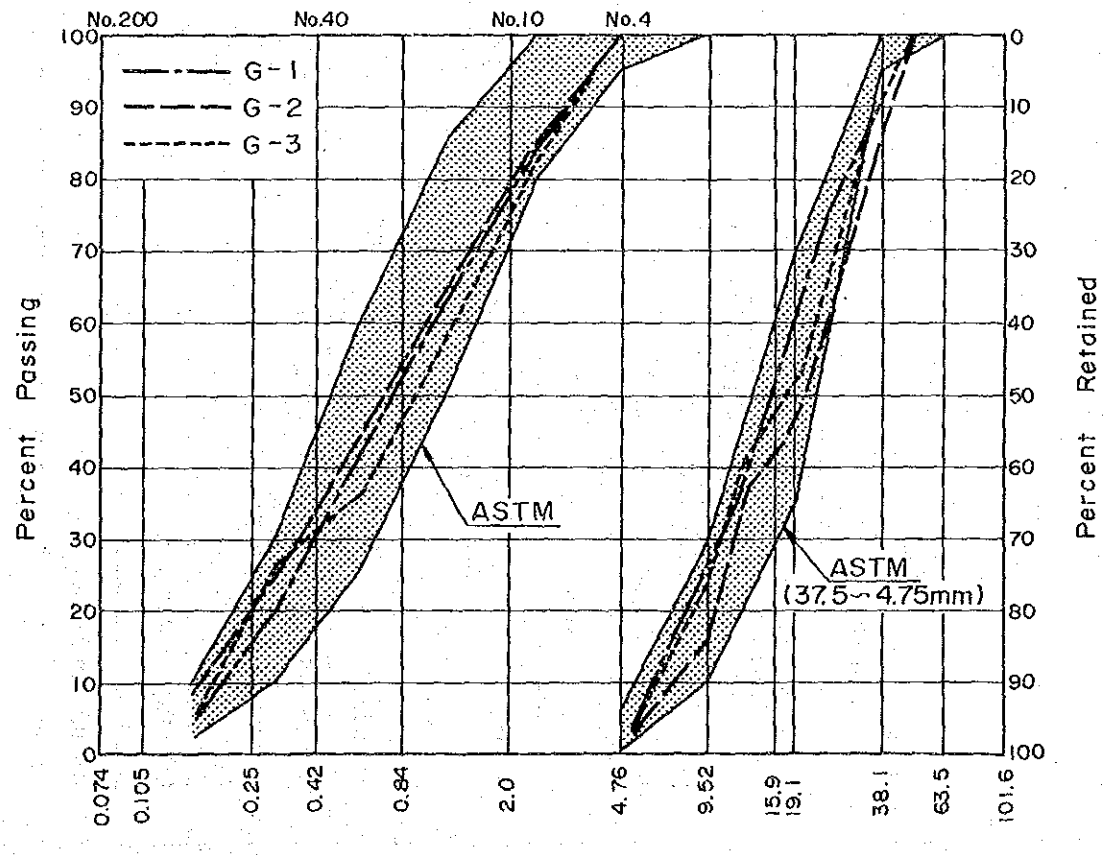

Fig. 7-20 Gradation analysis curve .

Table 7–19 Test Results and ASTM Standard (Concrete Aggregate)

		Fine Aggregate				Coarse Aggregate			
		G–1	G–2	G–3	ASTM C33	G–1	G–2	G–3	ASTM C33
Grading		See Fig. 7–20				See Fig. 7–20			
Fineness modulus		2.84	2.74	3.03	2.3～3.1	—	—	—	—
Bulk specific gravity	Dry	2.590	5.583	2.578		2.606	2.612	2.655	—
	Surface dry	2.643	2.645	2.628	—	2.645	2.650	2.696	—
	Apparent	2.736	2.753	2.715	—	2.712	2.832	2.768	—
Absorption (%)		2.06	2.39	1.96	—	1.51	1.49	1.53	—
Abrasion		—	—	—	—	16.3	18.2	17.0	less than 50%
Soundness		5.56	2.33	3.9	less than 10%	5.92	2.97	6.69	less than 18%
Unit weight (loose) (t/m^3)		1.640	1.707	1.520	—	1.776	1.780	1.739	—
Clay lumps		No	No	No	less than 3%	No	No	No	less than 2%
Quantity of soft particle (%)		5.6	3.8	35.6	less than 5% 1)	—	—	—	less than 1%
Organic impurities		0 – 0	0 – 0	0 – 1	2)	—	—	—	—

Note : 1) In case of concrete being subjected to erosion: less than 3%.

2) Color must be lighter than that of a standard.

7.6 In-situ Rock Test

7.6.1 General

In-situ tests were conducted on the foundation rock of the Yusufeli damsite. Test items include plate bearing tests and block shear tests as well as compressive strength tests at laboratory for concrete specimens which are incidental to the block shear tests.

(1) The plate bearing tests were conducted by the EIE engineers after the conference with the JICA Team for the test method.

(2) The block shear tests were conducted by the EIE and JICA Cooperation Team using test equipments which the JICA Team brought to the site. Some of the tests were continuously conducted by the EIE engineers even after the JICA Team left the site. The compressive strength tests for concrete specimens were conducted at the EIE Laboratory.

7.6.2 Test Period and Site Selection

The in-situ tests were conducted at the adits of the Yusufeli damsite from July to September, 1985. Four sections were selected as the test location and the details are indicated in Table 7-20. The number of the tests conducted at each section are as follows:

(a) the plate bearing tests were conducted twice at each section, totalled 8 times at 4 sections,

(b) the block shear tests were conducted with 3 blocks as a series, totalled 12 blocks, and

(c) 3 specimens for each section, totalled 12 specimens, were selected for the concrete compressive test.

The test sections were decided as follows.

At the outset, a geological site reconnaissance for the adits was carried out to grasp the rough outline of characteristics of the foundation rock of the damsite. Next, the rock classification for three elements, weathering, hardness and discontinuities was conducted.

Based on these results, a temporary rock evaluation was made to select test sections representing various rock characteristics.

For this evaluation we took into account that a uniformity in geologic conditions should spread to suit a test space, and sectional conditions and others of the adits should be suitable to the setting of test equipments and materials. Geologic conditions of each test section are as follows.

(1) RA-1 (TD 41 - 47m)

The base rock in this section is extremely fresh, hard and poor in crack. From the lower portion of side walls to the invert, granite is exposing, and diabase is spread in the upper portion with extremely compacted igneous contact between the two rocks. Ground water is coming out from the invert and side walls. All tests were conducted on the granite. The rock evaluation in this section is A1.
(Refer to (2)-(c)-vi) of 7.4.1 for the rock evaluation)

(2) LA-2 (TD 27 - 35m)

Granodiorite is spread in this section. Rocks are fresh and hard, but have lots of cracks which are weathered to brown color. The rock evaluation in this section is B.

(3) LA-3 (II) (TD 29 - 39m)

Diabase is in the invert, and granodiorite is in the upper portion of the adit, which are extremely hard but somewhat cracky. Some cracks are weathered to brown color, but are sufficiently compacted. The rock evaluation in this section is A2.

(4) LA-3 (II) (TD 72 - 80m)

This section is a shear zone with diabase as an original rock, which have lots of cracks. Cracks are filled with quartz-calcite veinlets. These rocks are brittle to impulse given by hammer and are broken into small pieces. The fault portions are clayey and soft. The rock evaluation in this section is B.

Table 7-20 Details of Test Location

Adit No.	Test Secton (m)	Rock Classification	Rock Evaluation	Plate Bearing Test			Block Shear Test			Remarks
				Test No.	Location (m)	Test Date	Test No.	Location (m)	Test Date	
RA – 1	41 ~ 47	1AII–III	(A1)	B–1	41.6	Sept. 12, '85	S–1	43.1	Sept. 28, '85	Granite
				B–2	46.0	Sept. 14, '85	S–2	44.55	Sept. 27, '85	
							S–3	46.95	Sept. 26, '85	
LA – 2	27 ~ 35	3AIV–V	(B)	B–3 *	29.0	July 29, '85	S–4 *	28.5	Aug. 19, '85	Granodiorite
				B–4 *	34.2	July 24, '85	S–5 *	30.4	Aug. 17, '85	
							S–6 *	33.4	Aug. 15, '85	
LA–3(II)	29 ~ 39	1–2AIII–IV	(A2)	B–5 *	29.55	Aug. 12, '85	S–7	31.8	Sept. 19, '85	Diabase
				B–6 *	32.6	Aug. 13, '85	S–8	34.6	Sept. 17, '85	
							S–9 *	37.25	Sept. 5, '85	
LA–3(II)	72 ~ 80	2C–DV	(B)	B–7 *	72.2	Aug. 16, '85	S–10	73.9	Sept. 23, '85	Shear zone of diabase
				B–8 *	77.1	Aug. 18, '85	S–11	76.15	Sept. 20, '85	
							S–12	77.8	Sept. 21, '85	
Total				8 Tests			12 Tests			

Note: * marked tests were executed by EiE–JICA Cooperation Team.
Others were done by EiE.

7.6.3 Test Method

(1) Plate Bearing Test

The plate bearing test is conducted to judge the deformation characteristics of the base rock. Through this test we obtained the modulus of deformation, the secant modulus of elasticity, the tangential modulus of elasticity and the creep characteristics.

The number of the tests is 2 spots at each section. We examined the deformation characteristics by mounting a loading plate, which is rigid enough and has 35.5 cm in diameter, in the vertical direction by means of a 200 ton jack. The loading pattern is indicated in Fig. 7-21. The maximum stress is 65 kgf/cm^2, and the creep time is set up at 6 hours.

(2) Block Shear Test

The block shear test is conducted to obtain the shear strength of the base rock. The number of the tests is 3 blocks at each section. After chipping the rock surface for shear plane of 3,600 cm^2 area for each block, we placed concrete in the test blocks. After solidification of the concrete, we mounted 2, 5 and 8 kgf/cm^2 vertical stresses on each test block by means of a 50 ton jack, and, thereafter, cut each block by three 100 ton jacks which were installed diagonally.

We obtained an shear strength from vertical stress and horizontal stress at the time of shear. In addition, in order to obtain a compressive strength of each test block, we prepared a sample concrete and kept it in the site for solidification, then conducted compression tests on cylindrical samples of concrete, at the corresponding time to the in-situ tests.

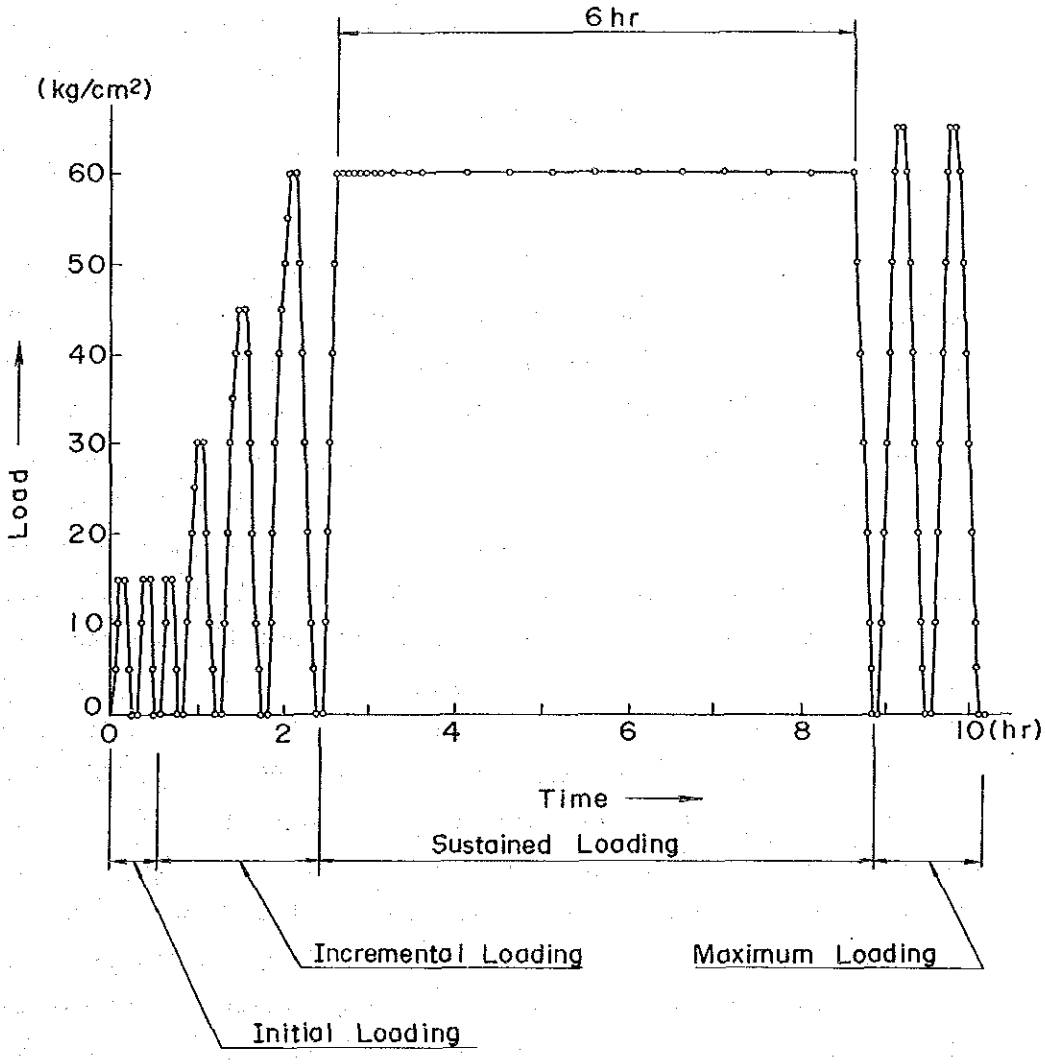

Fig. 7-21 Loading Diagram

7.6.4 Test Result and Evaluation

(1) Bearing Power of the Base Rock

It was confirmed that both A and B group base rocks have enough bearing capacity, at least more than 65 kg/cm^2. The relationships between load and deformation show linear statuses, and no yield characteristics were obtained. The above test results indicate that these rocks are hard enough.

(2) Plate Bearing Test

The plate bearing test results are indicated in Table 7-21, showing the deformation characteristics of the base rock. The modulus of deformation was obtained at the incremental loading section, and the secant and tangential moduli of elasticity as the average figure of the maximum loading two cycles. Note that the tangential modulus of elasticity was calculated at a section with the stress level of 20 - 65 kg/cm^2, an almost a linear status. Judging from the elastic and plastic deformation ratios, the plastic deformation showed roughly 33% for the A group base rock and roughly 43% for the B group. These figures indicate that the base rock are hard enough not to be influenced by cracks. The deformation modulus showed 68,100 - 142,000 kg/cm^2 for the A group base rock, and 29,400 - 78,200 kg/cm^2 for the B group, which indicates that the base rocks are hard and of little deformation characteristics. The tangential modulus of elasticity showed 91,100 - 206,400 kg/cm^2 for the A group base rock and 47,900 - 103,700 kg/cm^2 for the B group, which also indicates that these base rocks are hard and favorable.

Since the creep deformation is extremely low, the creep factor (Cf) indicated a wide range of 2 - 34%.

Convergences of creep curves showed slow tendencies for 2 hours, which are equivalent to 50% of the total 6 hour creep deformations, but it implies that there was little consolidation process in cracks etc.

(3) Block Shear Test

The results of the block shear tests are shown on Table 7-22. According to the observations of the shear planes after the tests, all of the test blocks were not sheared in the bed rocks and the observation results are as follows:

- Regarding test blocks S-1, 2 and 3 in adit RA-1, they were mainly sheared at the contact planes between concrete blocks and bed rocks and they were partly sheared in concrete.

- Regarding test blocks S-4, 5, 6 in adit LA-2 and test blocks S-7, 8, 9, 10, 11, 12 in adit LA-3, they were mainly sheared in concrete and partly sheared at the contact planes between concrete blocks and bed rocks.

The causes for the abovementioned results are considered as follows:

- The compressive strength of concrete block was expected to be 300 kg/cm^2 or more, however, most of strengths were less than 300 kg/cm^2.

- Accordingly, due to the lack of concrete strength, the concrete blocks were sheared in concrete or at the contact planes between concrete blocks and bed rocks before reach to 300 ton of possible max. shear load. Besides, phenomena which concrete aggregates were sheared are not found on the contact planes between concrete block and bed rock. This fact indicate that the cause for the lack of concrete strength is due to the quality of the cement.

In conclusion, as the shear strengths of the bed rocks could not be obtained directly, the shear strength of the bed rocks at Yusufeli damsite are assumed by the correlations between modulus of elasticity and shear strength which were collected at granitic rocks sites in Japan as shown in Fig. 7-22.

Fig. 7-23 shows the assumed shear strength of the bed rocks at Yusufeli site and the values of A and B groups are rather high.

Judging from Table 7-23, it is concluded that the foundation rocks at Yusufeli site are quite sound.

Table 7-21 Results of Plate Bearing Test

Adit	Measuring Number	Rock Evaluation	Maximum Deformation (mm)	Final Deformation (mm)	Modulus of Deformation (kg/cm^2)	Secant Modulus of Elasticity (kg/cm^2)	Tangential Modulus of Elasticity * (kg/cm^2)	Creep Deformation (mm)	Creep Factor (%)	Remarks
RA-1	B-1	(A1)	0.165	0.049	114,300	156,000	146,100	0.020	20	
	B-2	(A1)	0.326	0.107	68,100	79,500	91,100	0.031	15	
LA-2	B-3	(B)	0.353	0.069	61,000	62,700	76,500	0.007	2	
	B-4	(B)	0.722	0.303	29,400	41,600	47,900	0.013	3	
LA-3(II)	B-5	(A2)	0.123	0.040	142,000	210,900	206,400	0.016	20	
	B-6	(A2)	0.226	0.070	86,900	113,400	140,200	0.003	2	
LA-3(II)	B-7	(B)	0.270	0.102	78,200	106,500	103,700	0.054	34	
	B-8	(B)	0.441	0.207	42,900	72,800	93,900	0.018	8	

* Stress level
(20~65 kg/cm^2)

Table 7–22 Results of Block Shear Test

Adit	Block No.	Location (m)	Vertical Stress (kg/cm^2)	Compressive Strength of Concrete Block (kg/cm^2)	Vertical Stress of Shear plane (kg/cm^2)	Shear Stress (kg/cm^2)	Condition of Shear Plane
RA–1	S – 1	43.10	8	392	23.6	52.1	Sheared mainly at the contacts between the concrete blocks and the rock. Sheared partially inside the blocks.
	S – 2	44.55	5	358	22.0	56.7	
	S – 3	46.95	2	—	14.0	40.1	
LA–2	S – 4	28.50	2	162	17.6	51.9	Sheared mainly inside the concrete blocks. Sheared partially at the contacts between the blocks and the rock.
	S – 5	30.40	8	170	22.6	48.6	
	S – 6	33.40	5	179	18.8	46.1	
LA–3 (II)	S – 7	31.80	2	170	10.0	26.8	Ditto
	S – 8	34.60	5	179	20.9	52.9	
	S – 9	37.25	8	179	22.9	49.8	
LA–3 (II)	S – 10	73.90	2	179	12.3	34.3	Ditto
	S – 11	76.15	5	204	22.4	57.9	
	S – 12	77.80	8	204	24.8	56.0	

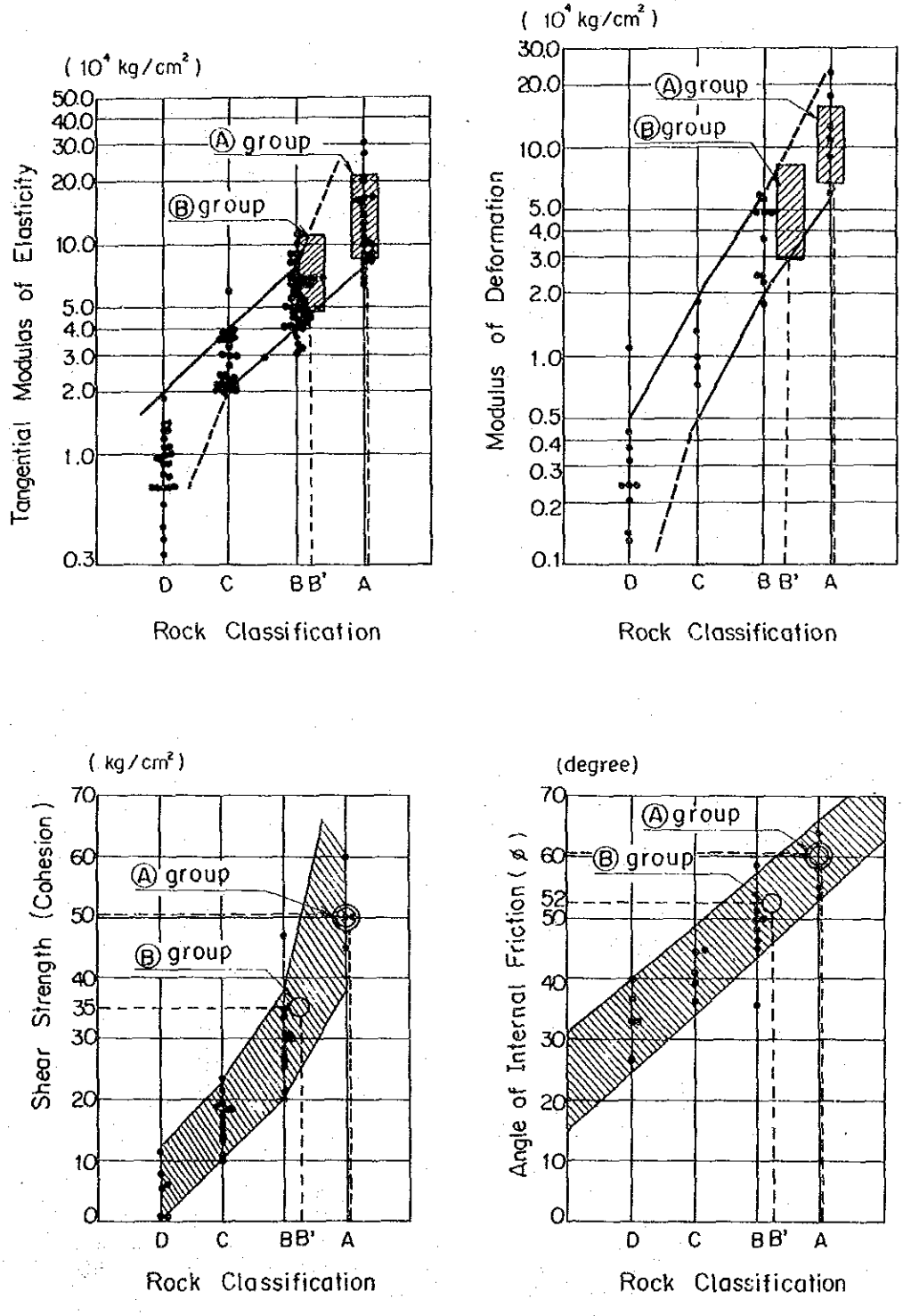

Fig. 7–22 Relation between Rock Classification and Deformation or Shear Strength

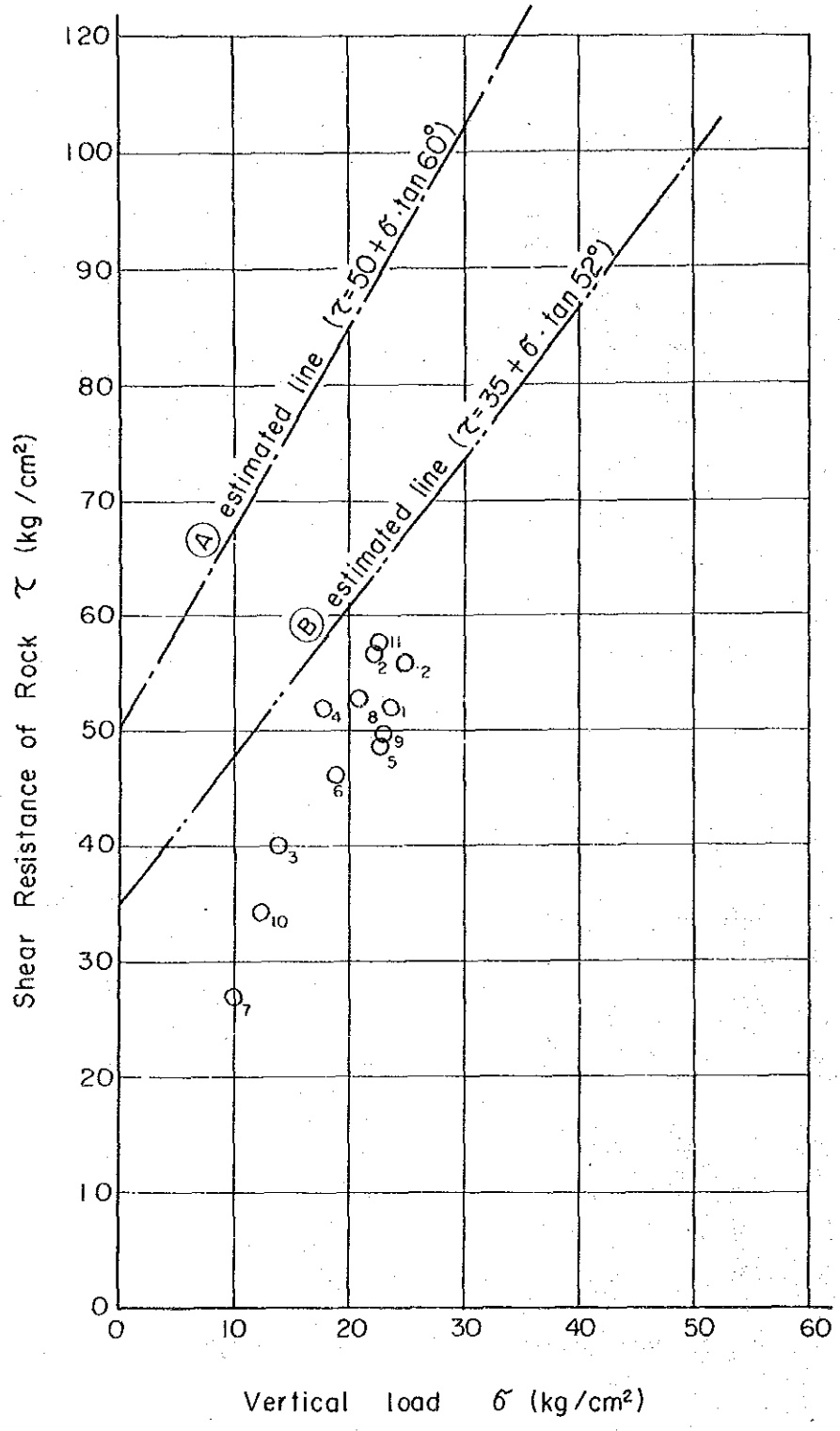

Fig. 7–23 Results of Shear Test and Presumed Share Strength

Table 7–23 Results of In-situ Rock Test

Rock Evaluation (Adit No.)	Test No.	Characteristic Deformation				Shear Strength		Remarks
		$\frac{\Sigma\,\delta\rho}{\Sigma\,\delta}$ (%)	Modulus of Deformation (kg/cm²)	Tangential Mod. of Elasticity (kg/cm²)	Ceep Deformation (mm)	Angle of Internal friction (degree ϕ)	Cohesion (kg/cm²)	
Ⓐ	B – 1 – 2 B – 5 – 6 S – 1	30 〜 33	68,000 〜 142,000	91,000 〜 206,000	0.003 〜 0.031	(Estimated Value)	(Estimated Value)	
(RA – 1 LA – 3)	– 2 – 3 S – 7 – 8 – 9	(32 ± 2)	(103,000 ±32,000)	(146,000 ±47,000)	(0.018 ±0.012)	60°	50	
Ⓑ	B – 3 – 4 B – 7 – 8 S – 4	20 〜 47	29,000 〜 78,000	47,000 〜 103,000	0.007 〜 0.054	(Estimated Value)	(Estimated Value)	
(LA – 2 LA – 3)	– 5 – 6 S – 10 – 11 – 12	(37 ± 12)	(53,000 ±21,000)	(80,000 ±24,000)	(0.023 ±0.021)	52°	35	

$\Sigma\delta\rho$; Final Deformation $\Sigma\delta$; Maximum Deformation

7.7 Conclusion of Engineering Geology

This is the conclusion of the engineering geology based on the field investigations (2 times) made by the JICA Team, and other data provided by EIE in regard to the Yusufeli and Artvin projects.

7.7.1 Yusufeli Project

(1) Reservoir

- Judgment can be made that there will be no problem with respect to the watertightness of the Yusufeli reservoir.
- Although two large-scale landslides of Gorgulu and Vecanket exist in the upstream area of the Yusufeli reservoir, it can be judged that their existence will not impede the construction of the Yusufeli dam. The influence they may have on the upstream area if they are reactivated after the reservoir is filled with water, however, needs to be investigated in the future.
- Besides the two landslides mentioned above, investigations are also necessary in regard to the possibility of the occurrence of new landslides. Even if such a possibility is recognized to exist, it will not impede the construction of the Yusufeli dam because all of new potential landslides will be limited to those areas further upstream from the two landslide areas mentioned above.
- However, to avoid the risks of new landslides, it can be said that the lower water level of the reservoir is better and has less influence on new landslides, especially in the area of Berta formation.

(2) Dam

- Although normal foundation treatments are necessary for the bedrock at the Yusufeli dam site, this bedrock can be evaluated as one of the best foundation rocks available for the foundation of the rock-fill dam with a height of about 270 meters.

. In spite of the scarcity of the past investigation works with respect to the areas suitable for the arch dam layout, the following judgments can be made as to the foundation of an arch dam with a height of about 270 meters, based on the existing investigation data.

* The strength of the bedrock in this dam site can be sufficiently suitable for the construction of a concrete arch dam with a height of about 270 meters.

* Well-developed joints and cracks being subjected to oxidation can be seen in the bedrock of the left bank of the dam site. Observations reveal that this has a noticeable effect on the permeability but no conspicuous effect on the bearing capacity. The deformation modulus of class A bedrock of the dam site is 68,000 - 142,000 kg/cm^2, and that of class B bedrock is 29,000 - 78,000 kg/cm^2.
  This means that although the development of joints and cracks accompanied by oxidation exist in the bedrock, they closely adhere to one another, and no weathered materials, such as seam, exist between joints and/or cracks. Therefore, such discontinuities can be improved through foundation treatment such as grouting.

* The total number of faults confirmed at the adits of the damsite (two adits in the left bank and two in the right bank amounting to a total of 403.80m) is 152, of which the number of shear zones with a thickness of more than 10 cm is 56 and those with a thickness of less than 10 cm is 96. Although some of these shear zones intercalate soft clay, they accompany breccia in general and are sufficiently consolidated in the adits located at the elevation higher than groundwater level (e.g. LA-3). They, however, are softened in the adit below groundwater level (e.g. LA-2). In-situ tests of these faults below groundwater level have not yet been performed.

* Should the faults (those with a thickness of more than 10 cm) confirmed at the above adits be extended in both

horizontal and vertical cross-sections, some places where the faults are concentrated at the deeper parts of the foundation can be found. Considering the conditions of shear zones below groundwater level or the conditions when the reservoir water will infiltrate into shear zones, the investigation for the places where the faults are concentrated, in-situ test for shear strength of soft fracture zones and the investigation of continuity of important faults must be performed in future.

* In-situ rock tests were carried out at TD 70 m of the adit LA-3 (II) where faults are concentrated and the results are as follows:

Secant modulus of elasticity	73,000 - 107,000 kg/cm^2
Modulus of deformation	43,000 - 78,000 kg/cm^2

The above values, however, were tested on the shear zone located above groundwater level, accordingly the values are more or less big.

* Comprehensive evaluation as the foundation of arch dam is that the bedrocks in the Yusufeli damsite bear to construct arch dam, more investigation, however, will be required.

. When any attempt is made to evaluate the dam site from the viewpoint of foundation treatment, consideration should be given to the permeability regardless of the type of dam to be employed. When the geological characteristics of both banks in the dam site are compared each other, the left bank abutment is especially complicated in regard to the permeability. This means that the permeability is influenced by many faults existing in the left bank abutment. As previously described, the greater part of cracks are recognized to have been affected by oxidation, but materials such as seam do not exist between cracks. From this fact, the site can be judged to have an good groutability.

(3) Appurtenant Structures

In the case of the rock-fill dam, the spillway is planned to be built on the left bank. It is judged that there is no problem with respect to the bedrock from the viewpoints of strength and slope stability.

In both cases, the rock-fill dam and the arch dam, the powerhouse is expected to be built on the right bank.

Judging from the results of the drillhole RSI-16, it is considered that there will be no problem with respect to the bedrock for an underground powerhouse. However, the drilled cores near the end of the hole are somewhat cracky because of the influence of the valley near by. This information shall be considered for the layout of the powerhouse.

The foundation rocks of penstock and tailrace tunnel seem to be generally good.

7.7.2 Material

(1) Impervious Core Material

- In conclusion, both Black soil and Red soil belong to clayey sand (SC) and/or silty sand (SM) in accordance with the Unified Soil Classification.
- They have good grain size distribution with 22-40% of fine particles (less than 0.075 mm).
- Their coefficient of permeability is 2.4×10^{-6} to 1.2×10^{-7} cm/sec, and the values are suitable for impervious core materials.
- The volumes of both materials are enough for the requirement.
- Black soil contains 15-17% of montmorillonite, accordingly, careful attention shall be paid for swelling and dispersion faculties.
- Swelling ratio of red soil is very small according to the test by one sample and it is judged that red soils are available for

impervious core materials. More detail tests, however, shall be executed during the definite study.

(2) Concrete Aggregate

. Every test specimen at the proposed sites is innocuous for the alkali aggregates reaction.

. Fine aggregates of G-3 contain abundant silt and its grain-size distribution is not good. Moreover, fine aggregates of G-1 and G-2 shall be washed by water to decrease the quantities of silt up to less than 3%.

. Every specimen is available as coarse aggregates. However, in case that they are used as ASTM size number 467 (37.5 - 4.75 mm), they shall be sorted using a grizzly because the quantities over 37.5 mm are too large.

(3) Rock Material

A quarry site for rock materials is proposed near the Yusufeli damsite. Quantities and qualities of the rocks near the damsite seem to be suitable judging from the data of adits and drillhole at the damsite.

7.7.3 In-situ Rock Test

It is confirmed by the results of the in-situ rock tests that the foundation rocks (both of A and B classes) at Yusufeli damsite have sufficient bearing strength more than 65 kg/cm^2.

7.7.4 Artvin Project

(1) Reservoir

There will be no problem in connection with the permeability of both reservoirs under the upstream and downstream dam sites.

- In the reservoir of the upstream dam site, neither existing landslide areas nor areas having a possibility of landslide are seen. From the viewpoint of slope stability, the reservoir of the upstream dam site is superior to that of the downstream one.

- In the reservoir of the downstream dam site, two large-scale landslides of Havuzlu and Demirkent exist.
  The existence of the landslides, however, is judged to be immaterial to the construction of the downstream dam site. Provided, however, that the influence they may have on the upstream area if they are activated after the filling of reservoir water needs to be investigated in the future.

- In the reservoir area of the downstream dam site, no geographical features capable of causing new large-scale landslides can be found.

- There is a possibility that the relatively thick slope washes in several places of the reservoir area of the downstream dam site can collapse after the filling of reservoir water.
  Their scales are, however, extremely small compared with the landslides, and they may have practically no effect on the downstream dam and the upstream area.

(2) Upstream Dam and Its Appurtenant Structures

- The bedrocks in the left bank of the upstream dam site are complicated because of the existence of faults and dyke rocks. On the contrary, the right bank is stable in spite of a existence of a fault in part. Therefore, the bedrock of the dam site is suitable for a rock-fill dam, but it has problems with respect to a concrete arch dam.

- The upstream plan includes a pressure tunnel of which route consists of gabbro, phyllite, and green rocks comprising of basic tuff and diabase etc. The section consisting of gabbro and green rocks has excellent bedrocks with a support work factor of several percentages. Due attention, however, should be given to the tunnelling of the section consisting of phyllite.

Especially, the sections passing Havuzlu landslide area and the Esenkaya valley are covered with thickness about 100 meters at the former and about 50 meters at the latter. The distribution rates of each kind of rock over the total length of the tunnel are as follows:

Gabbro section	10%
Phyllite section	40%
Green rock section	50%

. It is expected that a great deal of water will not flow out during the tunnelling work in the gabbro and green-rock sections.
In the section of phyllite, however, there is a great possibility of water flow out.

. The power plant site is situated in the green rock distribution section. This rock is sufficiently hard for use as the foundation of the penstock and the power plant.

(3) Downstream Dam and Its Appurtenant Structures

. For the downstream dam site, surface geological investigations and one drillhole have been performed. The thickness of gravel in the riverbed is confirmed to be 33.7 m.

. In this dam site, thin phyllite layers sporadically exist in part, but the greater part of the bedrock consists of the previously described green rock (gabbro and basic tuff). This rock is hard and is suitable for the foundation of a concrete arch gravity dam.

. The discontinuities that can be seen in this dam site consist of the bedding plane of green rock, the foliation of phyllite, several faults and major joints.

. The drillhole of SID-1 (at the river bottom) revealed large shear zone at the depth from 65.30 m to 81.40 m. The attitude of the shear zone is not clear so far. In addition, a major joint having long continuity and 35° inclination to the river

side is found at the right abutment, the details, however, are also not clear yet.

As mentioned above, some open questions still remain at this damsite.

CHAPTER 8 SEISMICITY

CHAPTER 8. SEISMICITY

CONTENTS

List of Figures

List of Tables

CHAPTER 8. SEISMICITY

8.1 Tectonics of Eastern Turkey

8.1.1 Geological Outline of Eastern Turkey

Eastern Turkey has been subjected to repeated orogenic movements from the begining of the Paleozoic Era and presents a complex geological structure, but basically it can be divided into four east-west oriented tectonic zones. Namely, they are in order from the north, the Pontids, Anatolids, Taurids, and Border Folds. Cretaceous to Paleogene rhyolitic-basaltic volcanic rocks are predominant in the Pontids while there is partial distribution of Jurassic to Cretaceous ophiolite. At the Anatolids, strongly deformed Eocene to Miocene marine clastic rocks and Quaternary volcanic rocks are distributed on the basement rocks of Jurassic to Cretaceous ophiolite and slightly metamorphosed rock. Continental deposits of Pliocene to Quaternary are distributed at mountainland basins. The basement of the Taurids consists mainly of Precambrian to Mesozoic strata and ophiolite, while Eocambrian to Pliocene neritic sedimentary rocks are predominant in the Border Folds.

8.1.2 Neotectonics of Eastern Turkey

(1) North Anatolian Fault and East Anatolian Fault

The eastern region of the Anatolian Peninsula is divided by two transform faults named North Anatolian Fault and East Anatolian Fault which make up plate boundaries. Particularly, these two transform faults prominently divide the previously-mentioned old tectonic zones. The former makes up the boundary between the Eurasian Plate (Black Sea Plate) and Anatolian Plate (Turkey Plate), and the latter the boundary between the Anatolian Plate and the Arabian Plate.

The North Anatolian Fault extends east-west presenting a gentle arc bulging northward at the northern part of Turkey and its total length is in excess of approximately 1,000 km. At least

at present it shows a right-handed horizontal displacement, the total horizontal displacement having been said to be 70 to 80 km in the past, but recently, there have been opinions expressed that it should be 20 to 30 km, and this point requires further study. The occurrence of the North Anatolian Fault is said to have been 10 to 12 million years ago, but the direction of displacement has not always been consistently right-handed horizontal and it appears there was a time in the middle of Pliocene Epoch when a left-handed horizontal displacement was indicated. Many active faults, earthquake-associated faults and mountainland basins are distributed along this fault, while there have been also volcanic activities, and it may be seen that this is a first-class structure of the Quaternary Period.

The East Anatolian Fault divides the Taurids, and on land it has a length of approximately 560 km with a strike of N60°E - S60°W. It shows a thrust-fault nature at the southwestern part, but a left-handed lateral displacement is prominent on the whole. It is covered by Quaternary volcanic rocks and the displacement topography is not necessarily distinct, while the degree of activity is slightly less compared with the North Anatolian Fault, but this is also a paramount structure of this region. The fault intersects the North Anatolian Fault east of Karliova to comprise a triple junction. As a consequence, the Anatolian Plate sandwiched by the two faults would apparently shift westward.

As described in the foregoing, the neotectonics of eastern Turkey is made complex reflecting the mutual movements between the plates in the field of tectonic stress from north-south compression caused by the northward-drifting Arabian Plate since the late Miocene Epoch.

(2) Active Faults in Eastern Turkey

The active fault groups listed below have developed in the tectonic stress field of eastern Turkey.

(a) Reverse or thrust fault group with east-west orientation

(b) Left-handed horizontal displacement fault group with NNE-SSW to NE-SW orientation

(c) Right-handed horizontal displacement fault group with NW-SE orientation

(d) Tension joint or normal fault group of north-south orientation

Particularly, the active fault groups of (a) and (b) are prominently developed and the former is connected with the occurrences of mountainland basins such as the Erzincan and Erzurum Basins.

Most of the active faults in this region indicate distinct cumulative displacement topographies as seismicity is strong as described in the following section, and earthquake faults are caused.

(3) Earthquake Faults of Eastern Turkey

Earthquakes in Turkey may be broadly divided into (a) shallow earthquakes corresponding with right-handed displacement activity of the North Anatolian Fault (for example, Erzincan Earthquake, 1939), (b) shallow earthquakes corresponding with left-handed displacement activity of the East Anatolian Fault (for example, Bingol Earthquake, 1971), (c) slightly deep-focus earthquake group related to the normal fault group of the east-west oriented graben zone of the Aegean Sea and its shoreline, and (d) shallow earthquake groups inside the respective plates other than the above earthquakes (for example, Caldiran Earthquake, 1976, and Horasan-Narman Earthquake, 1983).

Particularly, the earthquake which occurred at Erzincan in 1939 at the eastern part of the North Anatolian Fault registered M 7.9, the strongest of this century in Turkey. Since then, earthquakes belonging to the category of (a) have occurred every several to ten and several years, and it is a well-known

fact that the hypocenters of these earthquakes have shifted westward in remarkably orderly manner.

Within the limits of the investigations made, earthquake faults produced as results of these earthquakes belonging to (a) do not strictly coincide in cases, but approximately, they are produced by repeated cycles of motion of the active faults running roughly parallel in the vicinity of the North Anatolian Fault. In view of the cumulative vertical displacement of the active faults and the vertical displacements of the individual earthquake faults the return period is of the order of several hundred to several thousand years (< 5,000 yr).

The earthquake faults are in a number of multiple echelon arrangements composed of segments made of echelon fissures, the smallest of which are ten and several centimeters. Small-scale echelon arrangements with segment lengths of less than several hundred meters are arrayed in correspondence with the lateral displacement of related transform faults. On the other hand, large-scale echelon arrangements of segment lengths ten and several kilometers do not necessarily correspond with related transform faults. This is because they are affected by geological anisotropies near the ground surface such as existing fissures and volcanic rock mass.

According to the relationship of earthquake faults formed and earthquakes in this century in Turkey, in case of magnitude not less than 6.5 and depth of hypocenter shallower than 40 km, it can be expected that earthquake faults will be formed. Further, as already pointed out by a number of researchers, a relationship of $\log L\ (D) = aM - b$ is valid approxiamtely between total length (L) and displacement (D) of a fault and magnitude (M).

On comparison of earthquake faults of Japan and Turkey at equal magnitudes, those of Turkey are longer, while those of Japan have larger maximum displacements. For example, in the cases of the Erzincan Earthquake in Turkey and the Nohbi Earthquake in Japan with the same magnitudes of M7.9, the length of the

earthquake fault was approximately 300 km and maximum displacement was approximately 4.2 m for the former, whereas the length was approximately 80 km and maximum displacement approximately 8 m or more for the latter.

As for the Horasan-Narman Earthquake Faults produced comparatively recently (October 30, 1983) in eastern Turkey, they appear to have occurred where a topographically distinct active fault did not previously exist. These earthquake faults are in the northeast-southwest direction and comprise a sheared zone correlative to left-handed lateral displacement consisting of a group of many fractures of poor continuities of a length of 12 km and a width 4 km. The fracture group consists of left-handed lateral displacement faults of predominant strikes of N15° - 30°E, right-handed lateral faults of slightly poorly developed conjugate sets, and tension fissures of north-south orientation. Similarly to the neotectonics of this region, north-south compression can be imagined from these fractures, and it may be said there is good correspondence between the two.

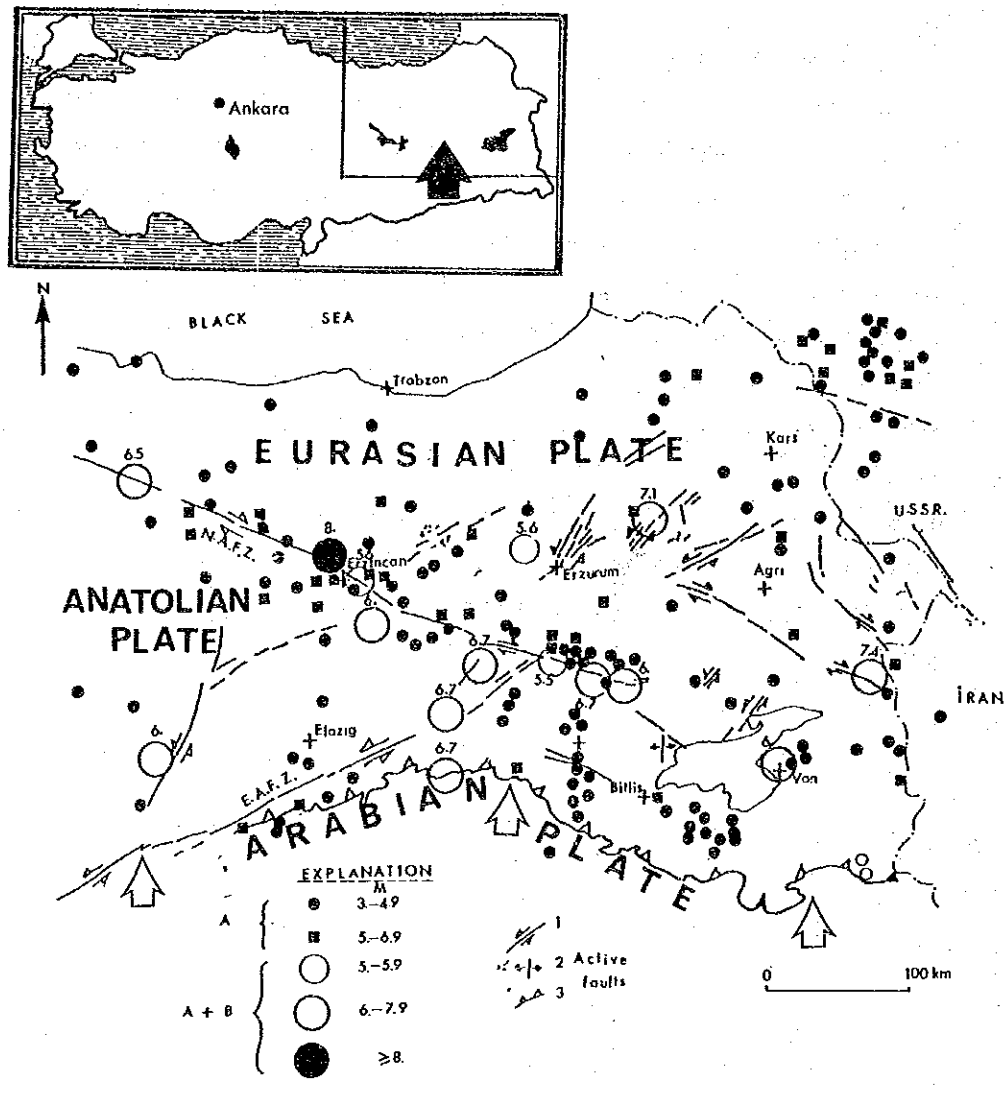

A. Epicenter based on measurement data
A+B. Epicenter based on measurement data and macroseismic data
1. Lateral fault 2. Tension fracture fissure and normal fault
3. Reverse fault and thrust (active fault)
NAFZ. North Anatolian Fault Zone
EAFZ. East Anatolian Fault Zone

Fig. 8-1 Seismotectonics of Eastern Turkey

8.2 Design Seismic Coefficient

The estimation of the maximum ground acceleration at Yusufeli site by probability analysis was performed to determine the design seismic coefficient. The seismicity data used in this study are those compiled by NOAA (National Oceanic and Atmospheric Administration Environmental Data Service) and are 1658 in number during the period 1901-1984. Of previously proposed attenuation models which express peak ground acceleration A (gal), in terms of earthquake magnitude M, and hypocentral distance R (km), or epicentral distance D (km), five models shown below are used in this study.

$$\text{Log } A = 3.090 + 0.347\ M - 2\ \text{Log } (R+25) \qquad (1)$$

proposed by C. Oliveira

$$\text{Log } A = 2.674 + 0.278\ M - 1.301\ \text{Log } (R+25) \qquad (2)$$

proposed by R.K. McGire

$$\text{Log } A = 2.041 + 0.347\ M - 1.6\ \text{Log } D \qquad (3)$$

proposed by L. Esteva and E. Rosenblueth

$$\text{Log } A = 2.308 + 0.411\ M - 1.637\ \text{Log } (R+30) \qquad (4)$$

proposed by T. Katayama

$$\text{Log}(A/640) = (D+40)(-7.6+1.724\ M-0.1036\ M^2)/100 \qquad (5)$$

proposed by S. Okamoto

A probabilistic model based on the "Theory of Extreme Values" can be established by taking an equal time interval of one year. Although a probability function of the maximum ground acceleration expected at a certain particular dam site is not known, it is reasonable to suppose that the function should be associated with the third-type asymptotic distribution.

The results thus obtained as well as the seismicity data distribution are shown in the Fig. 8-2 and the Tables 8-1 to 8-3.

Taking into consideration general dam behaviour on top of the above results, 0.15 and 0.30 are to be adopted as the design seismic coefficients used in the conventional pseudo-static stability analysis for a rockfill dam and an arch dam respectively at Yusufeli site.

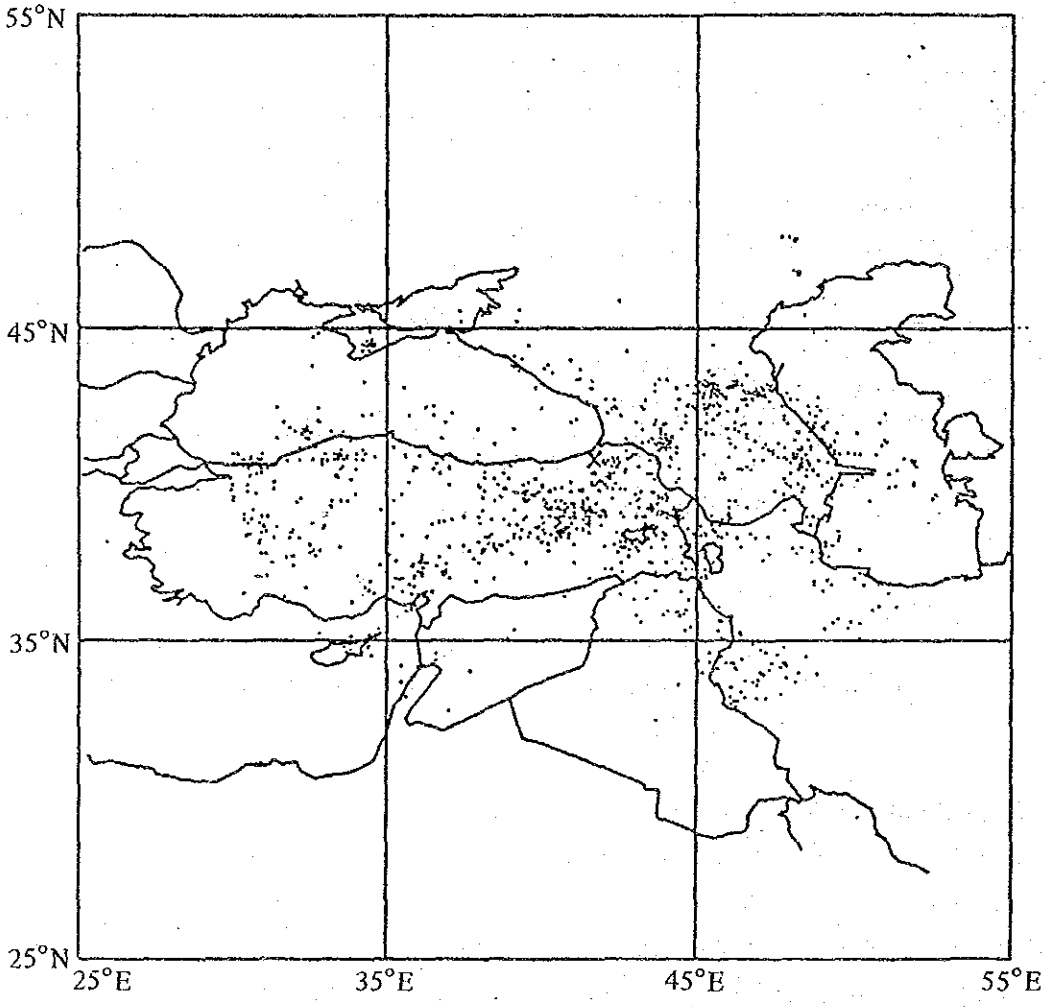

Fig. 8-2 Seismicity of All Data in 1901-1984
Total Number of Plots in the area of $\Delta \leqq 1000.0$ (km) is 1658.

Table 8-1 Distribution of Magnitude and Epicentral Distance of the Seismicity Data

	0 ≦Δ< 50	<100	<200	<300	<400	<500	<600	<700	<800	≦1000	Total
3.0≦M<3.5	0	0	0	1	0	1	1	0	3	3	9
<4.0	0	1	0	4	3	5	4	3	2	6	28
<4.5	3	7	7	38	26	33	27	14	32	60	247
<5.0	4	11	36	83	57	60	62	40	35	79	467
<5.5	3	3	33	55	47	60	37	48	22	57	365
<6.0	0	7	41	68	49	63	38	54	32	51	403
<6.5	1	5	11	19	11	11	11	9	19	15	112
<7.0	0	1	3	0	2	2	0	1	4	4	17
<7.5	0	0	0	0	1	2	0	2	2	1	8
<8.0	0	0	0	1	1	0	0	0	0	0	2
Total	11	35	131	269	197	237	180	171	151	276	1658

Δ : Epicentral Distance (km)
M : Magnitude

Table 8–2 Maximum Accelerations during a Year from 1901 to 1984

year	Oliveira,C Eq.(1)	McGuire,R.K. Eq.(2)	Esteva,L.& Rosenblueth,E. Eq.(3)	Katayama,T Eq.(4)	Okamoto,S. Eq.(5)
1901	0.5	5.9	0.6	1.8	0.0
1902	1.4	11.5	1.4	4.0	0.2
1903	10.3	43.8	9.1	22.5	34.7
1904	4.0	22.2	3.6	9.1	5.0
1905	6.9	31.7	6.1	14.0	15.6
1906	28.1	85.8	26.2	52.1	116.4
1907	2.3	16.0	2.2	6.2	1.3
1908	5.8	28.3	5.1	12.2	11.2
1909	1.8	14.6	1.9	6.2	0.9
1910	1.5	11.8	1.5	4.1	0.3
1911	0.3	4.8	0.4	1.5	0.0
1912	2.2	15.6	2.1	6.2	1.2
1913	3.1	19.9	2.9	8.5	3.4
1914	0.6	6.5	0.7	2.1	0.0
1915	2.2	16.0	2.2	6.5	1.3
1916	1.9	15.9	2.0	7.5	1.4
1917	0.6	6.4	0.6	2.0	0.0
1918	0.6	6.8	0.7	2.3	0.0
1919	0.6	6.6	0.7	2.1	0.0
1920	2.9	19.8	2.8	9.0	3.3
1921	2.1	15.0	2.0	5.8	1.0
1922	1.1	10.0	1.2	3.6	0.1
1923	1.3	10.9	1.3	3.9	0.2
1924	18.7	70.4	16.4	45.5	83.8
1925	9.3	40.4	8.3	20.0	28.9
1926	3.8	22.7	3.5	10.1	5.2
1927	0.6	6.8	0.7	2.5	0.0
1928	5.8	27.8	5.2	11.5	10.8
1929	2.6	16.3	2.4	5.9	1.5
1930	2.1	17.0	2.2	8.3	1.8
1931	3.3	19.3	3.0	7.5	2.9
1932	2.1	14.0	1.9	4.9	0.7
1933	0.8	7.7	0.8	2.5	0.0
1934	23.6	69.5	24.6	34.8	106.5
1935	6.1	32.4	5.6	16.4	16.9
1936	3.5	22.1	3.3	10.1	5.1
1937	1.7	13.1	1.7	4.9	0.5
1938	2.5	16.1	2.3	5.9	1.4
1939	9.3	48.6	8.8	32.5	39.0
1940	5.9	32.4	5.5	17.0	17.2
1941	3.7	22.6	3.4	10.1	5.4
1942	1.7	15.2	1.9	7.2	1.1
1943	5.8	28.3	5.1	12.2	11.2
1944	5.0	25.1	4.4	10.2	7.7
1945	2.3	16.4	2.2	6.8	1.5
1946	4.4	25.5	4.0	11.9	8.2
1947	6.1	30.6	5.4	14.3	14.1
1948	2.5	16.3	2.3	6.2	1.5
1949	6.8	35.9	6.2	19.6	22.3
1950	2.7	17.2	2.5	6.6	1.8
1951	7.5	35.1	6.7	16.9	20.4
1952	12.6	50.9	11.1	27.9	47.7
1953	3.3	19.6	3.0	8.1	3.2
1954	4.9	27.6	4.5	13.2	10.6
1955	1.6	11.9	1.5	4.1	0.3
1956	0.3	4.3	0.4	1.2	0.0
1957	0.2	4.0	0.3	1.2	0.0

unit:gal

year	Oliveira,C Eq.(1)	McGuire,R.K. Eq.(2)	Esteva,L,& Rosenblueth,E. Eq.(3)	Katayama,T Eq.(4)	Okamoto,S. Eq.(5)
1958	0.7	7.5	0.8	2.5	0.0
1959	0.0	0.0	0.0	0.0	0.0
1960	2.9	19.7	2.8	8.8	3.3
1961	2.1	14.6	2.0	5.5	0.8
1962	0.4	5.8	0.6	2.2	0.0
1963	1.6	12.6	1.6	4.7	0.4
1964	2.6	15.0	2.3	4.8	1.4
1965	1.7	11.9	1.5	3.9	0.3
1966	6.1	33.7	5.7	18.1	19.0
1967	2.5	16.3	2.3	6.2	1.4
1968	16.5	49.6	19.5	19.7	34.6
1969	7.3	28.2	7.1	9.6	17.7
1970	1.7	11.9	1.5	3.9	0.4
1971	2.1	15.4	2.1	6.2	1.1
1972	5.1	23.8	4.6	8.6	7.4
1973	0.5	5.6	0.6	1.5	0.0
1974	0.5	5.8	0.6	1.7	0.0
1975	9.7	37.0	9.0	15.1	32.9
1976	8.4	31.6	8.1	11.4	20.4
1977	6.1	25.7	5.6	9.0	10.9
1978	3.0	16.5	2.6	5.4	1.8
1979	1.2	9.2	1.1	2.7	0.1
1980	3.7	18.2	3.3	5.7	3.3
1981	1.8	11.6	1.6	3.4	0.3
1982	2.3	14.1	2.0	5.0	0.8
1983	17.2	61.0	15.4	33.6	57.9
1984	20.5	58.5	24.9	24.9	47.3

unit:gal

Table 8-3 Maximum Accelerations for Return Periods (gal)

Model (Eq.No.)	Proposer(s)	Return Period , Tr (year)					
		50	100	200	500	1000	10000
(1)	C.Oliveira	22	27	32	37	41	51
(2)	R.K.McGuire	71	83	93	106	115	136
(3)	L.Esteva & E.Rosenblueth	20	25	30	36	40	51
(4)	T.Katayama	41	49	58	69	77	98
(5)	S.Okamoto	93	115	133	150	160	175

CHAPTER 9 DEVELOPMENT PLAN

CHAPTER 9. DEVELOPMENT PLAN

CONTENTS

List of Figures

List of Tables

CHAPTER 9. DEVELOPMENT PLAN

9.1 Development Type and Scale

9.1.1 Review of Existing Master Plan

(1) Outline of Main River Development Plan

The master plan of the Coruh River Hydroelectric Power Project, studied by EIE in 1982, is an integral river development plan, in which 11 project sites are to be developed in series along the main river in a cascade style. In this master plan, 3 large reservoirs are to be constructed at Laleli Site, located at the uppermost part, Yusufeli Site and Deriner Site at the middle and lower parts, to regulate the river flow. The total head of 1,430 meters, from the most upstream Laleli Site to the most downstream Muratli Site would be utilized with 11 hydroelectric power plants having the total installed capacity of 2,000 MW, which would generate 7,470 GWh of electricity. The outline of this master plan is presented in Table 9-1.

The main stream of the Coruh River runs approximately 410 km (of which 390 km runs in the Turkish territory). The river has rapid flow, its gradient being 1/300, 1/150 and 1/250 at the upstream, middle stream and downstream part of the river respectively. The drainage area is 19,750 km^2 at the border of the Soviet Union, and the average annual flow there is 5.96 x 10^9 m^3 (189 m^3/s).

The geographical features of the Coruh River are its steep river gradient, as described above, plus high mountains of more than 3,000 m in elevation surrounding the river basin with steep slopes on both banks of the river. Another feature to be noted is that the Oltu River, a large tributary of the Coruh River, joins the main stream just upstream of Yusufeli Site, abruptly increasing the drainage area (by 1.9 times) at this confluence.

Accordingly, judging from the geological feature and the river flow, a development plan of the Coruh River which is based on the concept of constructing large reservoirs and power plants on the middle and lower parts of the river will be generally advantageous.

Table 9–1 Dam and Hydroelectric Power Plant (from M.P.R.)

Project	C.A	Annual Inflow	Reservoir		Dam		Installed Capacity	Annual Energy	Note
			H.W.L.	Capacity	Type	Height			
	Km^2	10^6m^3	m	10^6m^3	-	m	MW	GWh	
LALELI	4,760	785	1,480	950	Arch	134	85	181	
KILICCI	4,822	802	1,365	31.8	Gravity	59	27	75	
ISPIR	5,100	938	1,320	150	Fill	77	58	276	
GULLOBAG	5,915	1,335	1,160	37.6	Arch	94	64	292	
AKSU	6,338	1,616	1,040	146	Fill	148	116	356	
KARAKALE	6,853	1,825	935	283	Fill	175	202	802	
YUSUFELI	15,254	3,611	700	1,730	Arch	259	417	1,445	
ARTVIN (former INANLI)	15,397	3,611	500	34.3	Arch Gravity	129	193	746	
DERINER (former ARTVIN)	18,389	4,988	395	1,989	Arch (R.Fill)	250 (245)	511 (600)	1,994 (2,050)	Value of ( ) : From Feasibility Report
BORCKA	18,895	5,344	185	318	Fill	83 (94)	230 (300)	871 (1,029)	
MURATLI	19,748	5,905	92	58.8	Fill	45 (47)	100 (115)	431 (417)	

The scope of study presented herein covers the main river stretching downstream of Karakale Dam Site to the back water of Deriner Reservoir. Thus, the master plan aforementioned is to be reviewed with a particular focus on the Yusufeli and Artvin Projects proposed in the master plan.

At present, feasibility studies are being conducted by EIE for other 9 sites along the main river.

(2) Review of Master Plan

In the stretch downstream of Karakale Dam Site to the back water end of Deriner Reservoir, three project plans, (A), (B) and (C), are conceivable, including the proposal in the master plan, based on the site reconnaissance and considering such factors as geography, geology, status of landslides, reservoir efficiency, effective utilization of river flow, etc. The three project plans are shown in Fig.9-1.

In these three plans, a large reservoir is to be constructed at Yusufeli Site, which is approximately 800 m downstream from the confluence of the tributary Oltu River to the Coruh River, for the regulation of the river flow and for construction of a large hydroelectric power plant.

In Plan (A) and Plan (B), a dam and conduit type power plant or a dam type power plant is planned by constructing another reservoir at Artvin Site, which is located downstream of Yusufeli Site. The dam and conduit type power plant of Plan (A) is also suggested in the master plan. However, as the effect of the landslide (Havuzlu) which is directly upstream of Artvin Dam Site (the original dam site) must not be neglected, a new dam site (Artvin Upstream Dam Site) is selected at a location 3 km upstream of the original dam site based on the result of the reconnaissance. In the plan of the dam type power plant of Plan (B), the dam site (Artvin Downstream Dam Site) was selected at a location 8 km downstream of the original dam site around the back water end of Deriner Reservoir to utilize the head effectively.

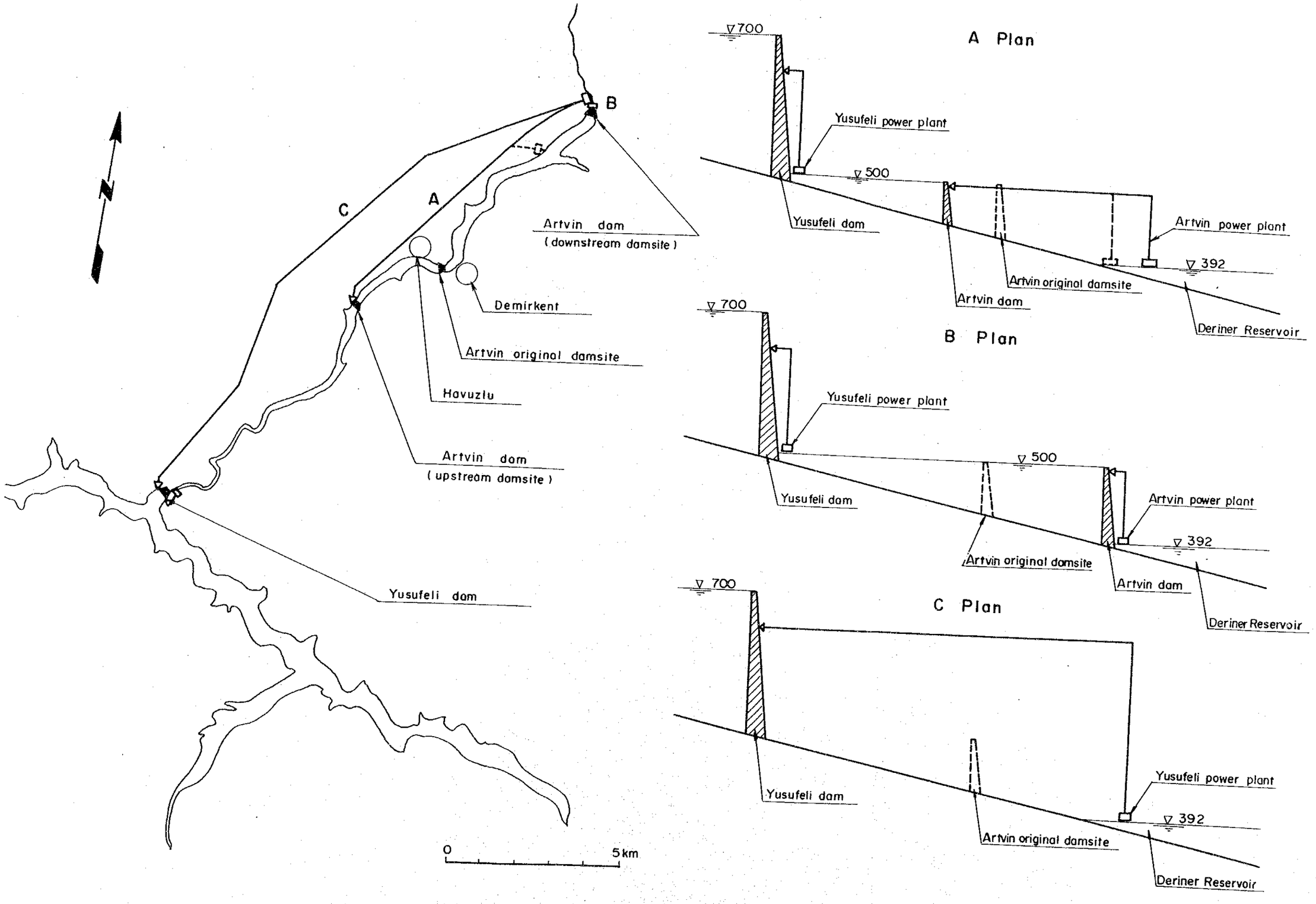

Fig. 9–1 Alternative Plan of Yusufeli and Artvin Projects

In Plan (C), the construction of Artvin Reservoir is not considered, and it is planned to construct a power plant at the end of the back water of Deriner Reservoir, which is a dam and conduit type power plant directly connected to Yusufeli Reservoir by a water conduit. It was found out that Plan (C) is not economical in the following preliminary study, and no detailed study was conducted on this plan.

Comparing Plan (C) with Plan (B), the construction cost is partly substantially increased by the conduit, while partly substantially decreased by the construction of Artvin Dam, power plant and electrical equipment.

As shown in Table 9-2, the direct cost of Plan (B) is smaller than that of Plan (C), besides, the benefit comparison indicates that Plan (B) is more favorable due to the difference of the power and energy generation taking the head loss into consideration.

Table 9-2 Main Cost Difference between Plans C and B

Item	Unit	Plan C	Plan B	C - B
Installed Capacity	MW	780	840	
Energy Generation	GWh	2,300	2,600	
Direct Cost				
Headrace and Surge Tank	10^6TL	87,500	-	87,500
Dam	10^6TL	-	37,100	-37,100
Powerhouse	10^6TL	9,100	19,700	-10,600
Electro-mechanical Equip.	10^6TL	60,000	85,500	-25,500
Total		156,600	142,300	14,300

Assuming that Yusufeli Town is not to be submerged by a reservoir, an alternative plan can be produced in which, instead of constructing a dam at Yusufeli Site, a dam having high water level of 580 m is constructed at Artvin Dam Site. In this alternative plan, a dam should be constructed further upstream of Yusufeli Site in order to make effective use of the head of the main stream, and a site near Kilazuli, 23 km upstream of Yusufeli Dam Site, can be selected based on the geographical

condition. Considering the elevation of Kalakale Dam Site, a reservoir having high water level of 810 m can be constructed near Kilazli, and the head available to the high water level of Artvin Reservoir can be utilized by a water conduit.

In this scheme, the flow and the residual head of the tributary Oltu River must be utilized, and one more dam would be proposed at a location 1 km upstream of the confluence of the Oltu River and Tortum River, considering the geographical condition.

The storage efficiency of such 3-dam plan can be compared with that of a 2-dam plan consisting of Yusufeli Dam and Artvin Dam. As shown in Table 9-3, the storage efficiency of the 2-dam plan is overwhelmingly superior, being nearly twice that of the 3-dam plan. Thus the further study on the 3-dam plan has been omitted in this report. The concept drawings of 3-dam plan are presented in Fig. 9-2.

Table 9-3 Storage Efficiency of Two Dam Plan and Three Dam Plan

Name	HWL (m)	Surface Area (km^2)	Gross Storage Capacity A ($10^6 m^3$)	Concrete Gravity Dam Volume B ($10^6 m^3$)	Storage Efficiency A/B
Yusufeli Dam	700	29.9	1,820	5.3	
Artvin Dam	500	4.1	170	1.5	
Total			1,990	6.8	293
Kirazli Dam	810	12.0	700	3.5	
Oltu Dam	700	4.0	180	2.2	
Artvin Dam	580	12.3	800	4.0	
Total			1,680	9.7	173

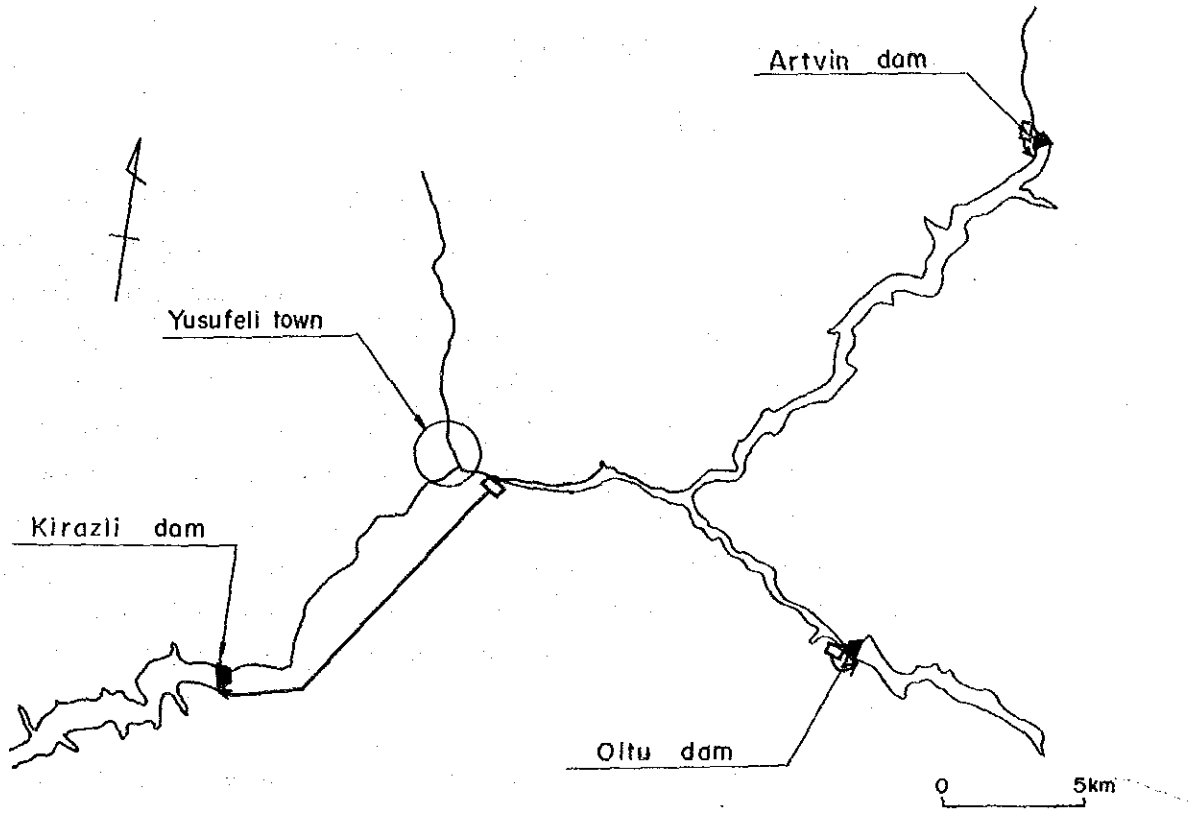

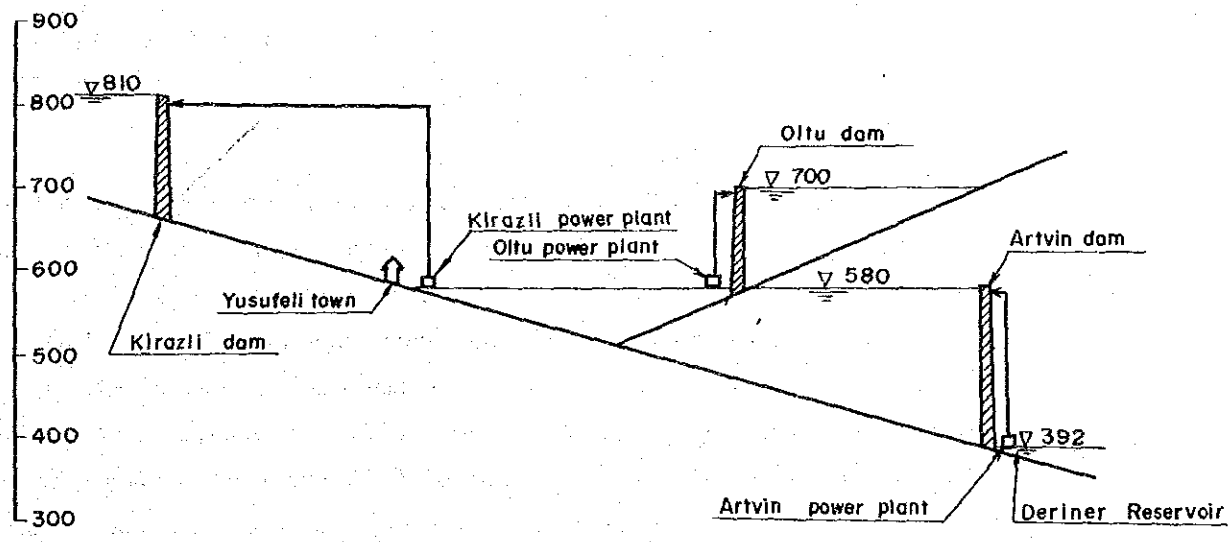

Fig. 9–2 Three Dam Plan

9.1.2 Evaluation Method for Development Type and Scale

(1) Fundamental View

The method used for examination of development type and scale of this project is that of considering an alternative thermal power plant that would be built without this project and taking the cost of the thermal power plant as the benefit of the project. In order to select the optimum development plan, an imported coal-fired thermal power plant and a heavy oil-fired thermal one are respectively used as the alternative facilities for the evaluation. Because, in Turkey, imported coal-fired thermal plants will be supposed to be main electric power facilities in future and heavy oil-fired thermal ones have been generally used as the alternatives in feasibility studies.

Generally, in Turkey, a conbination of a gas turbine power plant and a steam thermal power plant is used as the alternative thermal power facilities, but is not used in this study due to its unreality. Because the plant factor of a gas turbine power plant is generally 8% at most from economic point of view and therefore it is too short for the peak duration required of this project.

Study was done formulating a number of alternative plans for Yusufeli and Artvin Projects to select the optimum development schemes upon making comparison studies of these alternative plans.

In examinations of comparative plans, annual surplus benefit (B-C) and annual benefit cost ratio (B/C) obtained from equalized annual costs (C) for the project life (50 years) of the hydro power facility and the equalized annual costs (B) of the alternative thermal power facility having equivalent capacity and internal rate of return (I.R.R.) obtained from the total costs for the analysis period (construction period + project life) of the hydro power facility and those of the alternative thermal power facility are used as the indeces. The

criteria for comparisons are given in Table 9-4. Market prices without taxes are used for the costs in the comparisons.

The costs of the transmission line between Hopa and consuming cities in Yusufeli and Artvin Projects and the transmission line between the alternative thermal power plant and consuming cities are omitted since the future power transmission system plan has not yet been defined, and their influence on the evaluation of the project is small.

(2) Equalized Annual Cost Method

The equalized annual cost of a hydro power facility consists of depreciation and operation-maintenance cost and is estimated by multiplying annual cost factor with investment cost. Interest during construction would be included in the investment cost. The average interest rate of 9.5% is used for both foreign currency and local currency. The annual cost factor is obtained by the equation below and is to be 9.9% for civil facilities and 11.4% for electro-mechanical facilities.

$$\text{Capital Recovery Factor} = \frac{i(1+i)^n}{(1+i)^n - 1}$$

Civil facility	9.6%
Electro-mechanical facility	9.9%

where,

n :	service life, civil facility	50 years
	electro-mechanical facility	35 years
i :	discount rate	9.5%

Operation and Maintenance Cost (Ratio to Construction Cost)

Civil facility	0.3%
Electro-mechanical facility	1.5%

An alternative thermal power plant is supposed to be provided in Zonguldak City on the Black Sea near the load center of the West Anatolia Region, especially Ankara, with installed capacity of 600 MW (300 MW x 2) which is commonly used in feasibi-

Table 9-4 Basic Criteria for Comparison Study

Item	Description	
Method of Analysis	Annual Cost Method	Discount Cash Flow Method
Economic Index	Surplus Benefit (B-C) Benefit Cost Ratio (B/C)	Internal Rate of Return (I.R.R.)
Study Period	50 years	Construction period + 50 years
Discount Rate	9.5% 1/	
Cost	Investment Cost O/M Cost, Fuel Cost 2/ (Market Price without Tax)	Project Cost O/M Cost, Fuel Cost
Escalation	Not Considered	
Service Life of Facility		
Civil Facility	50 Years	
Electro-mechanical Facility	35 Years	
Oil Fired Thermal Plant	25 Years	
Coal Fired Thermal Plant	25 Years	
Substation	25 Years	
Transmission Line	35 Years	
Conversion Rate of Currency (As of July 1985)	US$1.00 = 550 T.L	

1/ In Turkey, a discount rate of 9.5% is generally used as the evaluation criterion for a hydro-power project.

2/ Investment Cost consists of project cost and interest during construction.

lity studies in Turkey at present. The costs per kW and kWh respectively obtained from the fixed and variable costs of this facility were used as the unit benefit of hydro. These particulars of a coal-fired thermal and an oil-fired thermal power plants are given in Tables 9-5, 6 respectively.

With regard to construction cost and fuel cost, they were calculated from standard international prices taking into account the situation in Turkey since it is difficult to convert the obtained actual prices in Turkey to 1985 prices due to the influences of inflation on values obtained for Turkey.

(3) Discounted Cash Flow Method

The construction cost and operation-maintenance cost of the hydro power plant are spread out by year. And the construction cost, operation-maintenance cost, and fuel cost of the alternative thermal power plant possessing an equivalent capacity are similarly spread out by year for the same period. The analysis period is to be from the commencement year of construction until the end of project life of the hydro power plant, with replacement of electromechanical equipment of the hydro power plant, the alternative thermal power plant, and transmission lines considered.

The discount rate at which present value of the cost of the hydro power plant would be equal to that of the alternative thermal one is taken to be internal rate of return (I.R.R.).

Operation-maintenance cost and fuel cost are the same as those in equalized annual cost method.

9.1.3 Yusufeli Project

(1) Basic Consideration

Yusufeli Project is much larger in scale than Artvin Project, and together with the fact that Yusufeli Project is located upstream of Artvin Project, it has a larger effect on the overall plan of the river development. For this reason, we

Table 9–5 Alternative Thermal Power Plant for Optimization Study (1)

Interest Rate = 9.5%
Price Level = As of July, 1985

Item	Unit	Description	
Type		Coal-fired Power Plant	
Installed Capacity	MW	600 (300 x 2)	
Annual Plant Factor	%	73	
Thermal Efficiency	%	35	
Annual Energy Production	10^6kWh	3,837	
Station Service Ratio	%	kW 7, kWh 8	
Investment Cost	10^6T.L	282,000	
Service Life	Years	25	
Construction Period	Years	4	
Capital Recovery Factor		0.10596 (i = 9.5%)	
Fuel Consumption Rate	kg/kWh	0.406	
O & M Cost Rate without Fuel Cost	%	3.0	
Unit Fuel Cost	T.L/kg	24.75	
Annual Cost		Fixed Cost	Variable Cost
Capital Recovery	10^6T.L	29,880.7	-
O & M Cost, Administration Cost	10^6T.L	7,614.0	846.0
Fuel Cost	10^6T.L	-	38,556.1
Total	10^6T.L	37,494.7	39,402.1
Annual Cost at Receiving End			
kW Cost	T.L	81,990 1/	
kWh Cost	T.L		11.45 2/

1/ $\frac{37,494.7 \times 10^6 \text{T.L}}{600,000 \text{ kW}} \times 1.312 = 81,990$ T.L/kW

2/ $\frac{39,402.1 \times 10^6 \text{T.L}}{3,837 \times 10^6 \text{kWh}} \times 1.115 = 11.45$ T.L/kWh

3/ & 4/ Adjustment Factor for kW & kWh

Item			
Transmission Loss Rate	(%)	kW, 3	kWh, 2.5
Station Service Rate	(%)	kW, 7	kWh, 8
Forced Outage Rate	(%)	4	
Scheduled Outage Rate	(%)	12	

$$\text{kW Adjustment Factor} = \frac{1}{(1 - 0.03) \times (1 - 0.07) \times (1 - 0.04) \times (1 - 0.12)}$$

$$= 1.312$$

$$\text{kWh Adjustment Factor} = \frac{1}{(1 - 0.025) \times (1 - 0.08)} = 1.115$$

5/ Interest during construction is included in the investment cost

Table 9–6 Alternative Thermal Power Plant for Optimization Study (2)

Interest Rate = 9.5%
Price Level = As of July, 1985

Item	Unit	Description	
Type		Oil-fired Power Plant	
Installed Capacity	MW	600 (300 x 2)	
Annual Plant Factor	%	73	
Thermal Efficiency	%	35	
Annual Energy Production	10^6kWh	3,837	
Station Service Ratio	%	kW 5, kWh 6	
Investment Cost	10^6T.L	193,000	
Service Life	Years	25	
Construction Period	Years	4	
Capital Recovery Factor		0.10596 (i = 9.5%)	
Fuel Consumption Rate	kg/kWh	0.251	
O & M Cost Rate without Fuel Cost	%	3.0	
Unit Fuel Cost	T.L/kg	89.937	
Annual Cost		**Fixed Cost**	**Variable Cost**
Capital Recovery	10^6T.L	20,450.3	-
O & M Cost, Administration Cost	10^6T.L	5,211.0	579.0
Fuel Cost	10^6T.L	-	86,617.2
Total	10^6T.L	25,661.3	87,196.2
Annual Cost at Receiving End			
kW Cost	T.L	54,960 1/	
kWh Cost	T.L		24.79 2/

1/ $\frac{25,661.3 \times 10^6 \text{T.L}}{600,000 \text{ kW}} \times 1.285 = 54,960$ T.L/kW

2/ $\frac{87,196.2 \times 10^6 \text{T.L}}{3,837 \times 10^6 \text{kWh}} \times 1.091 = 24.79$ T.L/kWh

3/ & 4/ Adjustment Factor for kW & kWh

Item			
Transmission Loss Rate	(%)	kW, 3	kWh, 2.5
Station Service Rate	(%)	kW, 5	kWh, 6
Forced Outage Rate	(%)	4	
Scheduled Outage Rate	(%)	12	

$$\text{kW Adjustment Factor} = \frac{1}{(1 - 0.03) \times (1 - 0.05) \times (1 - 0.04) \times (1 - 0.12)}$$

$$= 1.285$$

$$\text{kWh Adjustment Factor} = \frac{1}{(1 - 0.025) \times (1 - 0.06)} = 1.091$$

5/ Interest during construction is included in the investment cost

first studied the development plan and the size of Yusufeli Project, and then studied Artvin Project based on the optimum plan of Yusufeli Project.

Yusufeli Dam Site covering 15,250 km^2 of catchment area is located approximately 800 m downstream of the confluence of the Coruh River and the Oltu River. At this point, the catchment area contributed by the Oltu River amounts to about 90% of the total catchment of the Coruh River mainstream, and thus this location is ideal from the view point of the effective utilization of this river. The average inflow at the planned dam site is 120 m^3/s, and 61% of this annual inflow is concentrated in the 3 months from April to June, which is the season of snow melting and raining, while the average inflow during winter season, from December to February, decreases to 40% of the annual average. It is therefore key point in planning a hydroelectric project to store and regulate this large seasonal fluctuation of inflow by a large reservoir and to equalize the available power discharge.

The elevation of the river bed at the planned dam site is 496 m and the river width is approximately 30 m. The width of the valley at an elevation of 700 m is approximately 400 m. The slopes on both banks of the river are very steep, having gradients around 50 degrees. The base rocks are exposed, except in areas of partial sediment. In terms of geology, granite, granodiorite, granophyre and diabase intrude into one another, but the quality of the rock is very hard. Although there are many cracks, the cracks are held tight together, and it can be considered to be hard bed rock as a whole. Though the river bed deposit is about 50 m in depth, this site is suitable for dam construction in terms of both geography and geology. The dam type power plant, in combination with Artvin Dam, is the most suitable, as described in 9.1.1.

The examinations of development type and scale were made with 1/5000 topographical maps, and the optimum development plan is studied further in detail with 1/1000 topographical maps.

(2) Reservoir Operation Plan

The reservoir operation rules of Yusufeli Reservoir have been determined for each study case, based on considerations on the following factors.

i) The river water in a wet year is to be stored and released in a dry year, to make the firm discharge as large as possible.

ii) During a year, the reservoir is to be operated in such a way that the water in the wet season is to be stored and supplied in the dry season.

iii) The resevoir is to be operated so that the spill is as small as possible.

iv) The reservoir is to be operated so that a stable supply of power is assured for a long period and at the same time the energy generation is large.

The calculations of reservoir operation have been performed by an electronic computer system, and based on the monthly average inflow, for the period of 42 years from January 1942 to December 1983, in which the flow data are available.

The firm discharge is defined as the minimum discharge available for power generation for the 42-year period, and it is obtained by making it the largest with the inflow mass curve considering carry-over storage. The inflow mass curve and the effective storage capcity and the firm discharge, not counting evaporation from the reservoir surface, are shown in Figs. 9-3, 4 respectively. In the operation calculations of the reservoir, amount of evaporation has been counted.

In the calculation, the change of turbine and generator efficiency depending on the change of the reservoir water level has been taken into account. The maximum power discharge is limited by the rated output when the water level is higher than the rated intake water level, and the maximum power discharge

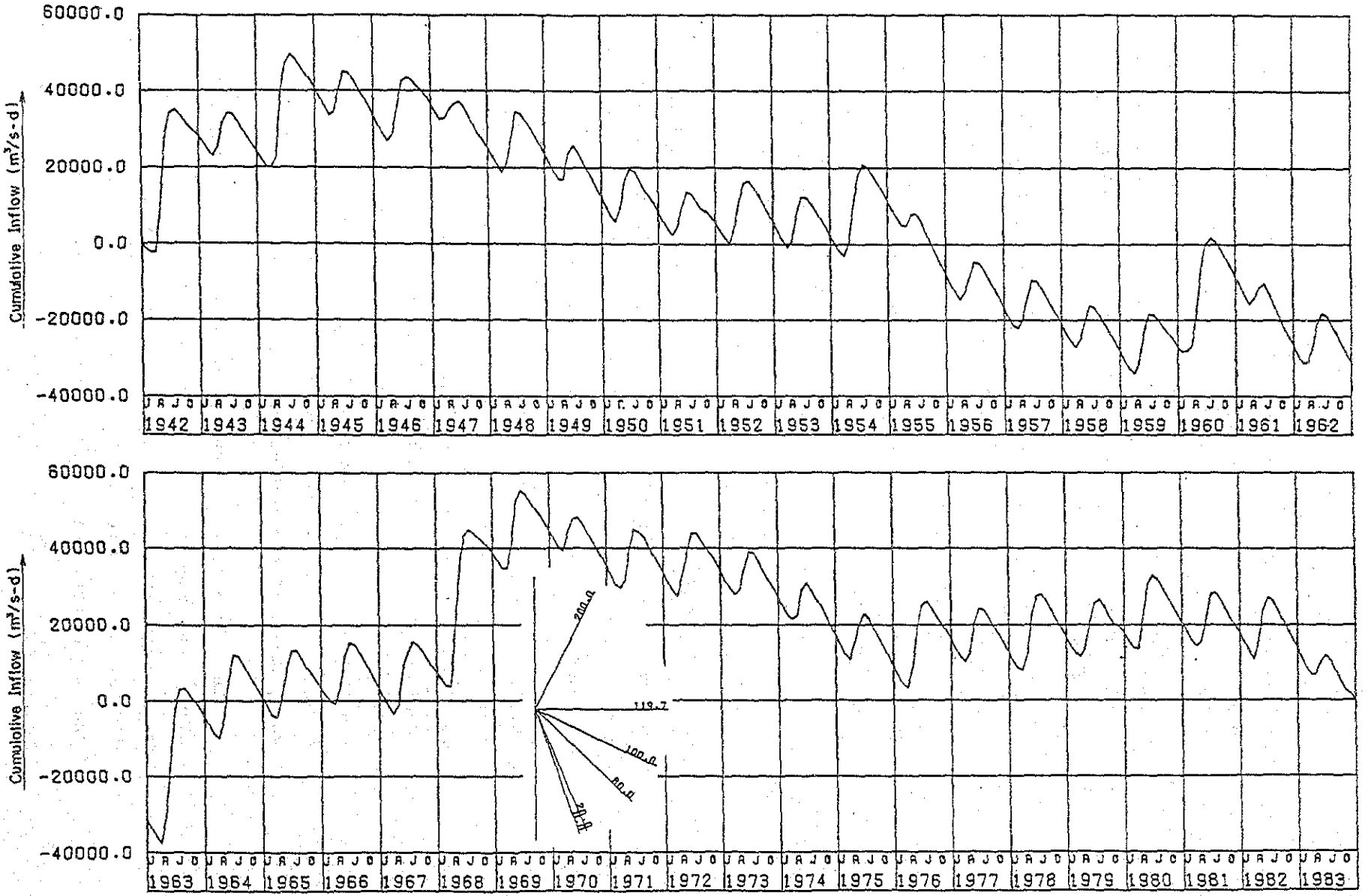

Fig. 9–3 Mass Curve at Yusufeli Dam Site

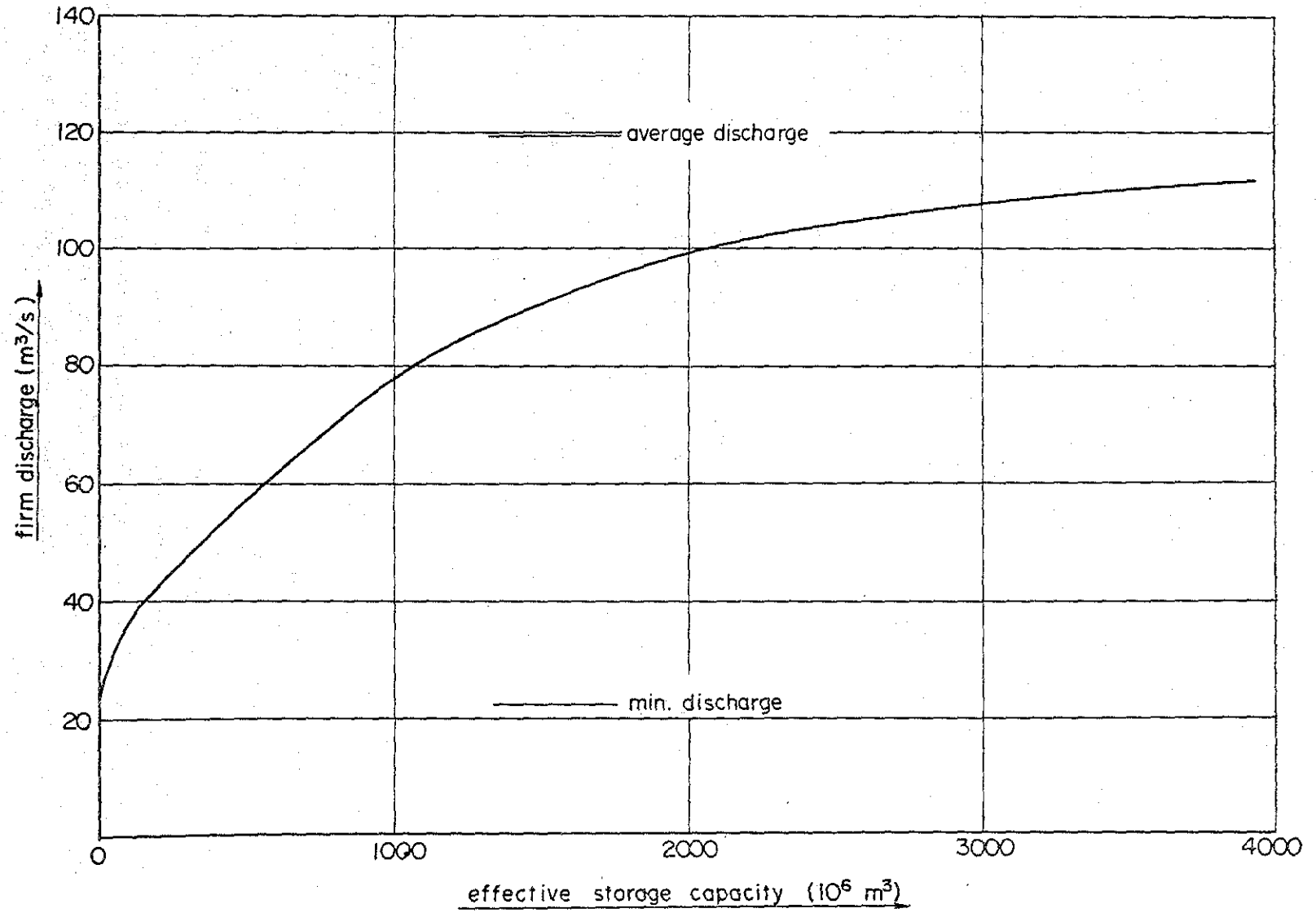

Fig. 9–4 Relation between Firm Discharge and Effective Storage Capacity

is reduced by the reduction of head when the water level is below the rated intake water level.
The rated intake water level was set at an elevation which is below the high water level by 1/3 of the available drawdown.

In selecting the rated tail water level, the tail water level has been calculated considering the back water level of Artvin Reservoir. There is negligible effect by the release of the Yusufeli Power Plant, and the rated tail water level has been set to be EL. 500 m, the same level as the high water level of Artvin Reservoir.

River cross sections used in non-uniform flow calculation were measured with 1/5000 topographical maps. Their standard intervals were set at 500 m, and a roughness coefficient of 0.05 was used. The procedure of the calculation of the power and energy generation, and the reservoir operation rule are illustrated in Figs. 9-5, 6 respectively.

The operation rule was simplified to be only one rule curve Vs for securing the firm discharge. The storage volume required to be secured every month in order not to undercut low water level by release of the firm discharge was calculated, and the envelope curve of this storage volume was taken to be Vs curve for each case. In the zone between high water level and Vs curve, half of the maximum available discharge was used.

(3) Study on Development Type and Layout

The examinations of development type and layout are carried out based on the plan with high water level of 700 m, effective storage capacity of 1120 x 10^6 m^3, and the maximum available discharge of 326 m^3/s.

As a dam type hydro power plant has been selected, various types of dam are conceivable. Rough studies are made of the four-types of concrete gravity dam, arch gravity dam, arch dam, and rockfill dam. The dam volume, excavation quantity, and their rough construction costs for each type of dam are as given in Table 9-7.

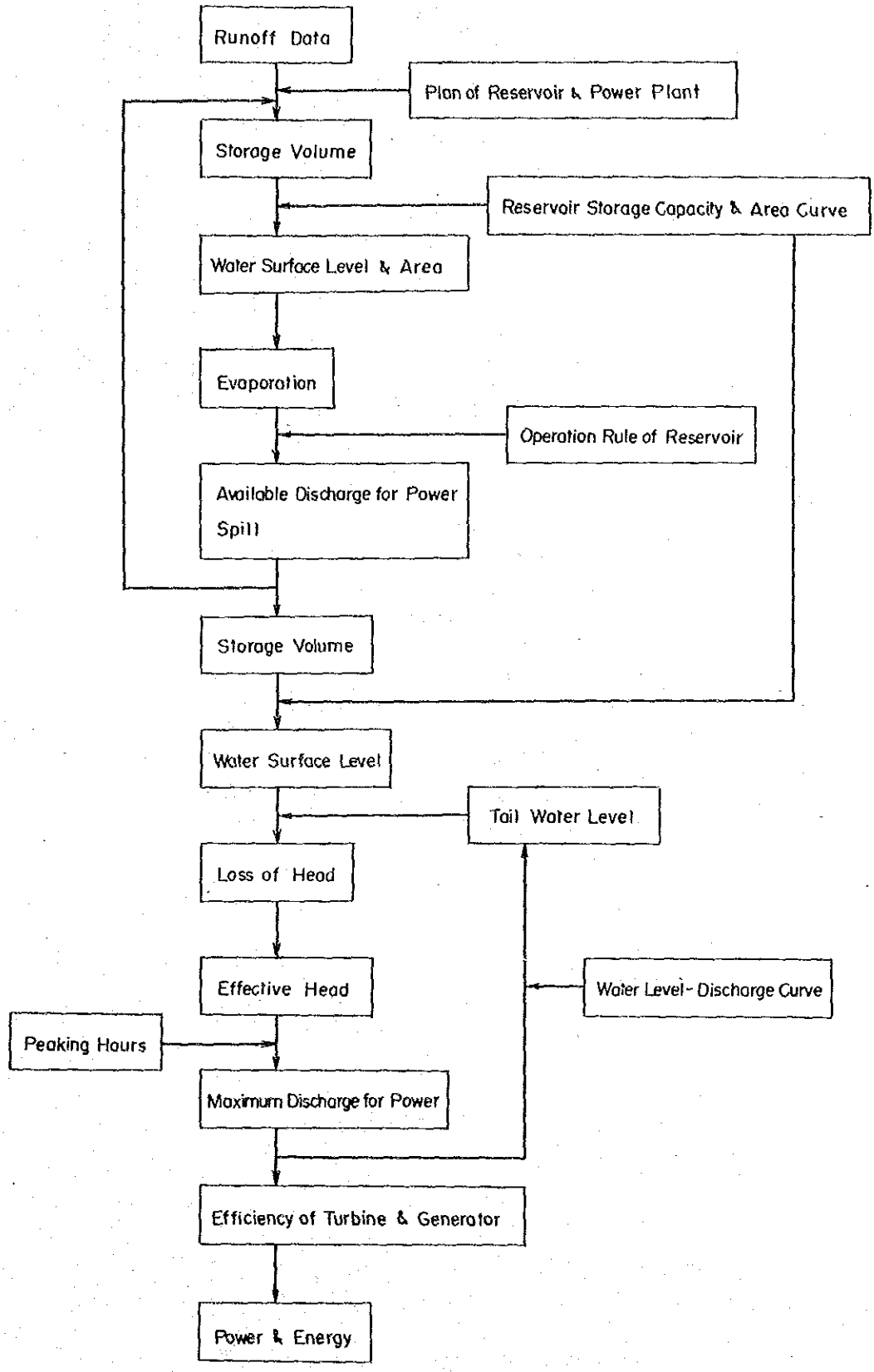

Fig. 9–5 Flow Chart of Calculation of Power and Energy

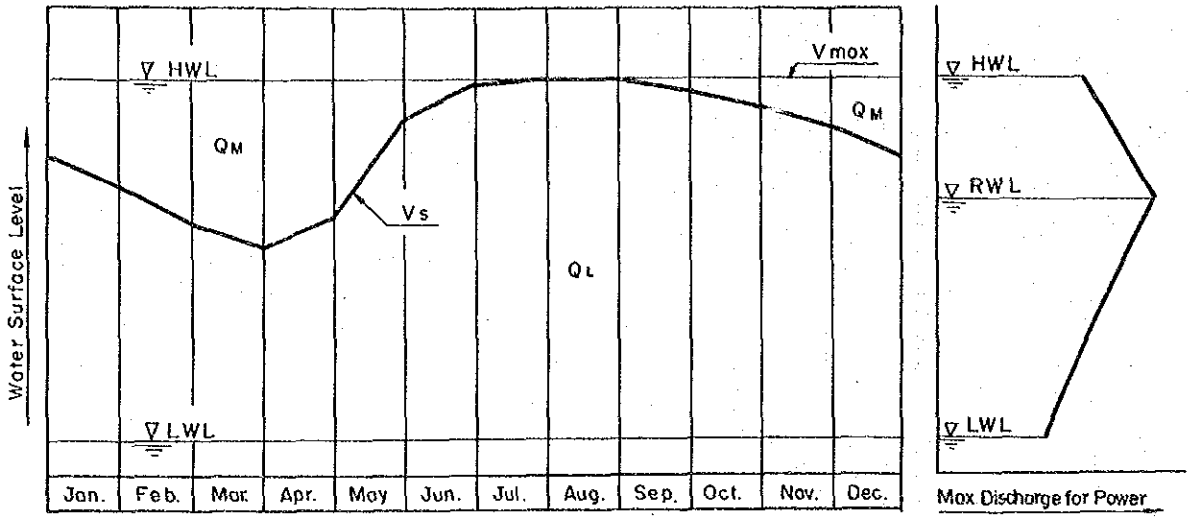

Symbols

V_{n-1}	:	Storage at the end of previous month
V_n	:	Storage at the end of current month
V_n'	:	Temporary storage at the end of current month
Vmax	:	Maximum storage (Effective storage capacity)
Vs	:	Secured storage for firm discharge
f_n	:	Spill in current month
q_n	:	Inflow in current month
Q_n	:	Available discharge for power in current month
Q_M	:	Medium discharge for power
Q_L	:	Firm discharge for power
Q_H	:	Maximum discharge for power, variable depending on water level
E	:	Evaporation, variable depending on water surface area

Operation Rule

$$V_n' = V_{n-1} + q_n - E$$

1. $V_n' \geqq V_{max}$
   - (1) $V_n' - V_{max} \geqq Q_H \longrightarrow Q_n = Q_H$
   - (2) $Q_H > V_n' - V_{max} \geqq Q_M \longrightarrow Q_n = V_n' - V_{max}$
   - (3) $Q_M > V_n' - V_{max} \longrightarrow Q_n = Q_M$

2. $V_{max} > V_n' \geqq V_s$
   - (1) $V_n' - V_s \geqq Q_M \longrightarrow Q_n = Q_M$
   - (2) $Q_M > V_n' - V_s \geqq Q_L \longrightarrow Q_n = V_n' - V_s$
   - (3) $Q_L > V_n' - V_s \longrightarrow Q_n = Q_L$

3. $V_s > V_n'$
   - (1) $V_n' \geqq Q_L \longrightarrow Q_n = Q_L$
   - (2) $Q_L > V_n' \longrightarrow Q_n = V_n'$

$V_n' = V_{max} - Q_n \geqq 0.0 \rightarrow f_n = V_n' - V_{max} - Q_n$

$V_n' = V_{max} - Q_n < 0.0 \rightarrow f_n = 0.0$

$V_n = V_n' - Q_n - f_n$

Fig. 9–6 Operation Rule of Reservoir

Because the dam scale is large, the proportion of dam cost to total construction cost is substantial and its economic influence on the whole project is great. Since the total construction costs of waterway and powerhouse are aproximately 10×10^9 TL for a surface powerhouse at the foot of the dam and approximately 15×10^9 TL for an underground powerhouse, a concrete gravity dam and an arch gravity dam are clearly disadvantageous economically when compared with an arch dam, and therefore, they are abandoned at this stage.

Table 9–7 Comparison of Dam Types

Item	Unit	Concrete Gravity Dam	Arch Gravity Dam	Concrete Arch Dam	Rockfill Dam
Dam Volume	10^3 m^3	5,300	3,600	2,800	19,200
Excavation Volume	10^3 m^3	2,400	2,000	2,400	1,500
Construction Cost	10^6 TL	144,000	106,000	90,000	45,000

The general layout of the structures, such as a spillway and a powerhouse, has been studied, based on considerations on the geography and geology of the site. With a rock-fill dam, two plans have been studied, one having an underground powerhouse in the right bank and the other having a surface powerhouse on the left bank. Two other plans have been also studied with the concrete arch dam, one having an underground powerhouse in the right bank, and the other having a surface powerhouse directly below the dam (the Master Plan). Thus 4 plans in total have been compared.

One of the alternatives of a rockfill dam with a chute spillway on the right bank and an underground powerhouse in the left bank turned out to be uneconomical at the preliminary study stage in terms of spillway excavation and dam embankment volume.

The investment costs of the 4 plans, with high water level of 700 m and the maximum available discharge of 326 m^3/s are presented in Table 9-8.

And one more alternative of an arch dam with a surface powerhouse just downstream of the dam body as shown in the Master Plan was also abandoned judging from the rough comparative study as follows.

i) The chute spillway in the Master Plan costs by far more than the center overflow type of spillway, which cannot be covered by the relatively small decrease of the construction cost of the waterway.

ii) The power waterway and the spillway incorporated in the dam body will require a special attention to the structural stability of the arch dam.

iii) The construction works will be concentrated in a limited area, so that it will cause a big congestion.

Accordingly, a comparative study of the basic layout was performed for the three cases shown in the Table 9-9 in more detail.

Although the power and energy generation are larger in the arch dam plans due to shorter conduit length, the rock-fill dam plan having an underground powerhouse in the right bank has an advantage over other plans, as indicated in Tables 9-10, 11. The changes in the dam volume and the construction cost for various height of the dam are given in Figs. 9-7, 8, for both rock-fill dam and concrete arch dam.

The outlines of the basic layout of alternative plans are described as follows.

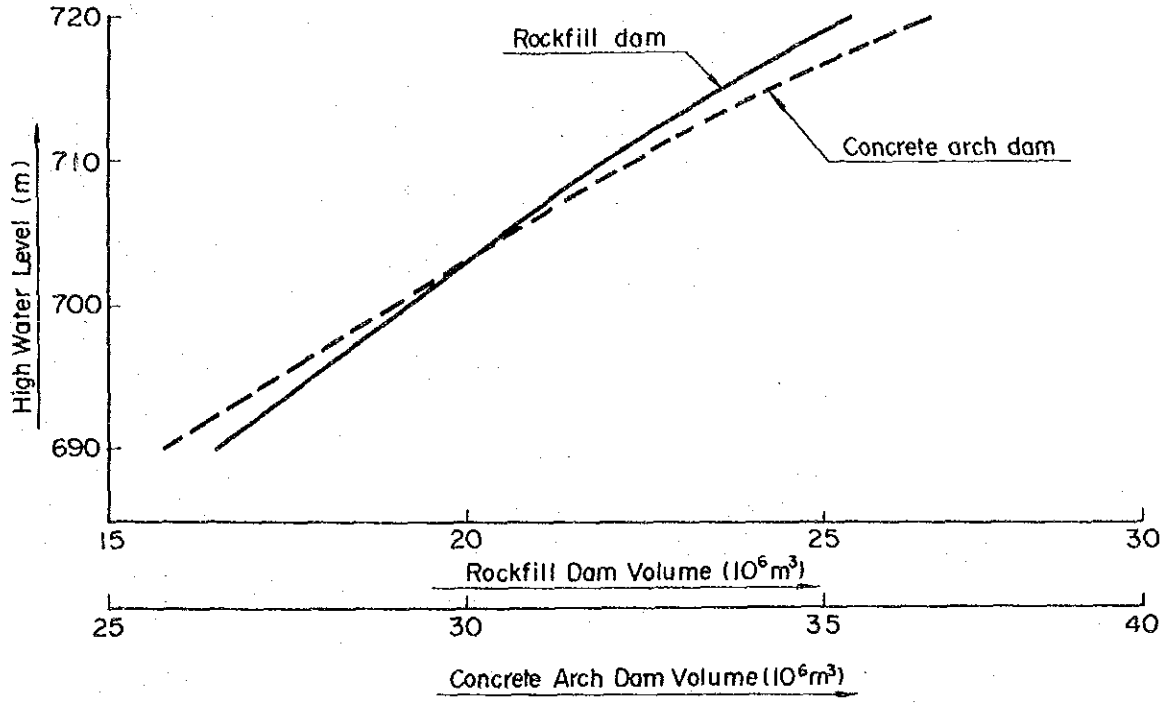

Fig. 9–7 Dam Volume for Various Height

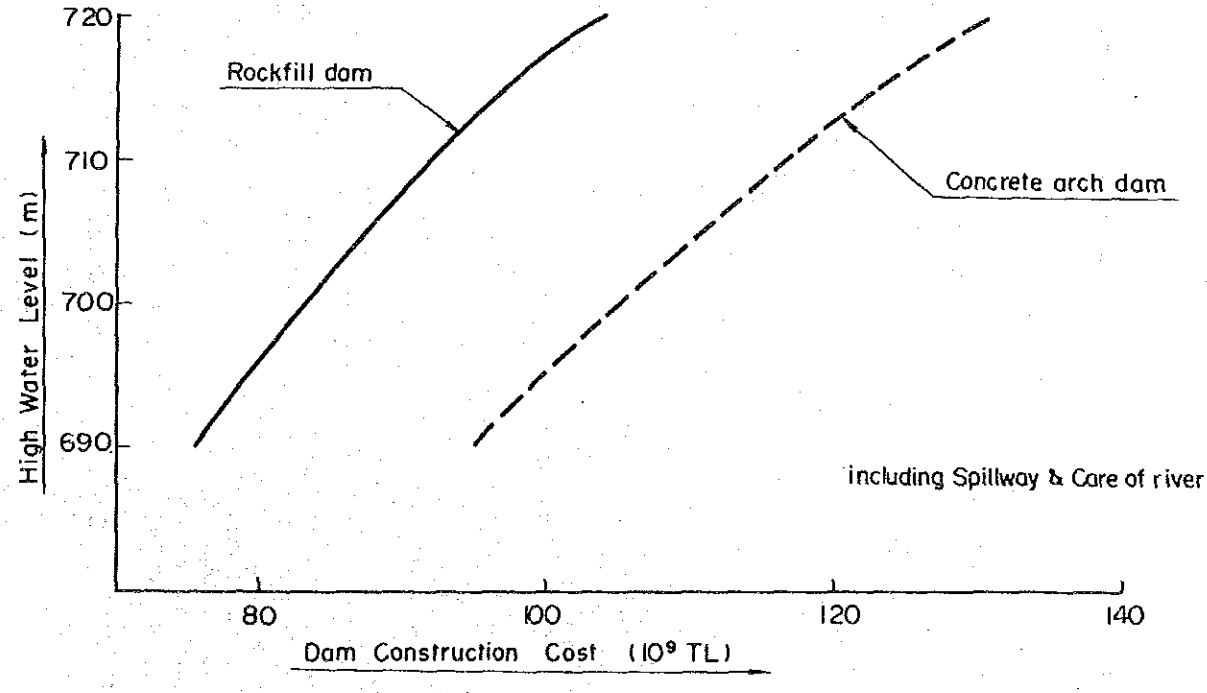

Fig. 9–8 Dam Construction Cost for Various Height

Table 9–8 Investment Cost of Layout Alternative Plans (Yusufeli Project)

(unit: 10^6 TL)

Item	Rockfill Dam Plan		Concrete Arch Dam Plan		Remarks
	Underground Type Power Plant	Surface Type Power Plant	Underground Type Power Plant	Surface Type Power Plant	
Civil Works	120,200	132,300	143,700	150,800	
Dam	80,600	92,500	102,700	112,600	HWL 700m
Care of River	(6,300)	(6,200)	(4,300)	(4,000)	
Dam	(50,000)	(52,000)	(98,000)	(95,000)	
Spillway	(23,500)	(33,000)	-	(13,000)	
Others	(800)	(1,300)	(400)	(600)	Bottom Outlet, etc.
Waterway	4,300	5,500	3,600	-	
Powerhouse	9,100	6,500	8,100	8,000	
Access Road	2,000	2,000	2,000	2,000	
Camp Facility	8,500	8,500	8,500	8,500	
Physical Contingency	15,700	17,300	18,800	19,700	
Hydraulic Equipment	4,300	4,100	4,200	3,000	
Electromechanical Equipment	40,600	40,600	40,900	41,300	
Transmission Line	2,100	2,100	2,100	2,100	between Yusufeli P.S. and Hopa S.S.
Total	167,200	179,100	190,900	197,200	
Project Controlling	25,100	26,900	28,600	29,600	
Land Acquisition	12,300	12,300	12,300	12,300	
Relocation of Road & Transmission Line	12,200	12,200	12,200	12,200	
Project Cost	216,800	230,500	244,000	251,300	
Interest during Construction	61,700	66,200	63,500	65,700	
Investment Cost	278,500	296,700	307,500	317,000	

Table 9–9 Structural Dimension (Yusufeli Project)

Item	Case		Rockfill Dam Underground powerhouse	Rockfill Dam Surface powerhouse	Arch Dam Underground powerhosue
Dam	H x L	(m)	260 x 400	260 x 410	260 x 456.5
	Top width	(m)	12	12	12
	Outer slope		1:2.2, 1:1.9	1:2.2, 1:1.9	55 (Base width)
	Dam volume (10^3 m^3)		19,200	20,100	2,800
Diversion tunnel	D x L x n	(m)	9.2 x 1,245 x 1	9.2 x 1,200 x 1	9.2 x 925 x 1
Spillway gate	B x H x n	(m)	13.5 x 15.0 x 4	13.5 x 15.0 x 4	10.5 x 12.0 x 6
Headrace	D x L x n	(m)	-	9.8 x 594	-
Surge tank	D x H x n	(m)	-	14.0 x 94	-
Penstock	D x L x n	(m)	(9.0-8.0-4.0) x 363 x (1-3) (No.2)	(9.8-8.0-4.0) x 285 x (1-3) (No.2)	(9.0-8.0-4.0) x 399 x (1-3) (No.2)
Tailrace	D x L x n	(m)	(5.7 - 9.8) x 403 x (3-1) (No.2)	-	5.7 x 142
Powerhouse	B x L	(m)	20 x 83	39 x 85	20 x 83

Table 9–10 Study on Optimum Layout of Yusufeli Project (1)

* Alternative Power Plant .... Coal-fired one

Item	Unit	Rockfill Dam Plan		Concrete Arch Dam Plan		Remarks
		Underground Type Power Plant	Surface Type Power Plant	Underground Type Power Plant	Surface Type Power Plant	
Installed Capacity	MW	513	513	516	520	
Maximum Discharge	m^3/S	326	326	326	326	
Rated Effective Head	m	178.3	178.3	179.3	180.8	
Firm Peak Power	MW	468.7	468.7	471.3	475.1	
Annual Energy	GWh	1,610.9	1,610.9	1,618.9	1,629.3	
Investment Cost	10^6TL	278,500	296,700	307,500	317,000	
Construction Period	Month	105	105	93	93	
I.R.R.	%	17.09	15.82	14.83	14.43	
B – C	10^6TL	24,820	23,020	22,240	21,690	
B/C	–	1.87	1.76	1.71	1.67	
Energy Cost	TL/kwh	18.3	19.5	20.0	20.4	

Table 9—11 Study on Optimum Layout of Yusufeli Project (2)

* Alternative Power Plant .... Oil-fired one

Item	Unit	Rockfill Dam Plan		Concrete Arch Dam Plan		Remarks
		Underground Type Power Plant	Surface Type Power Plant	Underground Type Power Plant	Surface Type Power Plant	
Installed Capacity	MW	513	513	516	520	
Maximum Discharge	m^3/S	326	326	326	326	
Rated Effective Head	m	178.3	178.3	179.3	180.8	
Firm Peak Power	MW	468.7	468.7	471.3	475.1	
Annual Energy	GWh	1,610.9	1,610.9	1,618.9	1,629.3	
Investment Cost	10^6TL	278,500	296,700	307,500	317,000	
Construction Period	Month	105	105	93	93	
I.R.R.	%	17.35	16.36	15.57	15.24	
B - C	10^6TL	33,880	32,080	31,330	30,830	
B/C	-	2.19	2.06	2.00	1.95	
Energy Cost	TL/kwh	18.3	19.5	20.0	20.4	

(a) Rockfill Dam: Underground Powerhouse Plan

The rockfill dam is of center impervious core. The outer slope of dam embankment is made 1 to 2.2 upstream and 1 to 1.9 downstream taking account of the study of plane sliding based on the assumed physical properties of the available materials and the design seismic coefficient of 0.15. The total embankment volume will amount to about 19 x 10^6 m^3 with the height of 260 m and the crest length of 400 m.

The spillway will be arranged on the left bank, which is an open chute type with four radial gates 13.5 m wide and 15.0 m high. The maximum water level will be 2.0 m above high water level giving the maximum spillway discharge of about 7,800 m^3/s.

The power waterway and powerhouse are arranged in the right bank. The power intake will be an inclined type and one line of inclined shaft penstock of 9.0 - 8.0 m in inner diameter tri-furcates at the lower horizontal portion.

The powerhouse is provided underground in the right bank being connected by an access tunnel about 450 m in length.

The turbine is a vertical Francis type and the unit number of main generating machine is studied. As a result, a three-unit plan is adopted because it is confirmed that the maximum unit output is well within the technical limit and that it is clearly more economical than a four-unit plan causing no trouble to the system operation.

The tailrace is a pressure tunnel type having inner diameter of 9.8 m after the confluence.

Care of river is planned based on design flood of 1,330 m^3/s that corresponds to 25 year return period flood. The crest elevation of the upstream cofferdam is 550 m, and one line of diversion tunnel with inner diameter of 9.2 m

for a typical horse-shoe section is arranged in the right bank being adjusted to the river configuration.

A bottom outlet will have to be provided to release a certain amount of water required downstream during initial filling of the reservoir.

The intake sill elevation of the bottom outlet is 555 m, and the discharge will be done to the diversion tunnel through the connecting inclined shaft downstream of the gate chamber.

(b) Rockfill Dam: Surface Powerhouse Plan

The dam axis is shifted upstream by about 100 m from (a) plan in order to allocate a surface powerhouse in good topography. This will result in a little more total embankment volume of about 20 x 10^6 m^3 and the spillway excavation on the right bank will be as much as 11 x 10^6 m^3.

The power waterway is arranged in the left bank. One line of headrace tunnel 9.8 m in inner diameter, 594 m in length will lead to the underground penstock which trifurcates at the lower horizontal portion before the powerhouse. Near the upper joint of penstock, a restricted orifice type of surge tank 14.0 m in inner diameter will be provided to contribute to the stable operation at the time of the instantaneous cut or the sudden increase of the load.

The switchyard is provided at the downstream end of the dam embankment adjacent to the surface powerhouse.

The same idea as for (a) plan, in principle, will be applied to the plan for the care of river and for the bottom outlet.

(c) Arch Dam: Underground Powerhouse Plan

The arch dam is of single-centered, constant thick double curvature with a parabolic configuration on a plan, which will inherently ensure the better stability of the abutment. As a result of the preliminary stress analysis by means of the trial load method, the thickness of the dam is to be 12 m at the top and 55 m at the base on the top of 30 m high foundation concrete and the total concrete volume will amount to 2.8×10^6 m^3.

The spillway is a center overflow type having six radial gates 10.5 m wide and 12.0 m high each. The maximum water level will be 3.0 m above high water level and the maximum discharge capacity is calculated to be about 7,700 m^3/s. An excavated stilling basin is provided 30 m in normal water depth and 150 m in flat bottom length.

The power waterway and the underground powerhouse are arranged in the right bank. The power intake structure is an inclined type. In terms of waterway configuration on a plan, a vertical shaft type of penstock is adopted to have a tri-furcation at the lower horizontal portion. Three lines of short tailrace tunnel remain straight down to the outlet. No surge tanks will be required.

A plan for care of river was studied on the basis of 10 year return period flood, that is 1,100 m^3/s, with an upstream cofferdam and a diversion tunnel combined together. In the result, the crest elevation of the upstream cofferdam is to be 530 m and inner diameter of the diversion tunnel is to be 9.2 m as an optimum combination.

A bottom outlet is provided through the dam body probably near the elevation of 575 m.

(4) Study on Reservoir Scale

The reservoir scale has been studied for the plan of rock-fill dam having an underground powerhouse in the right bank, which has been selected in the study of (3). The seasonal and yearly change of the monthly average inflow to Yusufeli Reservoir, for the period of 42 years, are indicated by the mass curve in Fig. 9-3. In terms of seasonal change, the inflow is generally large in the half-year period from March to August, and small in the period from September to February. The annual average inflow, calculated for the period of 42 years, is 3,777 x $10^6 m^3$ ($120 m^3/s$). The inflow in the period from March to August is 3,011 x $10^6 m^3$ ($189 m^3/s$), which is 3.9 times the inflow from September to February, which is 766 x $10^6 m^3$ ($49 m^3/s$). The total annual inflow also varies considerably from year to year during this period of 42 years. The annual inflow in the driest year in the 42 years (1955) was 2,093 x $10^6 m^3$, and that in the wettest year (1968) was 6,474 x $10^6 m^3$.

In order to effectively utilize the water resource of this river, Yusufeli Reservoir should be used to regulate these yearly as well as seasonal change of the river flow, and to secure stable power generation by supplementing water in the dry season and the dry year.

The reservoir high water level and the effective storage capacity must be so selected that the best overall economy is realized. For the study of high water level, 4 cases, with EL.690, 700, 710 and 720 m respectively, have been compared, taking into account such factors as sediment and effective storage capacity.

For the amount of the sediment, $400 m^3/km^2$/year was assumed based on the analysis in the study of "Meteorology and Hydrology". The sediment in a period of 50 years amounts to 304.8 x $10^6 m^3$. The elevation of deposits surface, due to this sediment, will be 618 m.

In comparing effective storage capacity of the reservoir, 4 cases of available drawdown, 30, 40, 50 and 60 m, have been

assumed for each case of high water level discussed above. Effective storage capacities for all combination of the study cases are given in the table below. The reservoir area, storage capacity curve of Yusufeli Reservoir is presented in Fig. 9-9.

H.W.L.(m)	Available Drawdown (m)			
	60	50	40	30
720	$1620 \times 10^6 m^3$	$1420 \times 10^6 m^3$	$1200 \times 10^6 m^3$	$950 \times 10^6 m^3$
710	1440 "	1270 "	1080 "	850 "
700	1260 "	1120 "	950 "	760 "
690	1100 "	980 "	840 "	670 "

The following conditions have been assumed in the comparative studies of high water level and effective storage capacity.

(a) As large hydroelectric power plant can be developed at this site, it is appropriate to design the power plant to carry the peak load, because the peak in the daily load curve will become more eminent in future. On the other hand, the peak duration of 6 to 10 hours seems reasonable for the design of this power plant, considering the fact that this site is near the Soviet border and far from the load center. The effect of the peak duration is studied separately in (5), and the peak duration time of 6 hours is assumed in the study of reservoir scale.

(b) The maximum power discharge and the installed capacity of Yusufeli Power Plant has been so selected that the peak power generation of 6 hours is realized with the firm flow, which is determined by the reservoir inflow and the effective storage capacity. The study on the maximum power discharge is described in (5).

(c) The low water level has been limited to EL. 630 m based on the assumed sediment of the reservoir as described above.

(d) The benefit of this project is measured by either the project cost or the investment cost plus operation-mainten-

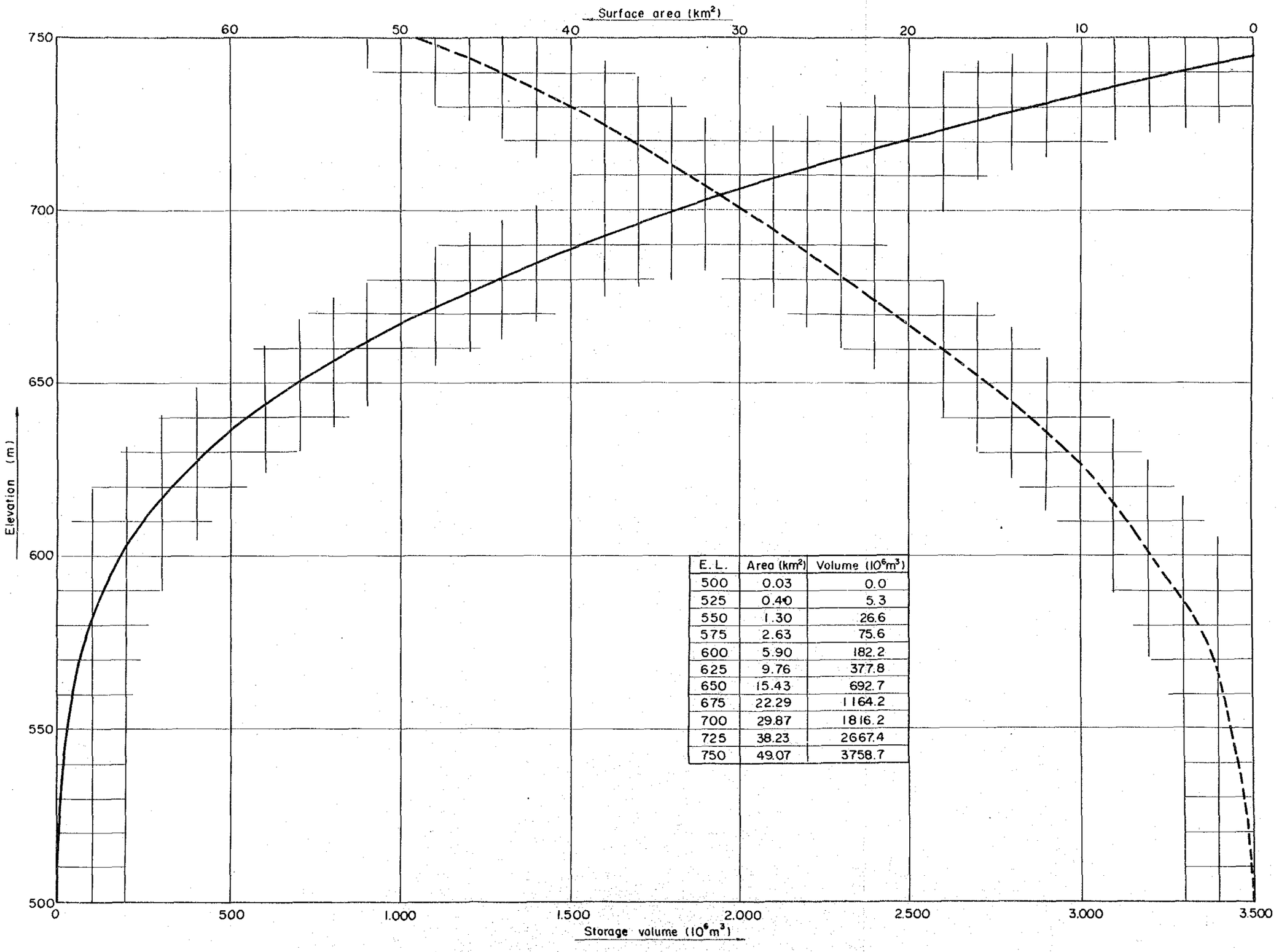

E. L.	Area (km²)	Volume (10⁶m³)
500	0.03	0.0
525	0.40	5.3
550	1.30	26.6
575	2.63	75.6
600	5.90	182.2
625	9.76	377.8
650	15.43	692.7
675	22.29	1164.2
700	29.87	1816.2
725	38.23	2667.4
750	49.07	3758.7

Fig. 9–9 Yusufeli Reservoir Storage Capacity and Area Curve

ance cost and fuel cost of a thermal power plant having equivalent power and energy generation. The power output and energy generation of this project which is used for the calculation of the benefit are defined by the following conditions, and to be termed as the "effective power output" and the "effective energy output" respectively.

i) The effective power output of this power plant at receiving end is expressed by the equation below deducting loss rates of 0.3% and 2.0% due to forced outage and scheduled outage, respectively, and 0.3% and 5.0% due to station service and transmission loss, respectively, from the firm peak power output. The firm peak power output is defined here as the average of 12 monthly minimum power outputs for the 42 year period.

Effective power output
= (1-0.003)(1-0.02)(1-0.003)(1-0.05)
x Firm peak power output

ii) The effective energy output of this power plant at receiving end is expressed by the equation below deducting loss rates of 0.3% and 3.0% due to station service and transmission loss, respectively, from the average annual energy generation for the 42 year period.

Effective energy output
= (1-0.003)(1-0.03)
x Average annual energy generation

The results of comparison studies on high water level and effective storage capacity of the reservoir for two cases of a coal-fired thermal and an oil-fired thermal power plants as the alternatives are shown in Table 9-12, 13, and Figs. 9-10 - 15, respectively.

In the case of a coal-fired alternative, in the range of high water level from 690 m to 720 m, the surplus benefit (B-C) is

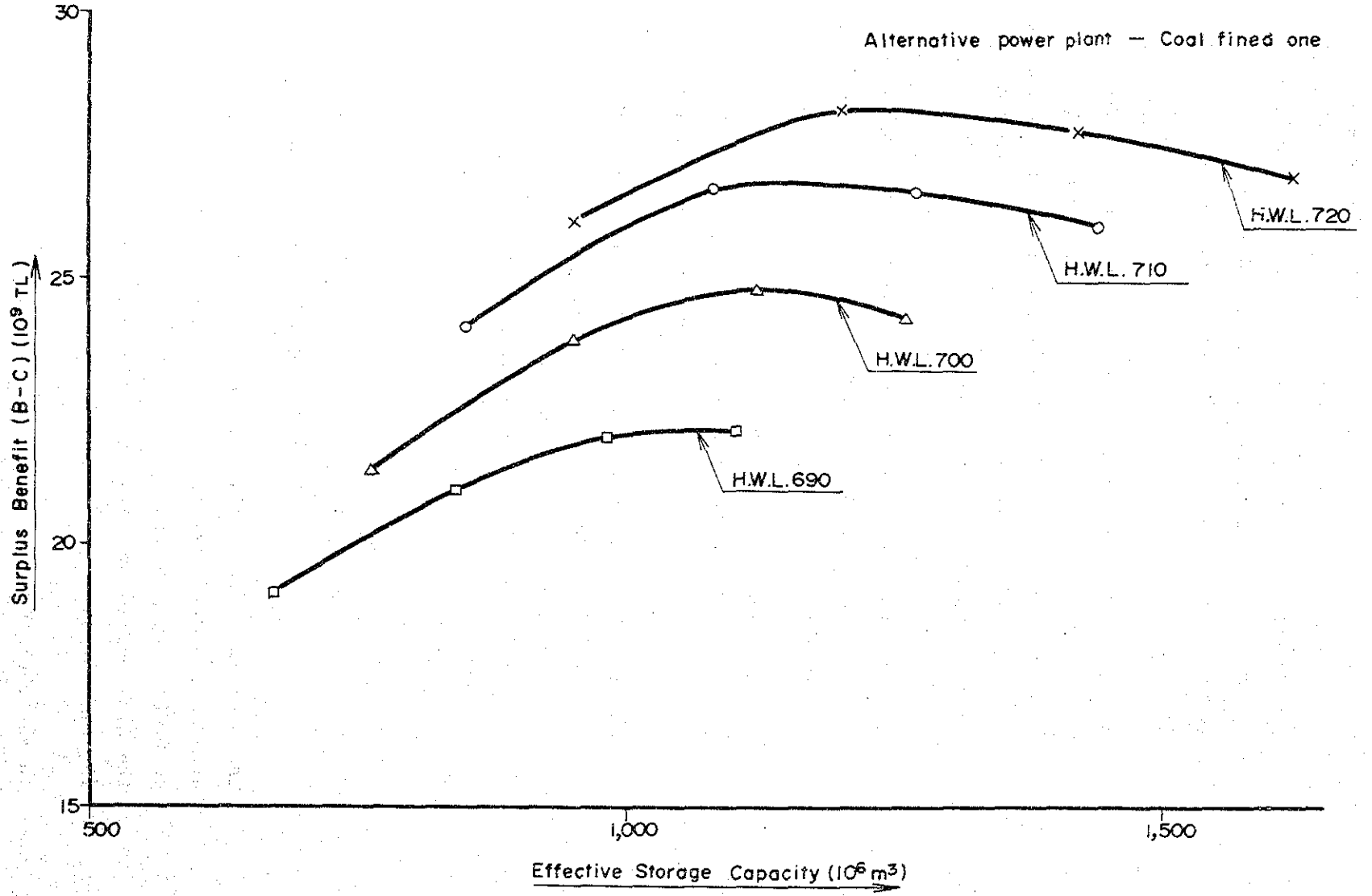

Fig. 9–10 Study on Optimum High Water Level and Effective Storage Capacity of Reservoir (B–C) (1)

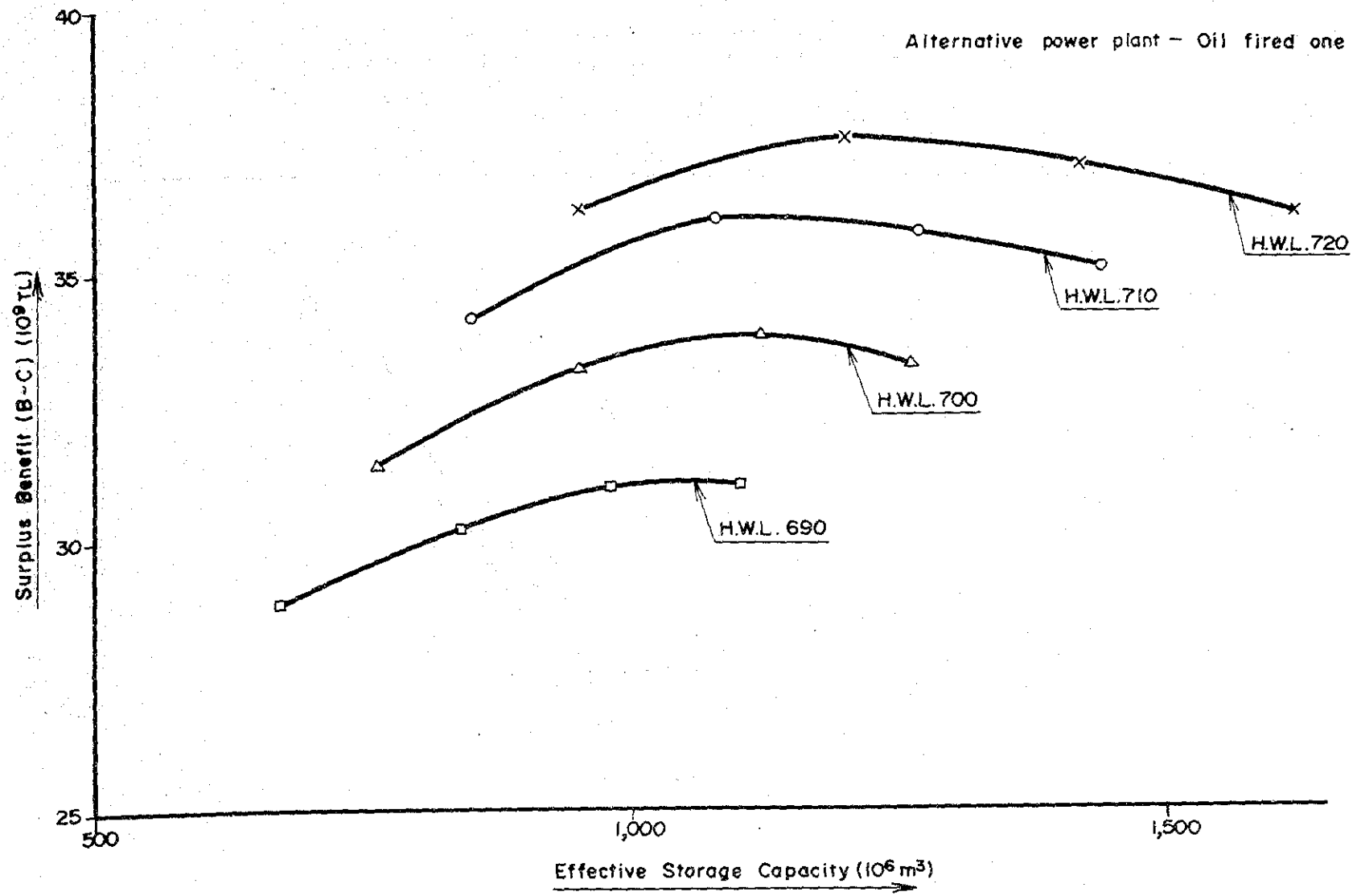

Fig. 9–11 Study on Optimum High Water Level and Effective Storage Capacity of Reservoir (B–C) (2)

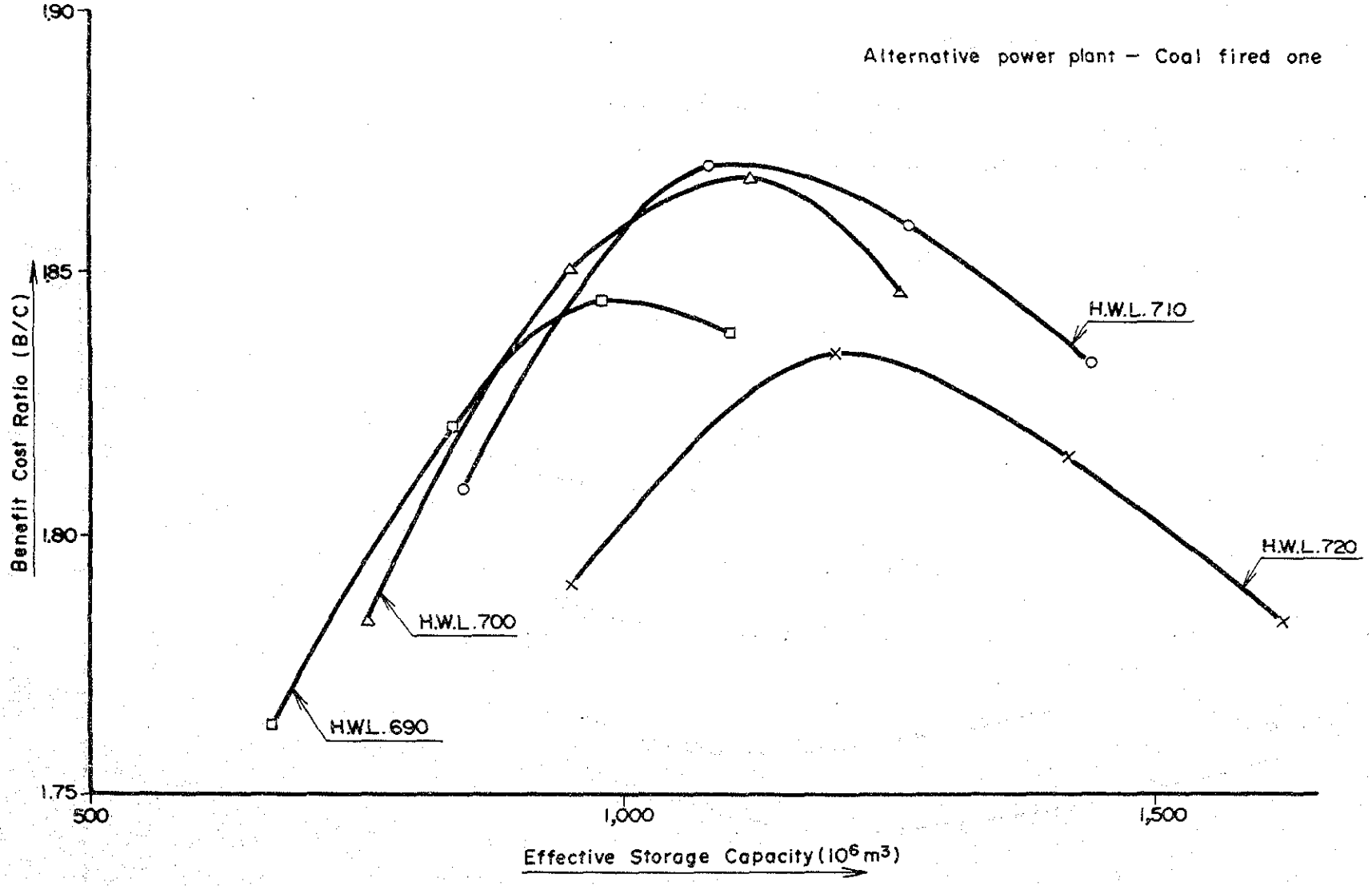

Fig. 9–12 Study on Optimum High Water Level and Effective Storage Capacity of Reservoir (B/C) (1)

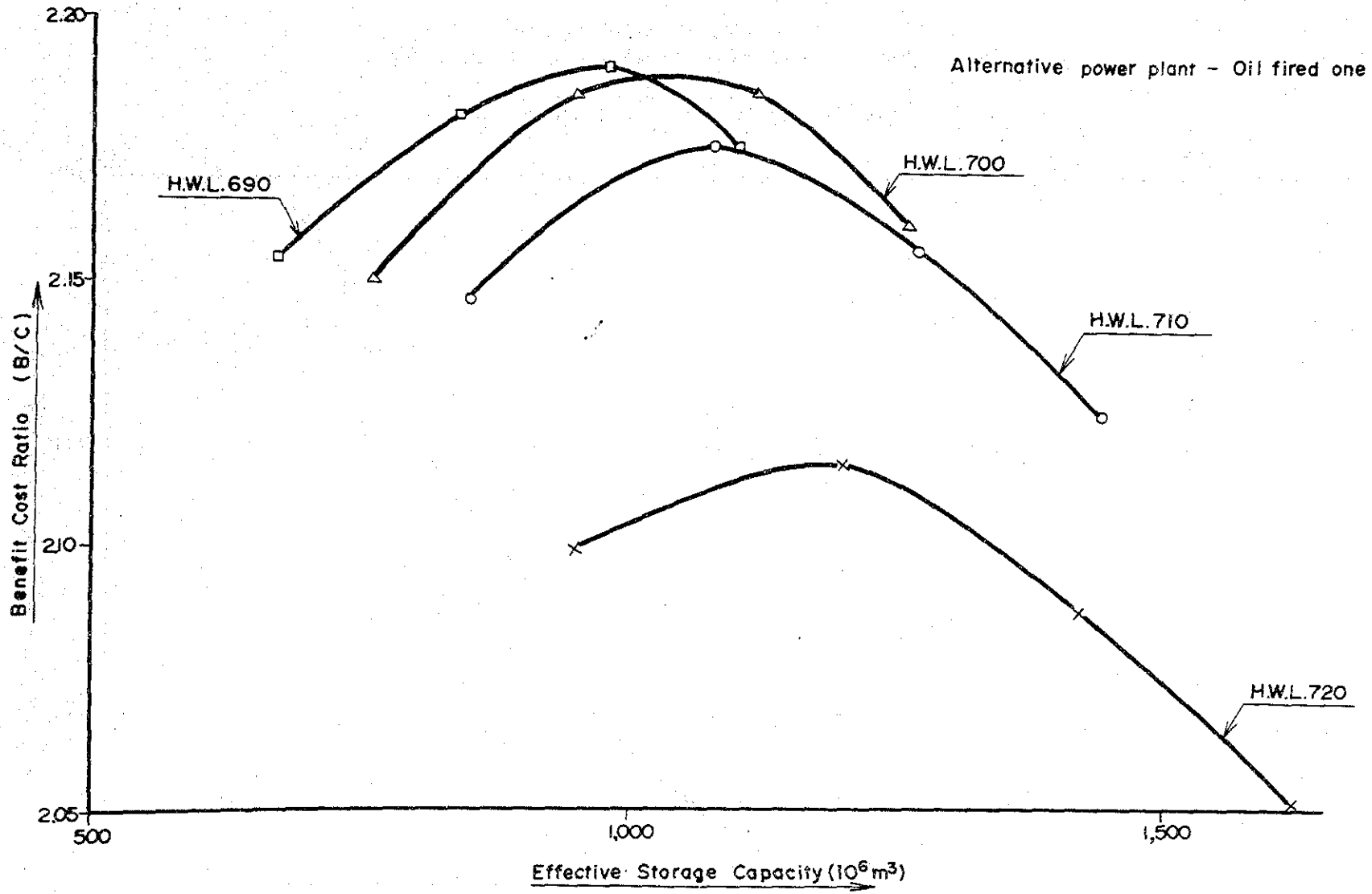

Fig. 9–13 Study on Optimum High Water Level and Effective Storage Capacity of Reservoir (B/C) (2)

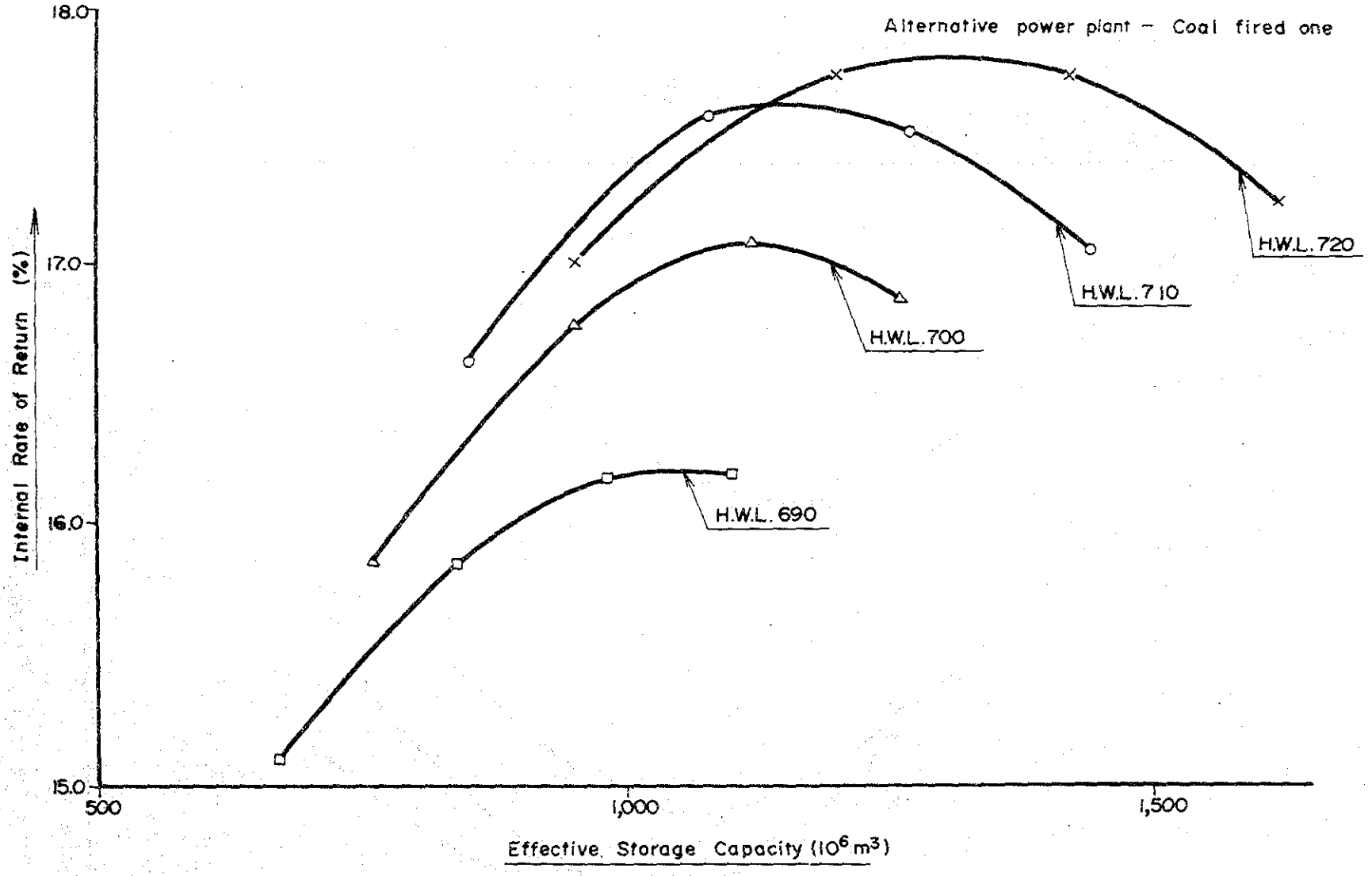

Fig. 9–14 Study on Optimum High Water Level and Effective Storage Capacity of Reservoir (I.R.R.) (1)

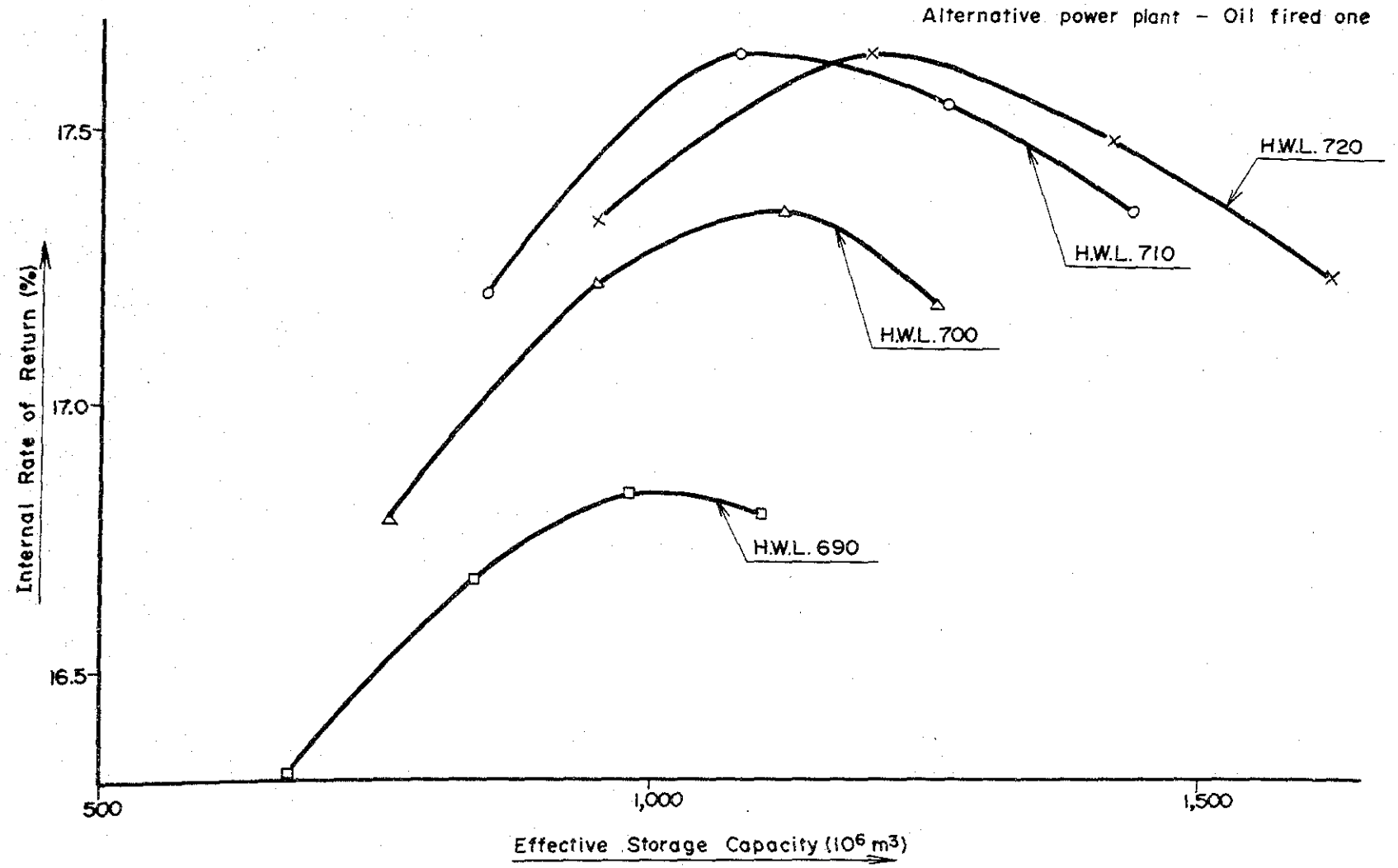

Fig. 9–15 Study on Optimum High Water Level and Effective Storage Capacity of Reservoir (I.R.R.) (2)

Table 9–12 Study on Optimum High Water Level and Effective Storage Capacity of Reservoir (1)

* Alternative Power Plant .... Coal-fired one

Case	H.W.L. (m)	Storage Capacity (10^6 m^3) Gross	Effective	Firm Discharge (m^3/s)	Maximum Discharge (m^3/s)	Effective Head (m)	Installed Capacity (MW)	Firm Peak Power (MW)	Annual Energy (GWh)	Investment Cost (10^6TL)	Annual Cost (10^6TL)	Energy Cost (TL/kWh)	I.R.R. (%)	Surplus Benefit (10^6TL)	Benefit-Cost Ratio
1			1,620	90.9	363	195.0	625	549.3	1,781.1	335,900	34,430	20.0	17.24	26,970	1.78
2	720	2,480	1,420	87.2	348	198.3	609	554.6	1,796.5	333,400	34,150	19.6	17.73	27,820	1.81
3			1,200	83.0	332	201.7	591	553.2	1,807.3	330,100	33,790	19.3	17.74	28,190	1.83
4			950	75.2	300	205.0	543	517.1	1,792.9	322,900	33,000	19.0	17.01	26,080	1.79
5			1,440	87.6	350	185.0	572	508.1	1,692.6	304,800	31,270	19.1	17.26	26,020	1.83
6	710	2,130	1,270	84.4	337	188.3	560	512.2	1,704.9	302,900	31,060	18.8	17.52	26,680	1.86
7			1,080	80.4	321	191.7	543	507.3	1,709.2	299,600	30,700	18.6	17.58	26,720	1.87
8			850	71.3	285	195.0	490	465.0	1,685.2	291,800	29,840	18.3	16.63	24,100	1.81
9			1,260	84.4	337	175.0	520	465.0	1,600.0	279,700	28,710	18.6	16.87	24,290	1.85
10	700	1,820	1,120	81.6	326	178.3	513	468.7	1,610.9	278,500	28,580	18.3	17.09	24,820	1.87
11			950	75.7	302	181.7	484	450.7	1,601.8	273,900	28,070	18.1	16.77	23,870	1.85
12			760	67.4	269	185.0	439	411.8	1,576.3	267,000	27,310	17.9	15.85	21,390	1.78
13			1,100	81.3	325	165.0	473	420.5	1,505.2	257,300	26,420	18.1	16.19	22,150	1.84
14	690	1,530	980	76.9	307	168.3	456	414.4	1,503.0	254,200	26,080	17.9	16.18	22,000	1.84
15			840	71.0	284	171.7	430	397.4	1,489.2	250,100	25,630	17.8	15.84	21,020	1.82
16			670	63.8	255	175.0	394	366.8	1,469.6	244,500	25,010	17.6	15.10	19,090	1.76

Table 9–13 Study on Optimum High Water Level and Effective Storage Capacity of Reservoir (2)

* Alternative Power Plant .... Oil-fired one

Case	H.W.L. (m)	Storage Capacity (10^6 m^3) Gross	Effective	Firm Discharge (m^3/s)	Maximum Discharge (m^3/s)	Effective Head (m)	Installed Capacity (MW)	Firm Peak Power (MW)	Annual Energy (GWh)	Investment Cost (10^6TL)	Annual Cost (10^6TL)	Energy Cost (TL/kWh)	I.R.R. (%)	Surplus Benefit (10^6TL)	Benefit-Cost Ratio
1			1,620	90.9	363	195.0	625	549.3	1,781.1	335,900	34,430	20.0	17.23	36,210	2.05
2	720	2,480	1,420	87.2	348	198.3	609	554.6	1,796.5	333,400	34,150	19.6	17.48	37,130	2.09
3			1,200	83.0	332	201.7	591	553.2	1,807.3	330,100	33,790	19.3	17.64	37,670	2.11
4			950	75.2	300	205.0	543	517.1	1,792.9	322,900	33,000	19.0	17.33	36,280	2.10
5			1,440	87.6	350	185.0	572	508.1	1,692.6	304,800	31,270	19.1	17.35	35,150	2.12
6	710	2,130	1,270	84.4	337	188.3	560	512.2	1,704.9	302,900	31,060	18.8	17.55	35,860	2.15
7			1,080	80.4	321	191.7	543	507.3	1,709.2	299,600	30,700	18.6	17.64	36,080	2.18
8			850	71.3	285	195.0	490	465.0	1,685.2	291,800	29,840	18.3	17.20	34,210	2.15
9			1,260	84.4	337	175.0	520	465.0	1,600.0	279,700	28,710	18.6	17.18	33,300	2.16
10	700	1,820	1,120	81.6	326	178.3	513	468.7	1,610.9	278,500	28,580	18.3	17.35	33,880	2.19
11			950	75.7	302	181.7	484	450.7	1,601.8	273,900	28,070	18.1	17.22	33,250	2.18
12			760	67.4	269	185.0	439	411.8	1,576.3	267,000	27,310	17.9	16.78	31,430	2.15
13			1,100	81.3	325	165.0	473	420.5	1,505.2	257,300	26,420	18.1	16.79	31,050	2.18
14	690	1,530	980	76.9	307	168.3	456	414.4	1,503.0	254,200	26,080	17.9	16.83	31,030	2.19
15			840	71.0	284	171.7	430	397.4	1,489.2	250,100	25,630	17.8	16.67	30,280	2.18
16			670	63.8	255	175.0	394	366.8	1,469.6	244,500	25,010	17.6	16.31	28,870	2.15

larger with higher dam height, and the energy cost is smaller with lower dam height. The benefit cost ratio (B/C) is best with the case of high water level 710 m. Internal rates of return (I.R.R.) are good and almost equal with the cases of high water levels 710 m and 720 m.

Considering the abovementioned economic indeces as well as physical conditions such as possibility of a landslide in the reservoir and difficulty of construction with a high dam, it is judged that the case of high water level 710 m will be optimum. In this case, effective storage capacity of 1080 x 10^6 m^3 with available drawdown of 40 m will be most advantageous.

In the case of an oil-fired alternative, similar results will be drawn, too. Accordingly design parameters of Yusufeli Reservoir have been determined to be high water level of 710 m, 40 m available drawdown, and 1080 x 10^6 m^3 effective storage capacity.

(5) Study on Maximum Power Discharge and Peak Duration

The installed capacity must be carfully selected considering the characteristics of the hydroelectric project site and the peak duration. If the installed capacity is too large, the effective power output is limited by the forecasted peak duration, resulting in latent power and reducing economy. If the installed capacity is too small, the effective power output is limited by the installed capacity and the peak duration becomes unnecessarily long.

Considering that this site is near the Soviet border, and far from the load center, the peak duration of 6 to 10 hours seems reasonable for the design of this power plant. In our study, the effects of the installed capacity have been examined for 12 cases which consist of combinations of 3 different peak duration hours and 4 different maximum power discharges. The peak durations assumed were 6, 8 and 10 hours, and the maximum power discharges were the values that give peak durations of 4, 6, 8 and 10 hours for the firm discharge, that is, 482, 321, 241 and